# NASA TECHNICAL MEMORANDUM

NASA TM-78285

# ADVANCED X-RAY ASTROPHYSICS FACILITY (AXAF)- SCIENCE WORKING GROUP REPORT

By Program Development Directorate

(NASA-TM-78285) ADVANCED X-RAY ASTROPHYSICS FACILITY (AXAF): SCIENCE WORKING GROUP REPORT (NASA) 182 p HC A09/MF A01 CSCL 03A

N80-29219

Unclas
G3/89 28222

May 1980

**NASA**

*George C. Marshall Space Flight Center*
*Marshall Space Flight Center, Alabama*

TECHNICAL REPORT STANDARD TITLE PAGE

| 1. REPORT NO. | 2. GOVERNMENT ACCESSION NO. | 3. RECIPIENT'S CATALOG NO. |
|---|---|---|
| NASA TM-78285 | | |

| 4. TITLE AND SUBTITLE | 5. REPORT DATE |
|---|---|
| Advanced X-Ray Astrophysics Facility Science Working Group Report | May 1980 |
| | 6. PERFORMING ORGANIZATION CODE |
| 7. AUTHOR(S) | 8. PERFORMING ORGANIZATION REPORT # |
| 9. PERFORMING ORGANIZATION NAME AND ADDRESS<br>George C. Marshall Space Flight Center<br>Marshall Space Flight Center, Alabama 35812 | 10. WORK UNIT NO. |
| | 11. CONTRACT OR GRANT NO. |
| 12. SPONSORING AGENCY NAME AND ADDRESS<br>National Aeronautics and Space Administration<br>Washington, DC 20546 | 13. TYPE OF REPORT & PERIOD COVERED<br>Technical Memorandum |
| | 14. SPONSORING AGENCY CODE |

15. SUPPLEMENTARY NOTES

16. ABSTRACT

The Advanced X-Ray Astrophysics Facility (AXAF) Science Working Group report documents the results of the studies by a group of 16 scientists appointed by the NASA Office of Space Sciences to examine the AXAF mission concept from a scientific viewpoint. This report contains (1) a brief description of the development of X-ray astronomy and a summary description of AXAF, (2) the scientific objectives of the facility, (3) a description of representative scientific instruments, (4) requirements for X-ray ground testing, and (5) a summary of studies related to spacecraft and support subsystems.

| 17. KEY WORDS | 18. DISTRIBUTION STATEMENT |
|---|---|
| | Unclassified-Unlimited |

| 19. SECURITY CLASSIF. (of this report) | 20. SECURITY CLASSIF. (of this page) | 21. NO. OF PAGES | 22. PRICE |
|---|---|---|---|
| Unclassified | Unclassified | 186 | NTIS |

# TABLE OF CONTENTS

## AXAF SCIENCE WORKING GROUP REPORT

## FOREWORD

X-ray astronomy is now approaching the end of its second decade. Its development has been extraordinary with results as surprising and significant as any in the physical sciences over the same period. Following the exploratory studies with small rocket payloads beginning in 1962, the seventies were heralded by the launch of the Uhuru satellite, which produced the first all-sky survey and discovered the powerful X-ray binaries and the X-ray emissions from the vast regions of space lying within galaxy clusters. A number of other small satellites, Copernicus, ANS, Ariel 5, OSO-8, and SAS-3, added further discoveries, for example, the strong X-ray emission from active galaxies and the strange X-ray "bursters". With these developments came the realization that X-ray observations are unique in their potential for revealing the most energetic and exotic phenomena in the universe. Over the past two years, the two HEAO spacecraft have brought, first an extension of the earlier small satellite surveys, and now, with HEAO-2 (the Einstein Observatory), a major advance in X-ray observations, extending the scope of X-ray astronomy to the study of normal stars, the detailed mapping of supernova ejecta both in the galaxy and in the Magellanic Clouds, high resolution spectroscopic anaylsis of the brighter sources, and the detection of clusters of galaxies and QSO's at the very edge of the known universe. Thus, the Einstein mission has firmly established the place of X-ray observations alongside those in the optical and radio, as a vital part of man's equipment for probing the heavens, in his oldest and most enduring intellectual quest, to understand the nature of the universe.

The congruence of three important factors make it now timely to embark on the next stage of this quest. First, as detailed in section 2, the exploratory studies of the 60's and 70's have brought X-ray astronomy to the forefront in scientific significance. Second, the Einstein Observatory has demonstrated the

power of imaging optics, and recent advances in both mirror technology and focal plane instrumentation will allow a considerably more powerful instrument to be built. Third, the Shuttle transport system, shortly to be inaugurated, will provide for extended space missions in which the full potential of a unique national facility such as the AXAF can be maintained over many years by routine servicing, installation of new instruments, etc.

It is our belief that the AXAF, as now envisaged, will provide an extremely powerful and unique tool for new and fundamental discoveries in astrophysics. It will also provide the third vital element, alongside ST and the VLA, in man's exploration of the universe through the remainder of the 20th century.

## PREFACE

The AXAF mission is essentially identical to the Large Orbiting X-ray Telescope (LOXT) PI experiment which was undertaken as the third mission in the HEAO program in 1970. In 1973 fiscal constraints required a severe reduction in the entire HEAO program and the 1.2 meter telescope of LOXT was reduced to the 0.6 meter Einstein telescope with reduced mission scope and duration.

In the following years, the 1.2 meter X-ray telescope mission was considered by a number of study groups and panels both within NASA and the NAS. The 1.2 meter telescope was endorsed in the "Scientific Users of the Space Shuttle" (NAS-Woods Hole 1973) and more recently in the document "A Program for High Energy Astrophysics (1977-1988)" by the Ad Hoc Planning Group of the HEA MOWP of NASA. In this document it was proposed that "major, general purpose instruments", such as the 1.2 meter high resolution telescope, should be managed as National Space Observatories.

In April 1976, the Smithsonian Astrophysical Observatory (SAO) submitted a proposal to the Office of Space Science (OSS), NASA Headquarters, titled, "Study of the 1.2 meter X-ray Telescope National Space Observatory". This document provided the primary initial technical foundation and stimulus for NASA's initiation of the Advanced X-ray Astrophysics Facility (AXAF) project, a national X-ray observatory in space.

In June 1977, the Marshall Space Flight Center (MSFC) was assigned responsibility for the definition and development of AXAF and in July 1977, SAO was awarded a contract to assist MSFC in the AXAF definition studies and associated technology efforts. This has now evolved into a joint MSFC/SAO team to manage the definition and development of the AXAF system, based on the premise that MSFC and SAO have complementary capabilities in space systems

engineering and in X-ray astronomy and optical systems design. The Phase A conceptual definition effort for AXAF was completed in the fall of 1978, and continuing definition effort by MSFC and SAO is directed toward providing the basis of a Phase B study effort, which is expected to be underway by FY81. The present plan calls for the final design and development activities (Phases C and D) to begin in FY83 and the launch of the AXAF to take place in mid-1987.

The OSS appointed an AXAF Science Working Group, chaired by Professor Riccardo Giacconi and co-chaired by Dr. Martin Weisskopf, AXAF Study (Project) Scientist, to assist NASA in establishing scientific requirements and to provide other guidance during the AXAF definition phase. The first meeting of this group took place in December 1977 and several subsequent meetings have been held. This group will be disbanded when NASA issues an Announcement of Opportunity (AO) for the AXAF science instruments. The membership of this group is as follows:

Riccardo Giacconi, Harvard/Smithsonian Center for Astrophysics, Chairman
Martin Weisskopf, Marshall Space Flight Center, Vice-Chairman

Elihu Boldt, Goddard Space Flight Center
Stuart Bowyer, University of California at Berkeley
George Clark, Massachusetts Institute of Technology
Arthur Davidsen, Johns Hopkins University
Gordon Garmire, California Institute of Technology
William Kraushaar, University of Wisconsin
Robert Novick, Columbia University
Minoru Oda, Tokyo University, Japan
Albert Opp, NASA Headquarters
Kenneth Pounds, University of Leicester, UK
Seth Shulman, Naval Research Laboratory
Harvey Tananbaum, Harvard-Smithsonian Center for Astrophysics
Joachim Trümper, Max Planck Institute, FRG
Arthur Walker, Stanford University

The "AXAF Science Working Group Report" has been prepared by this group and edited by Martin Zombeck (CFA), and is intended to provide a description of the AXAF for the astronomical community. It is organized in the following manner. Section 1 gives a brief description of the development of X-ray astronomy

and a summary description of the AXAF and its capabilities. Section 2 discusses the scientific objectives of the facility. This section is topically organized and reviews present observational status, theoretical understanding, the nature of outstanding problems, and the contributions that the AXAF can make toward the solutions to these problems. Section 3 contains a more detailed description of the AXAF telescope assembly and a description of representative scientific instruments. The latter description is intended to both stimulate instrument development and show potential users of the facility the potential power of the AXAF for imaging, spectroscopy, and polarimetry. The requirement for X-ray ground testing is outlined in Section 4. Section 5 summarizes the work performed by MSFC concerning spacecraft and support subsystems.

# ADVANCED X-RAY ASTROPHYSICS FACILITY (AXAF)

## 1.0 INTRODUCTION

### 1.1 X-ray Astronomy

X-ray astronomy was born less than twenty years ago, and has developed at an increasingly rapid pace. Spurred on by a host of unsuspected discoveries, it is today a powerful and indeed essential tool for astronomical observations, equalling in importance the more established disciplines of visible and radio astronomy, for the study of the most significant astrophysical problems. This has been brought about by a set of basic physical reasons and by developments in technology. It is the rule that whenever extremely energetic events or explosions take place in the universe, they result in the acceleration of particles to high energies, or in the heating of gases to very high temperatures. The high energy particles by collisions with photons and fields, the high temperature gases by free-free and free-bound transitions, emit much of their energy at X-ray wavelengths. Thus, whenever objects are found in which energetic events take place, such as mass exchange binary systems (containing a white dwarf, neutron star, or black hole), pulsars, nuclei of active galaxies and quasars, and condensations of galaxies into rich clusters, they are inevitably found to emit copious quantities of X-rays. Moreover, intergalactic and interstellar space is essentially transparent to X-rays with energies above 1 kilovolt. The earth's atmosphere is, however, entirely opaque to X-rays of this energy so that the start of X-ray astronomy had to await the development of space technology. When instrumented rockets and satellites became available, the fully laboratory-based technology of X-ray physics could be applied to astronomical research.

It is this combination of fundamental physical reasons and technological developments of the space age which has caused the field of X-ray astronomy to blossom.

Following the early discoveries of the 1960's with rocket-borne instru-

ments, X-ray astronomy moved in the 1970's to sophisticated satellite instruments which have surveyed the sky with a thousand-fold increased sensitivity that has revealed to us a rich new field awaiting future exploitation.

In the main body of the report a more detailed review of the previous work in the field is given. Here we wish to highlight only a few of the most important discoveries and results:

- the discovery of X-ray emission from the coronas of stars of all spectral types at levels exceeding by orders of magnitude the theoretical expectations;

- the discovery of X-ray emission from pulsars and supernova remnants;

- the mapping of supernova remnants and the study of their elemental composition and physical conditions;

- the discovery of the hot ($\sim 10^{6}$°K) interstellar medium;

- the discovery of the existence of close mass exchange binaries containing neutron stars and possibly black holes;

- the measurement of mass and moments of inertia of neutron stars;

- the discovery of rapidly varying X-ray emission from active nuclei of galaxies (Seyferts, N-types, BL Lacs, quasars, emission line galaxies, radio galaxies);

- the discovery of X-ray emission from the most distant known galaxies and clusters;

- the discovery of tenuous hot gas pervading the intergalactic spaces within clusters of galaxies with a total mass comparable to that of the galaxies themselves, and enriched with the products of nuclear burning inside of stars;

- the discovery of the X-ray background, apparently due to discrete sources at cosmological distances and possibly with a diffused component with cosmological implications.

X-ray astronomy has already demonstrated its power as a tool to study the properties of highly condensed or relativistically collapsed objects, such as neutron stars, black holes, and the cores of active nuclei of galaxies.

It has also proven to be the essential means for investigating the existence and properties of matter in physical states that are not accessible to direct study by optical or radio observations, for example, the hot intergalactic medium in clusters of galaxies. X-ray astronomy contributes to the investigation of some of the great problems of modern astrophysics such as the end point of stellar evolution, the existence of massive black holes, the nature of the energy source in the nuclei of active galaxies and quasars and the question of the density of matter in the universe.

The High Energy Astronomy Observatories, HEAO-1 and HEAO-2 (the Einstein Observatory), have recently achieved major improvements in observational capabilities compared to the previous instrumented satellites. HEAO-1 carried out a sky survey and various pointed observations with detectors of larger area and greater sensitivity than had been previously used. The Einstein Observatory, on the other hand, employed for the first time in satellite X-ray astronomy, the technology of X-ray image-forming focusing optics in the study of galactic and extragalactic X-ray sources. The Einstein results clearly show the tremendous advance in observational capabilities that focusing optics provide to X-ray astronomy. In many respects the Einstein Observatory is a full scale test for the AXAF. However, Einstein will have a relatively short life compared to previous satellite missions, so that it can not provide a permanent observational capability of the kind that is needed to study in detail the thousands of sources which it can detect. The greater capability of AXAF is needed to extend the deep sky surveys of the Einstein Observatory to fainter and therefore more distant sources. The AXAF is designed to provide all astronomers

with an X-ray observatory which is well matched to the problems under investigation and which represents a suitable complement to the capabilities of the Space Telescope in the optical region and the Very Large Array in the radio region of the spectrum.

## 1.2 Summary Description of the AXAF

AXAF is to be a free flying X-ray observatory that is Shuttle-launched, maintainable on-orbit, and retrievable. As a long-lived national facility (10-15 years), the science instruments and the expendables will be replaceable on-orbit.

AXAF (Figure 1.1)is conceived as a 1.2 meter diameter, 10 meter focal length X-ray telescope with interchangeable focal plane instrumentation. It will provide 0.5 arcsecond imagery over a several arcminute field and slightly reduced resolution for the full field of 1° in the X-ray band from 0.1 to 8 keV. With the increase in mirror area and resolution and with high efficiency detectors now under development, a factor of 100 or more increase in sensitivity over Einstein is projected.

High resolution spectroscopy of the strongest sources and high sensitivity (non-dispersive) spectroscopy of the weaker ones with the AXAF will allow detailed tests to be made of theoretical models of galactic and extragalactic sources. Polarimetry will provide critical data on the physical state of non-thermal sources. The combination of a high efficiency and high resolution telescope with high sensitivity quantum cameras will allow the detection of bright galactic nuclei to distances (measured by the redshift $Z = \Delta\lambda/\lambda$) as large as $Z = 10$ and the detection of clusters to $Z \gtrsim 3$. With the use of high sensitivity spectrometers, it will be possible to detect and study the iron lines emitted in the intergalactic gas pervading the clusters to $Z = 2$.

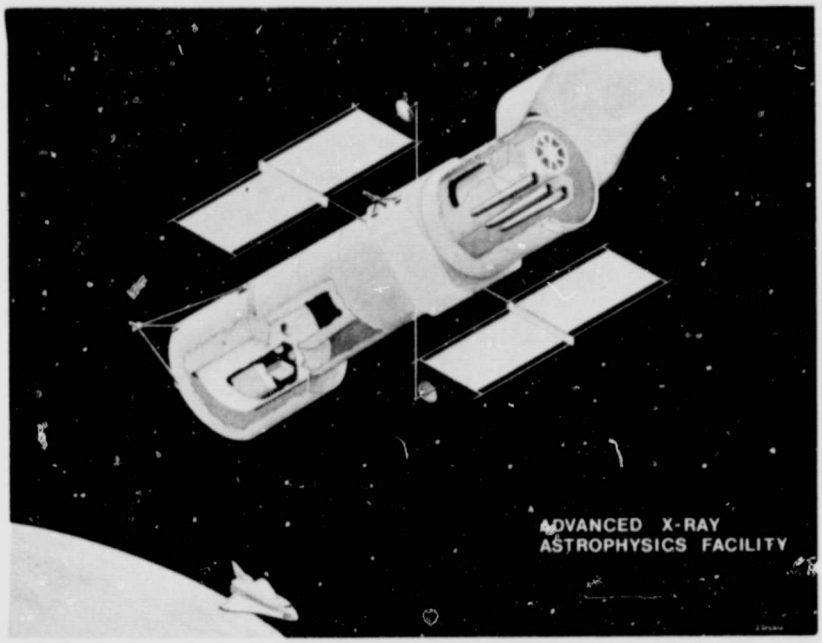


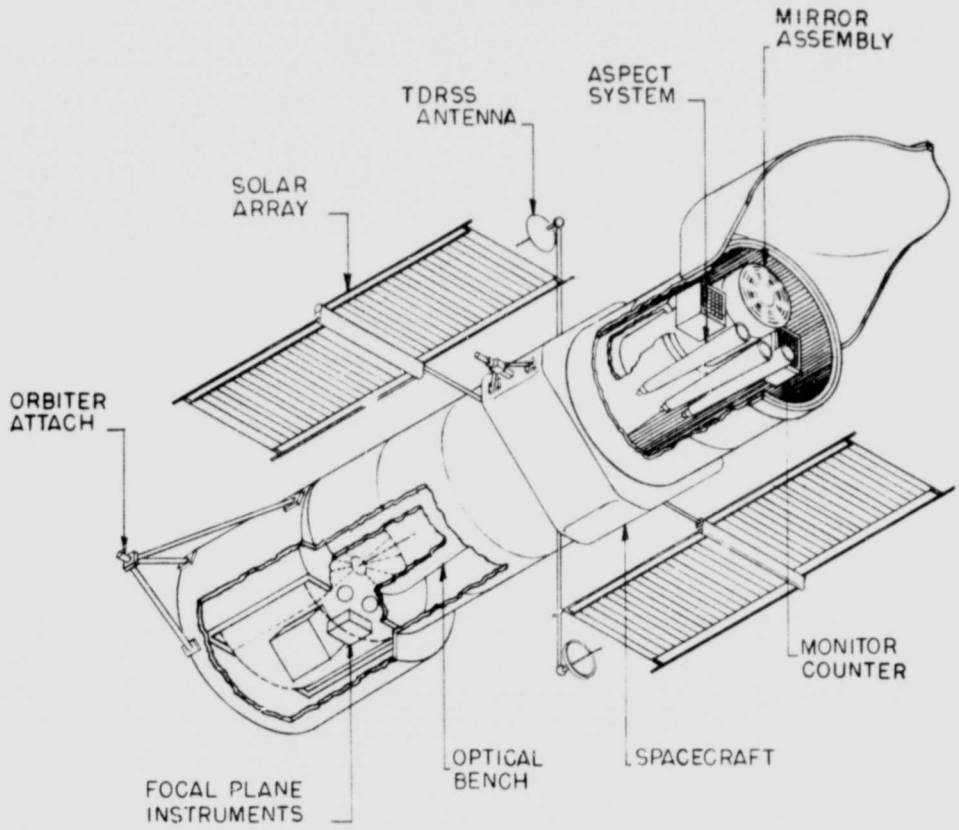


**Figure 1.1** - The Advanced X-ray Astrophysics Facility, a free-flying observatory that is Shuttle-launched, maintainable on-orbit, and retrievable. AXAF is conceived as a 1.2 m diameter, 10 m focal length X-ray telescope with interchangeable focal plane instrumentation.

These distances are greater or comparable to those attainable with the Space Telescope in the study of objects of the same kind. They are the distances at which evolutionary effects in the development of the universe are expected to appear clearly. We do not yet know, in fact, whether stars, galaxies and clusters had formed at these early epochs.

AXAF will be used to investigate the nature of processes occurring in the objects discovered by the ST and VLA. It will also undoubtedly discover new objects which will then be studied by the ST and VLA.

It is important in this respect to point out that if one had studied in detail the first 160 X-ray sources in the X-ray astronomy catalogs of the early 1970's (Figure 1.2), one would have discovered neutron stars and pulsars, black holes (?), radio galaxies, Seyferts, N-type galaxies, BL Lac objects, quasars, and clusters of galaxies. What new and unsuspected marvels await us in the AXAF era we do not know. It is clear, however, that progress in astrophysics now requires observations of the highest attainable quality at all wavelengths.

If X-ray astronomy is to move from its current exploratory state to take its place among the established branches of observational astronomy, then continuity in the observations is a primary requisite. The HEAO X-ray missions achieved major increases in sensitivity beyond previous X-ray experiments. In the case of the Einstein X-ray telescope, with a limited life of $\sim$ 3 years, the deep surveys will have covered less than 10 degrees$^2$ at the ultimate sensitivity limit and the moderate sensitivity surveys will have covered an additional few hundred degrees$^2$ (or less than 1% of the sky). Thousands of new objects will have been discovered which will require more sensitive exposures to study their structure, spectra, time variability, and polarization. The AXAF will be able to meet these requirements by means of:

(1) Long life (10-15 years). This not only permits the detection of a great

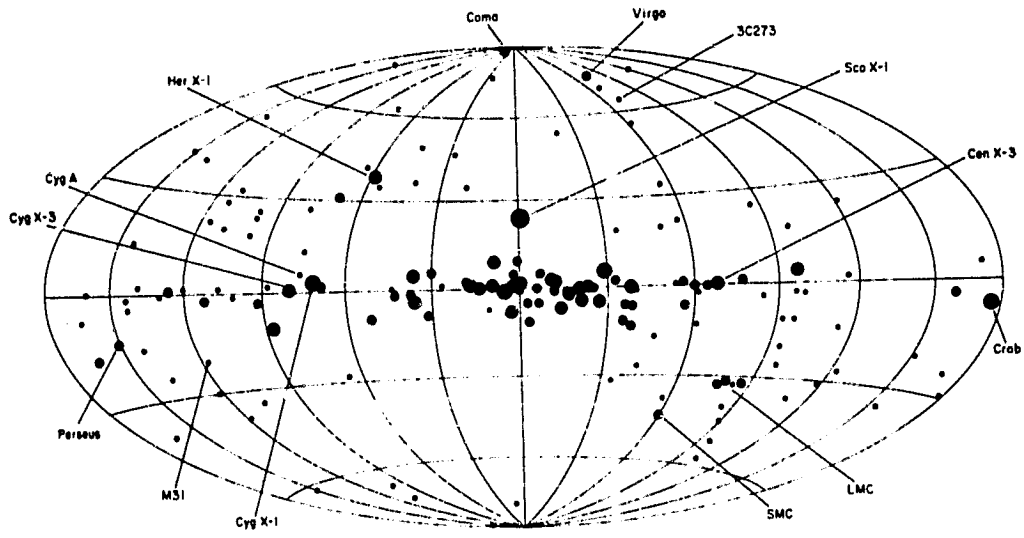


Figure 1.2 - The X-ray sky as reported in the Third Uhuru Catalog. The map is in galactic coordinates and the size of each dot is proportional to the logarithm of the source intensity.

number of targets of interest, but will also allow astronomers to receive data, fully comprehend their significance and import, carry out related optical or radio observations, and then again seek new data to clarify the nature of phenomena of interest. In addition, it is clear that the time scales of interest in X-ray astronomy extend to years, as for instance, in the study of changes in the orbital periods of binary X-ray sources. In order to insure a long-term utilization of the facility, we assume that a program of refurbishment can be carried out for focal plane instruments every three years. This would serve both for maintenance and for replacement of older instruments with newly developed ones.

(2) High angular resolution ($\sim$0.5 arcsecond). A number of extremely important astrophysical problems cannot be attacked at the Einstein 4 arcsecond resolution level. Many of the arguments which have been advanced to support this view in the optical wavelength range are applicable in X-ray astronomy as well. In particular, in extragalactic research the study of the nuclei of active galaxies demands that the resolution achieved by comparable to the characteristic sizes of interest. A resolution as fine as 0.5 arcsecond would permit us to study the nucleus of our own galaxy with a resolution of $2 \times 10^{-2}$ pc, of a nearby galaxy with 20 pc resolution.

For clusters of galaxies at 100 Mpc, a resolution of 0.5 arcsecond would allow us to resolve 1/50 of the linear size of a galaxy in a cluster. For the study of clusters at very great distances ( $Z > 3$ ), a high resolution X-ray telescope would prove particularly valuable since the radiation tends to be red-shifted to the range of greatest sensitivity and the high angular reso-

lution would permit the detailed study of the angular structure and measurement of angular size.

(3) Greater sensitivity. For the AXAF, we expect the sensitivity to increase by a factor of 100 or more over the Einstein Observatory from the increase in mirror area, the increase in high resolution imaging detector efficiency, and the reduced background due to the high resolution of the mirror assembly. This increase in sensitivity is extremely important not only because of the improved ability to explore further in the universe and expand our catalog of X-ray sources, but also because the increased sensitivity will make it possible to study in detail known objects within reasonable observing time. Qualitatively new information may be forthcoming from the low surface brightness features which will be revealed. Sources as faint as $3 \times 10^{-16}$ erg $cm^{-2}$ $s^{-1}$ ($10^{-9}$ Sco X-1) will be detected. This flux density corresponds to an X-ray luminosity of $3 \times 10^{37}$ ergs $s^{-1}$ at a distance of 30 Mpc. (The faintest objects than can be seen with the largest ground-based optical telescopes have apparent magnitudes of about 25, corresponding to an energy flux density of about $10^{-15}$ erg $cm^{-2}$ $s^{-1}$ or $10^{38}$ ergs $s^{-1}$ at 30 Mpc.) Table 1.1 illustrates the range of objects that can be detected with AXAF at this sensitivity level. A comparison of the sensitivity of various astronomical facilities in the radio, visible, and X-ray range is given in Figure 1.3. High resolution spectroscopic measurements, which in the Einstein Observatory are only marginally possible for a few targets due to the long observation times required (weeks), will become routine for a very large number of targets. Spectroscopy with $\lambda/\Delta\lambda = E/\Delta E \sim 1000$ for sources $10^{-4}$ Sco X-1 and polarimetry to a precision of one percent for sources $10^{-3}$ Sco X-1 will be possible.

Table 1.2 lists further examples of observations which exploit the AXAF capability. Listed are the luminosities and redshifts of point-like extragal-

TABLE 1.1

Detection of Point Sources

($10^5$ seconds observation time)

| Luminosity Distance | Object | Minimum Detectable X-ray Luminosity (ergs/sec) | Corresponding Linear Dimension of 1" Detection Cells |
|---|---|---|---|
| 150 pc | star | $10^{27}$ | 50 AU |
| 0.7 Mpc | point source in M31 | $2 \times 10^{34}$ | 3.5 pc |
| 19 Mpc | point source in Virgo Cluster | $1 \times 10^{37}$ | 100 pc |
| 300 Mpc | normal spiral galaxy | $3 \times 10^{39}$ | 1.5 Kpc |
| 1000 Mpc | active galaxy in Hydra Cluster | $3 \times 10^{40}$ | 5 Kpc |
| $2 \times 10^5$ Mpc | quasar | $1 \times 10^{45}$ | 1 Mpc |

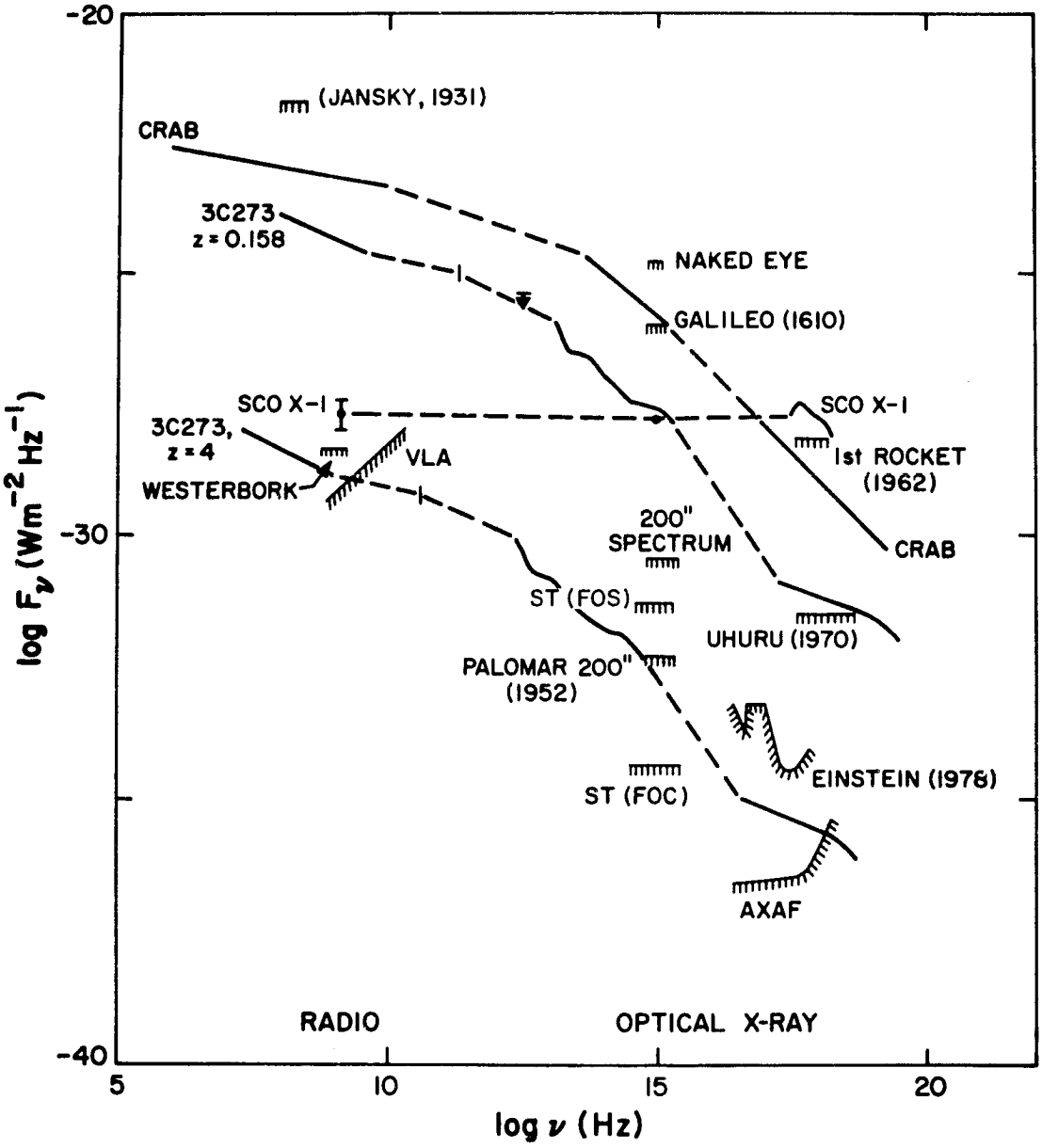


Figure 1.3 - Sensitivity of major astronomical facilities in radio, optical, and X-ray regions of the electromagnetic spectrum as shown at different epochs. The quasar 3Cs73 has been placed at Z of 4 in order to illustrate the detectability of a very distant object.

TABLE 1.2

Observational Capability of the AXAF

1. Point-Like Extragalactic Sources

| Luminosity | Example | Z |
|---|---|---|
| $5 \times 10^{41}$ ergs/s | (Radio Galaxies) | 0.5 |
| $5 \times 10^{43}$ | (Seyfert Galaxies) | 3 |
| $1 \times 10^{45}$ | (QSO's) | 4-10 |

2. Clusters of Galaxies

- Detect to Z of 1-4
- Map structure - temperature and density distribution for nearer members

3. Iron Lines in Clusters

- Detect to $Z \sim 1.5$ for brightest clusters
- Measure temperature and iron distribution for nearer clusters

actic sources that can be seen with exposures of the order of one day. The ability to detect QSO's at redshifts of 4-10 may prove very important in gaining an understanding about when QSO's were created, how they evolve, and what they are. Seyfert galaxies have so far been studied optically to redshifts of $\sim 0.2$. AXAF should be able to detect such sources, and pinpoint them for radio and optical studies out to $Z \sim 3$. Since X-ray Seyferts already have been observed to have a luminosity function ranging from $10^{42}$ to $10^{45}$ ergs $s^{-1}$, a complete study of their properties - particularly at larger distances - may well explain their relation to BL Lac objects, quasars, and other active galaxies. Detailed spectral data may also help to decide between thermal-Compton and synchrotron-Compton models for these sources. By studying the time variations of these active galaxies, we may be able to determine the nature of their energy source, thought by many to be a massive black hole at the core of the nucleus.

AXAF will be able to detect clusters of galaxies to Z of 1 to 4, which may be the range of epochs at which the clusters were formed. Also the greater sensitivity of AXAF will allow detailed mapping and spectroscopy of many X-ray clusters, as well as direct redshift measurements from the iron line feature to redshifts of $\sim 1.5$. Detailed X-ray, optical, and radio studies may help separate the contributions from thermal bremsstrahlung and from inverse Compton scattering for these sources.

Table 1.3 summarizes the basic characteristics of the AXAF. These will be discussed in greater detail in Section 3.

## Table 1.3 AXAF Characteristics

### Summary of Performance Requirements and Parameters of the AXAF

| | |
|---|---|
| X-ray Telescope Assembly (XTA): | 6 nested pairs of Wolter type I grazing incidence mirrors |
| Mirror Assembly | 1.2 meter outer mirror diameter |
| Focal Length | 10 meter (plate scale: 50 μm/arcsec) |
| Angular Resolution (on axis) | 0.5 arcsec goal |
| Spectral Range | 0.1 - 8 keV (1.5 - 120 Å) |
| Encircled Energy (on axis) | 60% in 1 arcsec diameter circle at 2.5 keV |
| | 35% in 1 arcsec diameter circle at 5 keV |
| Effective Collecting Area | 1400 $cm^2$ at 0.5 keV; 1100 $cm^2$ at 2 keV; 200 $cm^2$ at 7 keV |
| Field of View | 1° |

Overall Spacecraft:

| | |
|---|---|
| Attitude Control (reaction wheels and magnetic torquers) | 30 arcsec pointing; stability consistent with 0.5 arcsec *post facto* aspect determination |
| Length | 14 meters |
| Diameter | 4-1/4 meters |
| Weight | 21,000 pounds |

Scientific Instruments (generic types):
- High resolution imaging
- Moderate resolution imaging, high efficiency
- High resolution spectroscopy
- Moderate resolution, high efficiency spectroscopy
- Polarimetry
- Broad band filter spectroscopy
- Monitors

| | |
|---|---|
| Orbit: | |
| Inclination | 28.5 |
| Altitude | 460 km |
| Power (articulated solar arrays): | |
| Average power | 600 - 1200 watts |
| Data Management: | |
| Maximum Acquisition Rate | 1000 kbps |
| Onboard Storage | $10^9$ bits |

## 2.0 SCIENTIFIC OBJECTIVES OF THE AXAF

This section presents the scientific objectives of the AXAF. It is topically organized and reviews present observational status, present theoretical understanding, the nature of outstanding problems, and the contribution that AXAF will make toward the solutions to these problems. A capsule summary of the objectives is given first, followed by a more detailed discussion.

### 2.1 Summary of Scientific Objectives

**Stars:**

Determine the X-ray luminosity function for stars for all spectral types and luminosity classes.

Determine the physical conditions and composition of stellar coronae by measurement of X-ray emission lines.

Study the relation of coronal X-ray emission to the convective zone structure and more generally with the mechanism for the transport of energy from the stellar interior.

Relate coronal emission to stellar age, rotation period, and surface magnetic fields.

Study sun-like cycles, coronal structures, spots and flare activities by observation of short and long term variability.

Make high resolution spectral and polarization measurements of binary X-ray sources to study the accretion disks and magnetospheres surrounding the compact objects.

Detail properties of all stars in specific associations.

**Globular Clusters:**

Make high angular resolution studies (0.5 arcsecond) of globular cluster sources to "weigh" the X-ray sources (low mass binary or massive black hole?) and identify their optical counterparts.

Study the X-ray emission from the general population of stars in the globular clusters.

Determine the luminosity function of globular cluster sources in galaxies of the local group.

Supernova Remnants:

Make spectrally resolved images of extended supernova remnants to determine thermal and non-thermal structure of remnants and distribution of elements.

Determine the evolution of SNR's through study of density, composition, and temperature distribution.

Extend present measurements to high temperatures ($10^8$ °K) to study the hot components of young SNR's and to study Fe XXV and Fe XXVI line complexes.

Study temperatures and macroscopic bulk veolocities through line profile measurements.

Detect SNR's in galaxies of the local group and correlate with galaxy properties.

Study cooling mechanisms for neutron stars produced in SN events.

Study physics of low density shock waves and the heating of ISM.

The Interstellar Medium:

Determine the morphology, dynamical behavior, temperature, density, and composition of the hot component of the interstellar medium.

Study the composition, ionization structure, and morphology of the cool component of the interstellar gas and dust.

Normal Galaxies:

Detect high luminosity stellar ( $\gtrsim 10^{37}$ ergs $sec^{-1}$) sources in galaxies to 20 Mpc. Extend detailed source counts to all galaxies (2500) in Virgo.

Correlate stellar content with galactic morphology and evolution for early- and late-type galaxies.

Study the epoch of formation of young galaxies.

Determine the X-ray luminosity function for all known types of galaxies.

Active Galaxies:

Study luminosity function and evolution for narrow emission line galaxies, Seyfert galaxies, BL Lac objects, N-type galaxies, radio galaxies, and QSO's.

Study the possible evolutionary relations between different types of galaxies.

Extend the study of active galaxies to extremely large distances ($Z = 4\text{-}10$).

Study the energy source and emission processes in active nuclei through time variability, spectroscopy, and polarization measurements.

Clusters of Galaxies:

Study the formation and evolution of clusters of galaxies with extension to $Z = 1\text{-}3$ and with direct determination of Z through Fe line redshift measurement up to $Z \leq 2$.

Study the origin and heating mechanisms for the intracluster medium.

Study the matter content of clusters with particular emphasis on underluminous (in optical) matter.

Study the distribution of temperature and element abundances within individual clusters.

Study interactions of individual galaxies with intra- or intercluster medium.

Cosmological Studies:

Develop new methods for determination of fundamental constants through (a) number counts of clusters of galaxies, (b) combined microwave and

X-ray measurements which yield $H_o$ and $q_o$ directly, and (c) the possibility that binary X-ray sources provide a "standard candle" by which $H_o$ may be independently estimated.

Study the isotropy of the universe using the statistics of deep survey source counts in different directions.

X-ray Background:

Study the nature and cosmological implications of the diffuse X-ray background.

## 2.2 Low Luminosity Galactic Sources

### 2.2.1 Status of Results

Our knowledge of low luminosity galactic X-ray sources has changed drastically over the past few years, particularly so since the flight of the Einstein Observatory. With the aid of hindsight, the early, restricted research goals now seem overly conservative. The crucial fact which occasioned this perceptual revolution was the recognition that low luminosity ($< 10^{35}$ erg $s^{-1}$) X-ray emission is not an exceptional property of restricted categories of stars, but rather is the norm. This state of affairs began to emerge with the detection in rocket and explorer satellite observations of X-rays from a wide variety of stars, such as Algol, Capella, and other RS CVn stars, Sirius, the white dwarf HZ43, various cataclysmic variables, and flare stars. Its broad significance became clear as a result of the Einstein Observatory stellar surveys, which allow a limiting sensitivity $\sim 10^3$ greater than previous stellar observations. Thus, whereas AXAF might have been thought useful for only studying - in far more detail - a relatively small number of "special" types of stars, we now know that stars throughout the H-R diagram fall within the AXAF's observational capability. Emitters include early- and late-type stars

of all luminosity classes, as well as pre-main sequence and other exceptional stars. Because stellar X-ray emission very likely reflects the evolutionary state of the star, highly sensitive stellar X-ray observations join more traditional tools of stellar astronomy in constraining theories of stellar structure and evolution. We are no longer looking simply at exceptional processes (viz. accretion in close compact binary systems), but rather at what is apparently the normal functioning of stellar outer atmospheres, which we apparently do not understand at all. This new view of stellar coronae is a vast surprise, and is a serendipitous result of the great sensitivity improvement over earlier studies allowed by Einstein: the further radical sensitivity improvement expected from AXAF will open additional, new avenues of research which we can now perceive, as well as others whose existence is as yet hidden from us. We should expect to be surprised once more.

### 2.2.2 Types of Investigations

The remarkable enlargement of the horizons delimiting stellar X-ray astronomy should not obscure the fact that exceptional low luminosity X-ray sources may exist, and are deserving of detailed study in their own right. We do not as yet understand the generality (if any) of processes leading to stellar X-ray emission. We therefore distinguish between two types of studies, which are, to a large extent, complementary:

(1) Survey observations: Stellar X-ray astronomy is presently in a state of affairs comparable to that of optical stellar astronomy a century ago. Of the $\sim$ 6000 stars which are now estimated to be observable in X-rays (e.g., in less than $10^4$ sec per observation) by the Einstein Observatory, approximately 5 - 10% will have been looked at during the lifetime of this Observatory. Only roughly half of these observed stars will have low-resolution spectra available; for the remaining half only total fluxes will be available. Given the statistics

of galactic stellar distributions and our present estimates of measuring X-ray luminosities for various types of stars, it is now evident that, by the end of the Einstein mission:

(a) we will have very restricted data for construction of the X-ray equivalent of a "color magnitude" diagram; in many portions of the optical H-R diagram, comparable X-ray data will either not exist of be statistically sparse (Figure 2.1);

(b) we will have fairly complete data for stellar luminosity functions, for several classes of stars, and incomplete samples for others, particularly late-type giants and supergiants (Figure 2.2).

It is therefore presently clear that we will only be able to start stellar (X-ray) spectral classification, and will be restricted to only the crudest correlation studies with other spectral regimes. AXAF has the capability of drastically altering this situation. Assuming an approximately 100-fold increase in limiting sensitivity over Einstein, all the $\sim$ 6000 stars accessible (but not observed) by Einstein can be observed in a relatively short time by AXAF. In addition, the numbers of stars accessible to AXAF is vastly larger, as the available volume for sampling increases roughly by a factor of 1000. In addition, the quality of low-resolution spectral information should be substantially improved; AXAF therefore provides the ideal (and only) means for generating an X-ray "H-R" diagram.

(2) Detailed diagnostic studies: Certain subclasses of stars, (viz. RS CVn, white dwarfs, dwarf novae, etc.) have for some time been recognized as classes of low luminosity X-ray sources. In several of these cases, substantial studies covering a variety of spectral regimes and involving detailed modeling have been carried out in the past; the principal limitation upon the X-ray diagnostic observations have been the relatively low sensitivity of spectrally

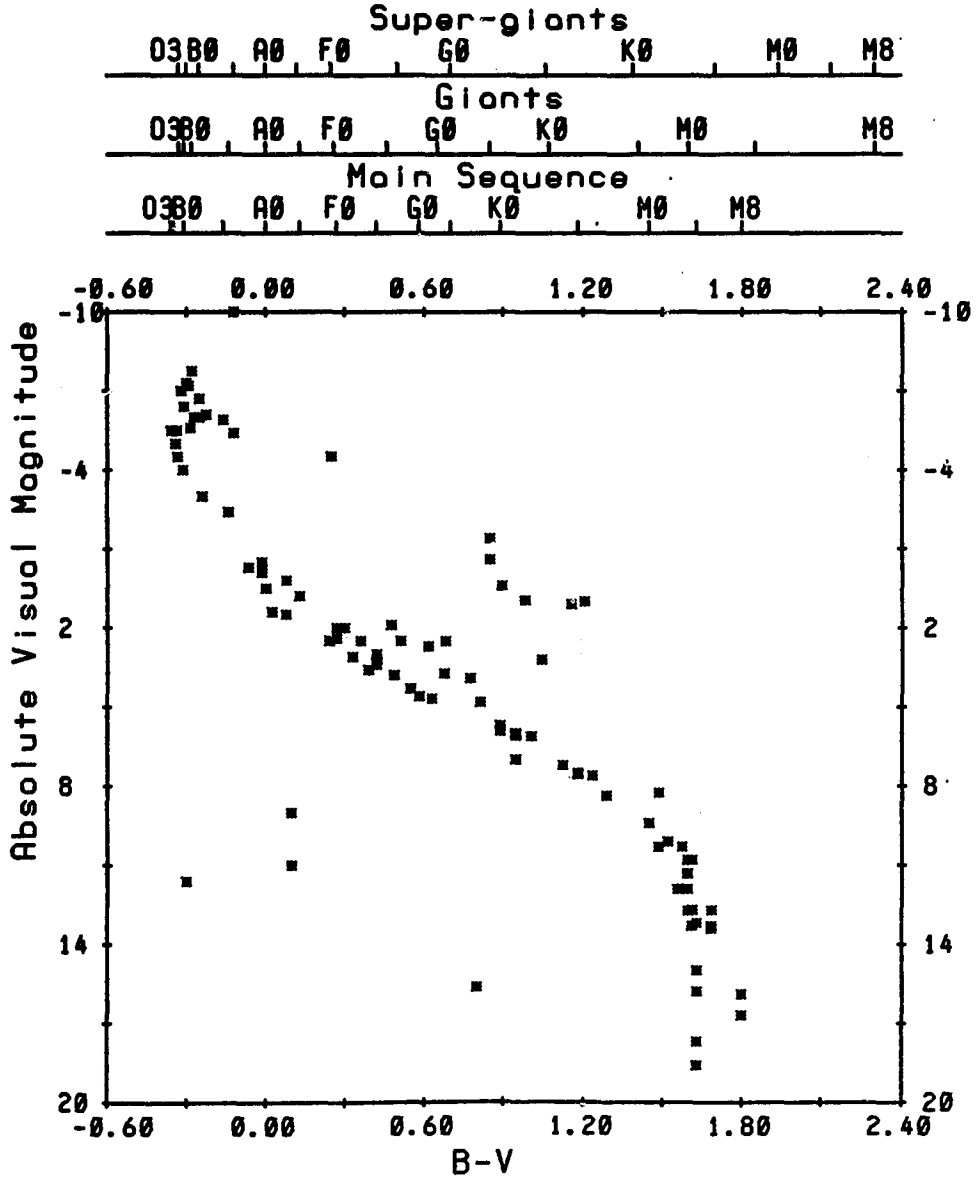


Figure 2.1 - Herzsprung-Russell diagram of stars detected as soft X-ray sources by the Einstein Observatory; the stars shown, for which both spectral type and luminosity class are necessarily known, constitute 1/2 of the total number of stars so far detected as sources in this survey. It is apparent that along the main sequence, contrary to predictions based upon theories of acoustic coronal heating, stars of all spectral types show emission. Along the giant branch, emission has so far been found up to spectral type K; along the supergiant branch, only early-type stars have so far been detected as soft X-ray sources.

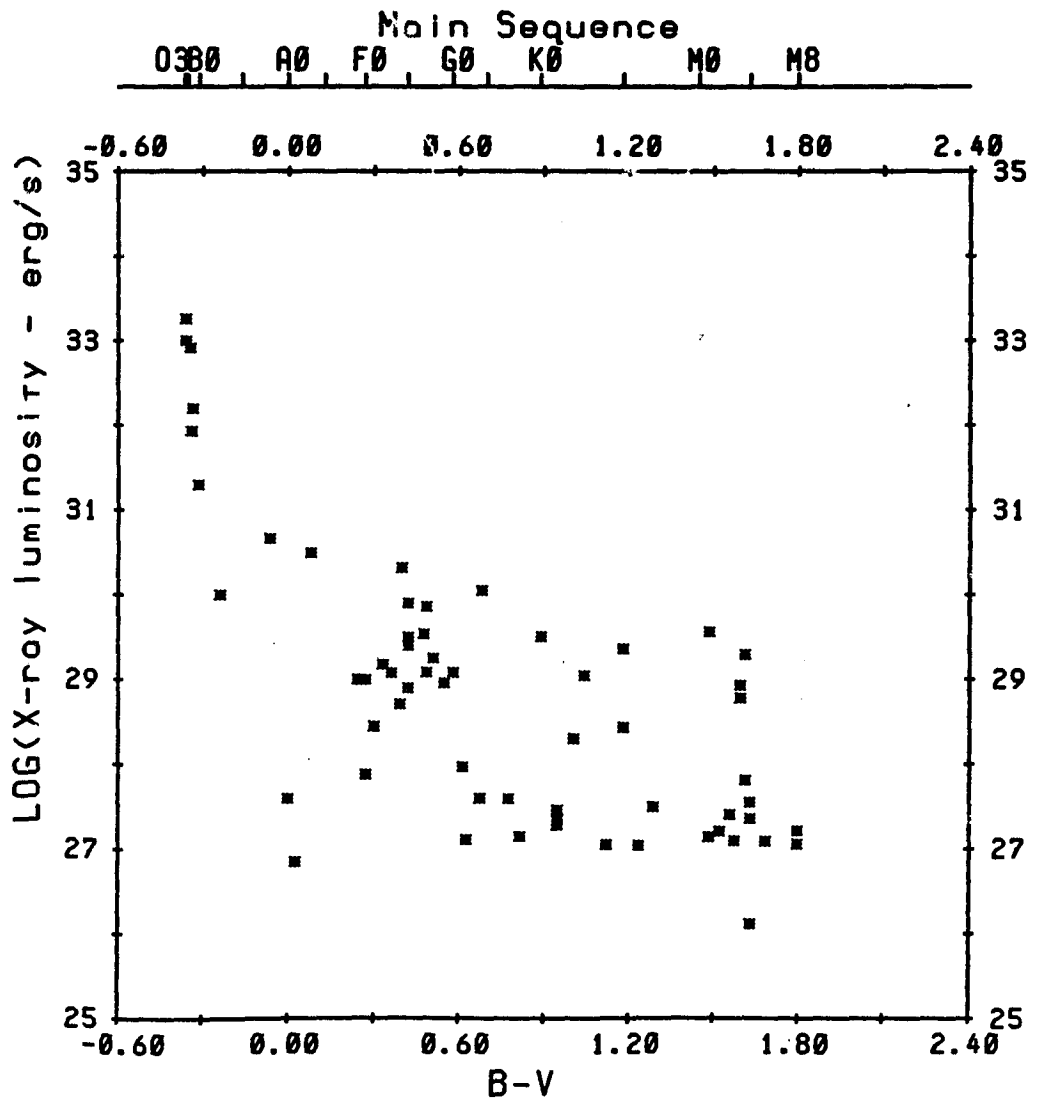


Figure 2.2 - X-ray luminosity of main sequence stars observed as part of the Stellar Survey with the Einstein Observatory. The stars shown are a small aubset of the detected stars for which distance information (parallax) is available. Comparison of the X-ray-to-optical luminosity ratio of this sample of stars with the far larger sample of stars whose distances are not known, shows that the mean of the X-ray luminosity function varies from $10^{33}$ ergs $s^{-1}$ at spectral type 0 to $10^{27}$ ergs $s^{-1}$ at spectral type A, increase to $10^{29}$ ergs $s^{-1}$ at F, drops to $10^{27.3}$ ergs $s^{-1}$ at spectral type G, and remains approximately at this level through spectral types K and M. Significant variations about these means are found in the full data sample, but are particularly striking in the late K to M spectral type region, where an appreciable fraction of the stellar population has X-ray luminosities two orders of magnitude in excess of the mean.

resolved observations with resolution better than that obtainable with gas proportional counters. Thus, the high resolution Einstein spectrometers were limited to observations of only the brightest sources in the observed sample, with the dispersive instruments particularly limited to only the five or so brightest stars. Meaningful atmosphere modeling can therefore be carried out at present for only a small handful of stellar low luminosity sources. Comparative modeling of distinct classes of stars is completely ruled out.

### 2.2.3 Science Objectives

As discussed above, it has only most recently been recognized that X-ray observations from stars are relevant to, and can provide significant constraints for, stellar structure and evolution. Stars in general constitute a class of low luminosity galactic X-ray sources very likely associated with stellar coronae, with X-ray emission characteristic of stars from youth (pre-main sequence) to old age, crossing virtually all spectral type and luminosity class boundaries. Although the conventional picture relating coronal emission to stellar surface turbulence (via acoustic wave generation and dissipation) is inadequate, a connection between coronal formation and the vigor of surface motions seems unavoidable; we simply do not understand the mechanism providing this coupling. Elucidating this connection is one of the principal goals of future stellar X-ray astronomy. The key element is that AXAF will not just perform the necessary tasks better than present instruments, but rather that it alone has the capability to carry out many of the most significant research goals which now confront us.

It is already clear that attributes of stars other than just the extent of surface convective activity must be important in determining the level and character of stellar X-ray emission. The principal additional processes are: stellar rotation, stellar convection, and dynamo processes leading to stellar

surface magnetic fields. None is readily determined so that the X-ray data may provide a unique tool for studying these stellar attributes and their variation as stars evolve. Stellar X-ray astronomy thus has as its goals: (1) Determination of the X-ray luminosity function, e.g., the mean emission level and the range of statistical spread about this mean, for stars of distinct spectral type and luminosity class. These data are necessary for studying:

(a) the variation of coronal emission with changing convective zone structure and (using statistical spread) extent of solar-like activity cycles;

(b) correlation of coronal emission levels with stellar age, rotation period, and surface magnetic fields (especially in Ap, Am, and normal A stars);

(c) contribution of stars (particularly of late-type dwarfs) to diffuse emission in star clusters, our galaxy, and other galaxies and galaxy clusters. Given present estimates of AXAF's limiting sensitivity, and assuming the provisional mean X-ray luminosities derived for late M dwarfs from Einstein data, AXAF will be able to probe for dM stars down to V $\sim$ 22 mag. The X-ray observations therefore also provide an observational tool for studying the space distribution of such stars comparable in power to the most sensitive ground-base optical telescopes. X-ray data therefore can play significant roles in determining the galactic mass distribution in Z (height above the galactic plane). In addition, detailed high sensitivity spectral data can be used, together with optical and ultraviolet observations to study the detailed structure of stellar extended atmospheres, and to understand the mechanisms responsible for coronal heating and stellar mass loss. Presently available data allow such modeling for only a few bright stars; we have at present no means for comparative studies of coronal atmospheres (other than in terms of simple integral measures, such as total luminosity). AXAF is uniquely able to

gather the necessary data.

(2) Determination of variability in X-ray emission on long and short ($\leq$ 5000 second) time scales. Examples of research areas to which these data are relevant are:

(a) placing limits upon the spatial inhomogeneity of coronal emission as a function of stellar type (from short-term variability data);

(b) measuring stellar rotation. For example, for main-sequence stars later than $\sim$ F5, surface rotation speeds are too low to be measurable by direct spectroscopic means, so that the observation of periodicity in the X-ray light curve (due to the existence of coronal emission regions whose lifetime is long when compared to the rotation period) remains as the only present tool for determining rotation rates for such stars (other than "spot" stars). Similar considerations (related to the masking effects of surface "macro-turbulence") apply to certain rapid rotators as well.

(c) verifying the stellar "spot" interpretation of periodic stellar optical light variations, which is based upon the hypothesis that strong stellar magnetic fields locally inhibit convective activity; the target class of such stars is the late dwarf emission line stars. Again, AXAF will contribute uniquely to these research areas because of its great sensitivity.

## 2.3 The Massive X-ray Binaries

### 2.3.1 Previous Results

The first compact X-ray sources shown to be binaries were the pulsing sources Her X-1 and Cen X-3 whose binary natures were inferred from the observations by the Uhuru satellite of periodic X-ray eclipses correlated with sinusoidal Doppler shifts in the pulse period (Figure 2.3). Many more X-ray sources have since been shown to be binaries, and almost all the pulsing

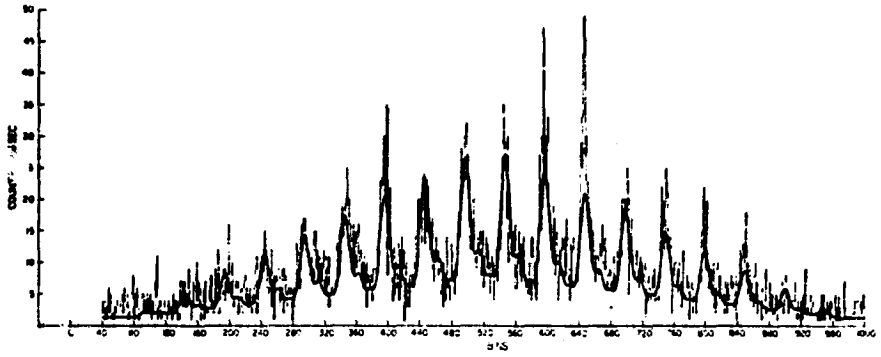

Counts accumulated in 0.096-s bins from Cen X-3 during a 100-s pass on 1971, 7 May. The functional fit obtained by minimizing $\chi^2$ is shown as the heavier curve.

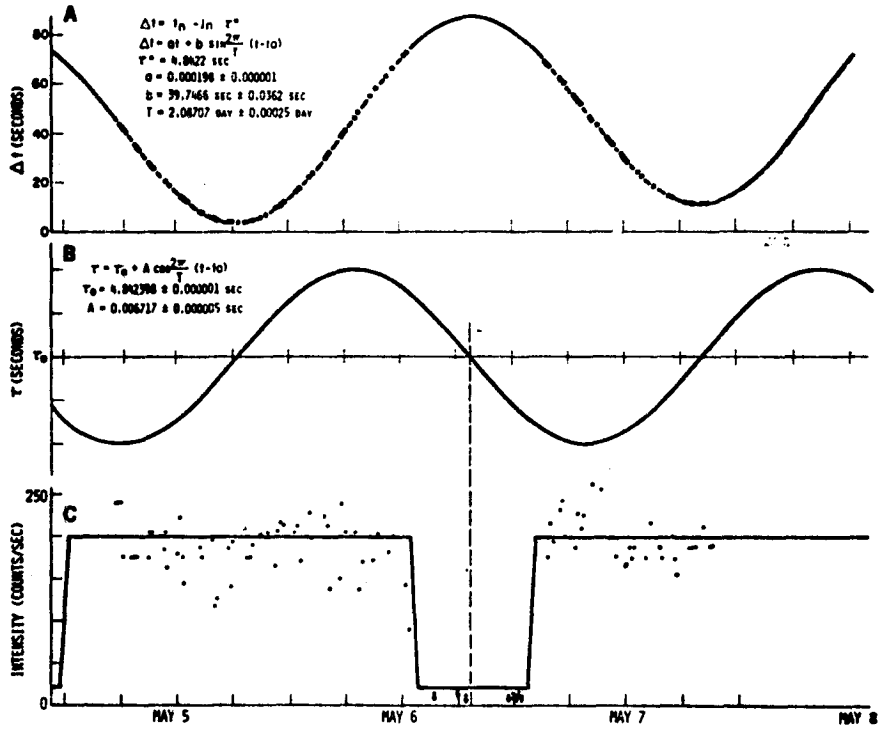


**Figure 2.3** - [Bottom] The intensity observed from Cen X-3 (dots) and the light curve predictions for 1971, 5-7 May. [Top] The difference $\Delta t$ between the time of occurrence of a pulse and the time predicted for a constant period, plotted as a function of time. A best fit function and the values of the parameters are given. [Center] The dependence of the pulsation period $\tau$ on time as derived from the best fit phase function. Note the coincidence of the null points of the period with the centers of the high and low intensity states.

sources known at this time are either known or strongly suspected to be binaries. Indeed, all bright ($L_X = 10^{36} - 10^{38}$ ergs $s^{-1}$) compact X-ray sources of stellar mass (except those radio pulsars which also emit X-rays, like the Crab pulsar) could be binaries, a possibility which make the study of binary X-ray sources one of the most interesting and important topics in X-ray astronomy.

A generally accepted model for binary X-ray sources has emerged, in which each source is powered by accretion of matter by a compact object, i.e., a neutron star, a degenerate dwarf, or a black hole (Figure 2.4). This matter is supplied by the normal companion in one of more of the following ways: Roche lobe overflow, conventional stellar wind, or mass loss produced by X-ray heating of its outer layers. Each unit of accreted mass releases a large amount of gravitational energy as it falls into the deep potential well of the compact object, much of this energy being radiated as X-rays. The compact objects in pulsing X-ray sources are believed to be strongly magnetic neutron stars, the magnetic field channeling the accretion flow towards the magnetic poles and the rotation of the neutron star producing the pulses. The mechanism is capable of producing a remarkable variety of pulse forms as shown by the summary of data in Figure 2.5. On the other hand, black holes may be the compact objects in some sources like Cyg X-1, which do not pulse periodically, but show large variations on many different time scales.

Previous studies of binary X-ray sources divide into two main categories: temporal and spectral. A rich variety of phenomena has been discovered from the time variability studies. The pulse periods of pulsing sources exhibit three types of variability which give extremely valuable information about neutron stars and accretion processes.

First, the pulse period undergoes periodic Doppler shift due to binary

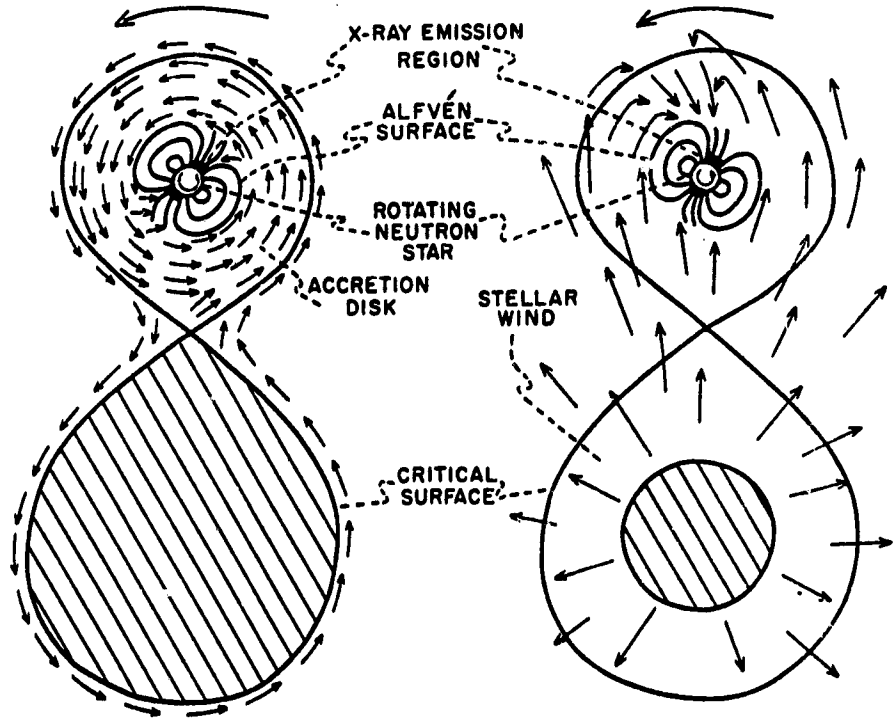


**Figure 2.4 - Two regimes of mass-transfer and accretion in binary systems. The accreting object is taken to be a neutron star, but that choice is not an absolute requirement of the model (Blumenthal and Tucker).**

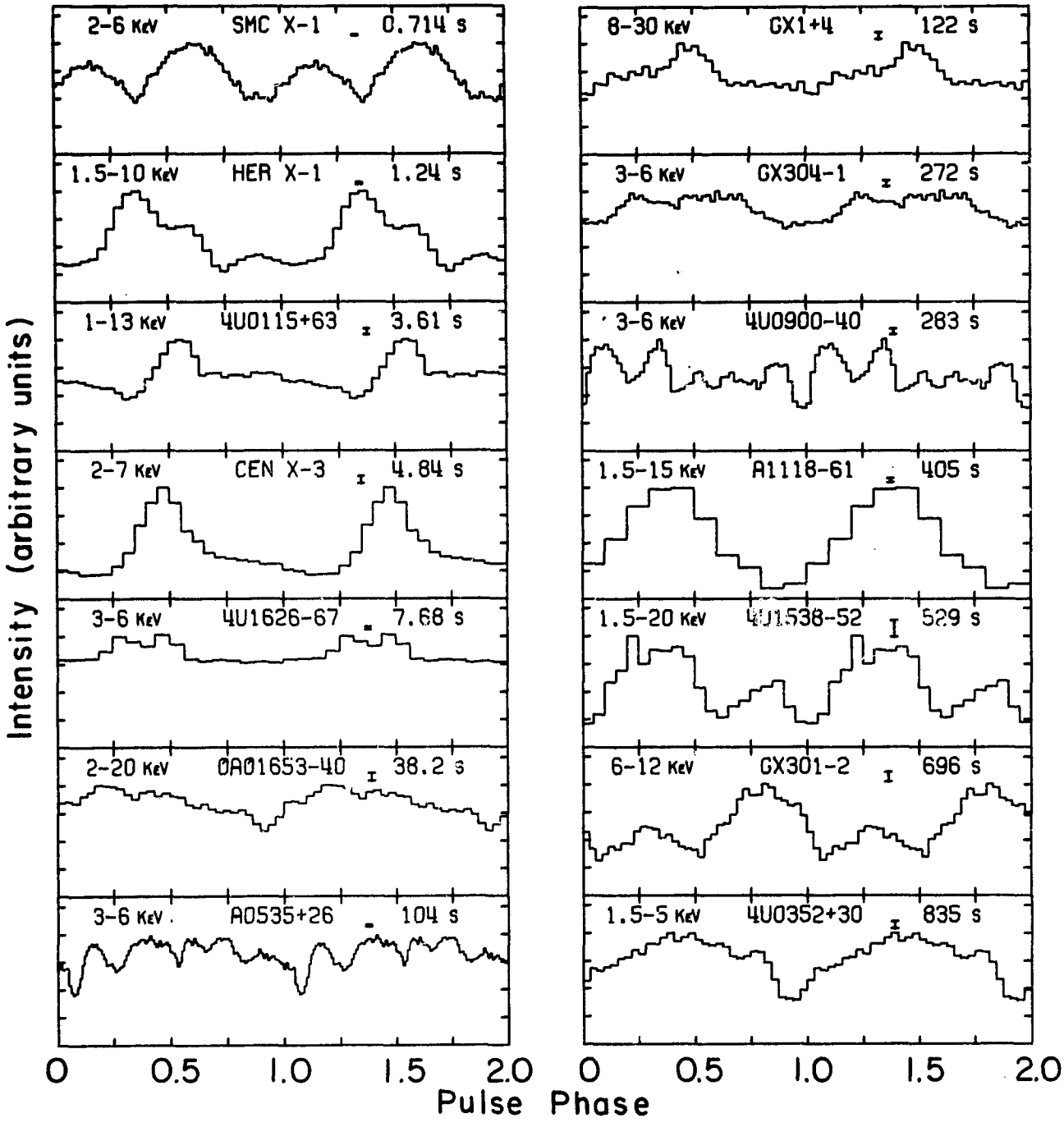


Figure 2.5 - The compact objects in pulsing X-ray sources are believed to be strongly magnetic neutron stars, the magnetic field channeling the accretion flow towards the magnetic poles and the rotation of the neutron star producing the pulses. The mechanism is capable of producing a remarkable variety of pulse forms.

orbital motion. This variation gives information on the neutron star mass when supplemented by other data on the binary orbit, i.e., the projected orbital velocity of the optical companion. Figure 2.6 summarizes the mass limits derived from data on five X-ray pulsars and the binary radio pulsar.

Second, the pulse period shows a steady long-term decrease which gives information about the accretion flow and the structure of the neutron star. The combined effect of the angular momentum added to the star by accreting matter and the magnetic viscous torques is to speed up the rotation of the neutron star. The amount of angular momentum added per unit mass of accreted matter is larger for the case of accretion from a disk, such as is formed when the companion loses mass by Roche overflow, than it is in the case of accretion from interception of a stellar wind. The rate of spin up depends upon the rate of addition of angular mementum and inversely on the moment of inertia of the accreting body. Figure 2.7 shows the agreement between current observations and the theoretical relation between the spin up rate, the pulse period, and the X-ray luminosity for neutron stars accreting from disks.

Third, the pulse period shows short-term fluctuations which can be caused by fluctuations in the external torque acting on the neutron star and/or internal torque fluctuations due to processes inside the neutron star. Analysis of the relation between these fluctuations and the accompanying X-ray luminosity fluctuations gives valuable clues to the internal structure of the star, for example, the coupling time between the solid crust and the superfluid core.

For non-pulsing sources like Cyg X-1, auto-correlation analysis of the timing data extracts the basic scales of time variability, which in turn, can give information about accretion flows (e.g., disks) and X-ray production processes around black holes.

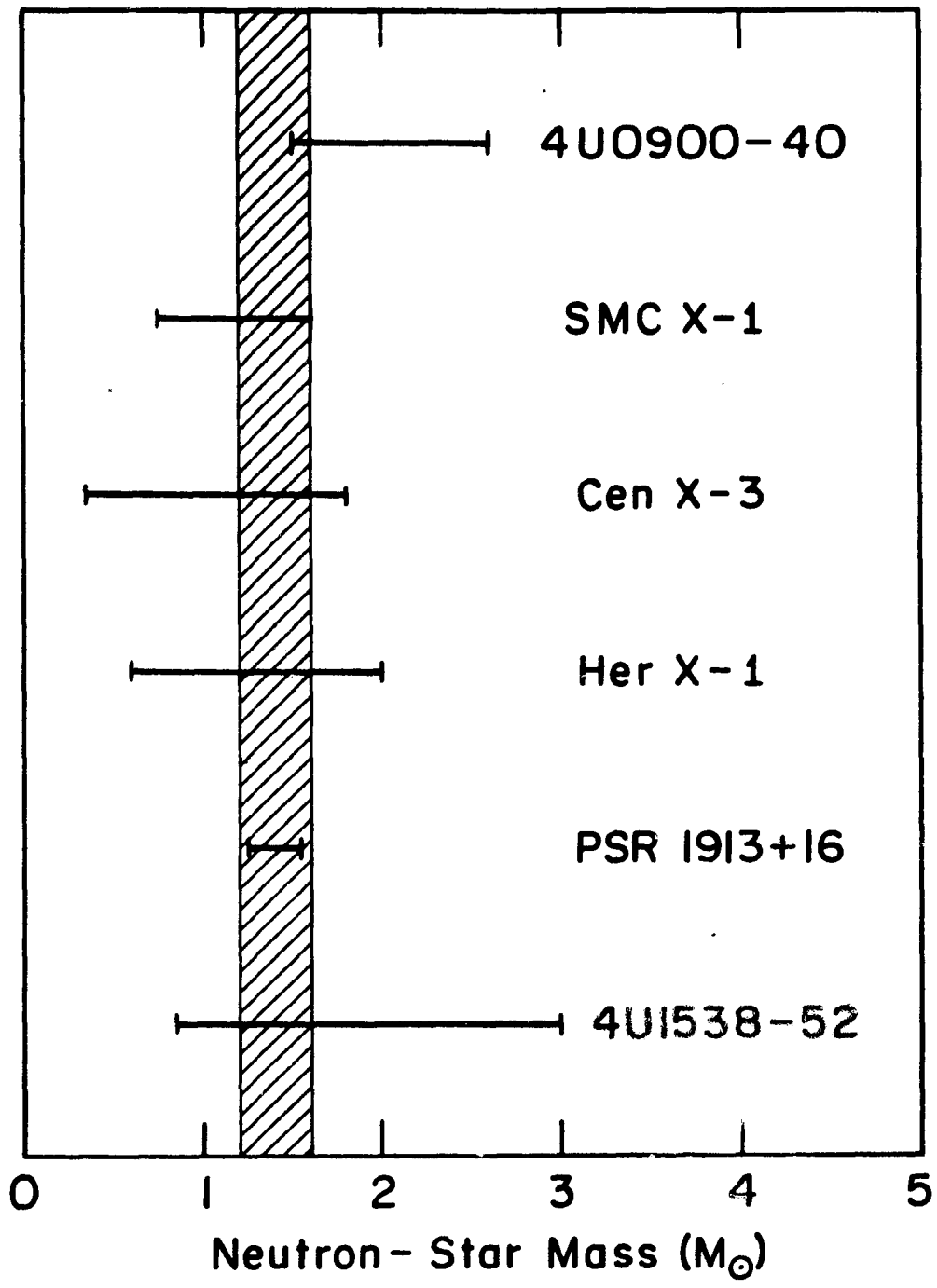


Figure 2.6 - Summary of the mass limits derived from data on five X-ray pulsars and the binary radio pulsar.

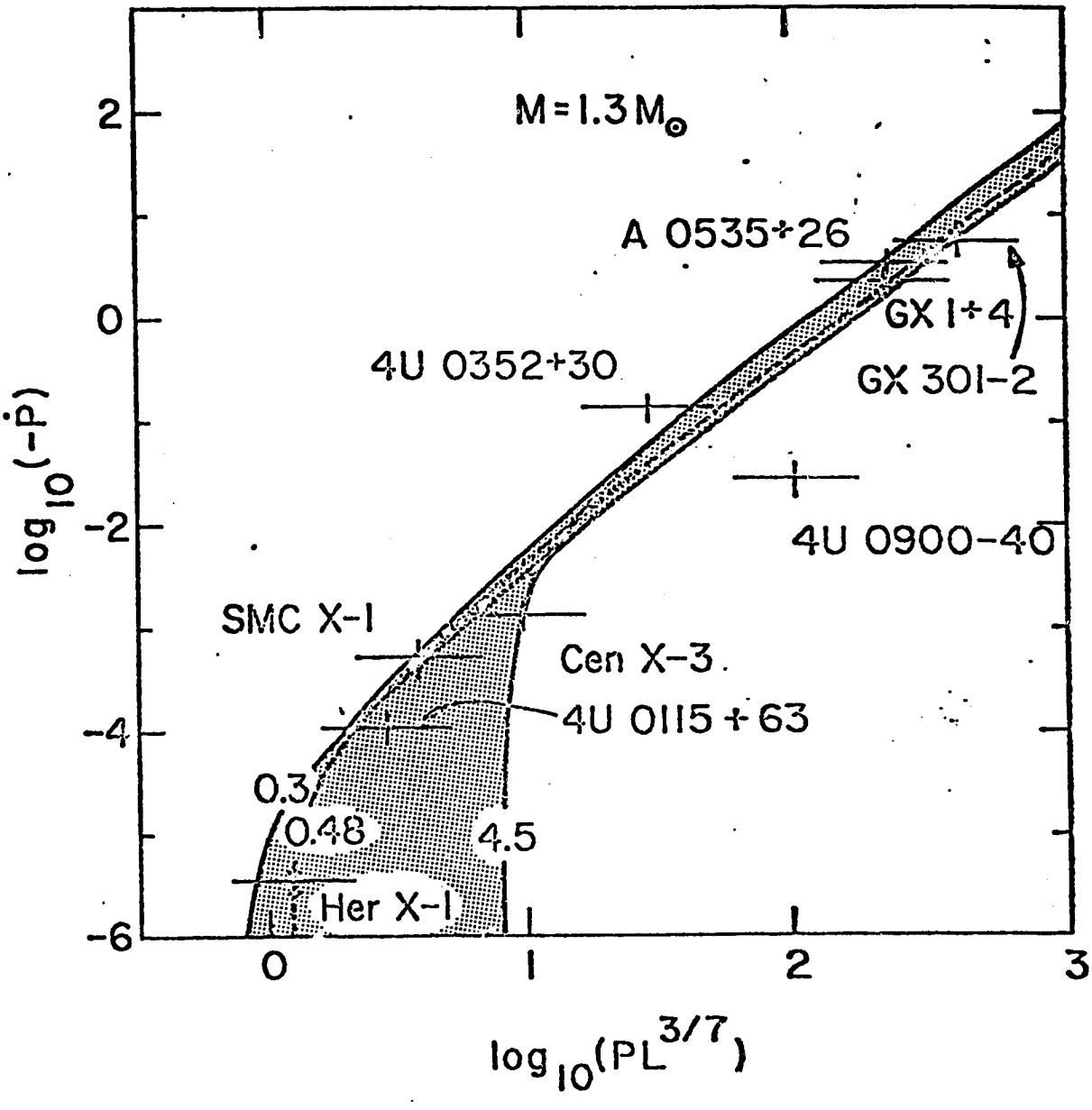


**Figure 2.7 - Observational and theoretical relations between the spin-up rate, the pulse period, and the X-ray luminosity for neutron stars accreting from disks. (F.K. Lamb).**

Spectral studies of binary X-ray sources have also given information about accretion flows and neutron star properties. The continuum spectra have usually been described by exponentials with absorption at low energies. In general the pulsing sources have relatively hard spectra (effective temperatures > 10 keV), compared to the non-pulsing sources. In addition, Her X-1 emits a strong flux of soft X-rays which is believed to be produced when the hard X-rays illuminate a shell of matter surrounding the companion star.

Detection of fluorescent iron lines in these sources has provided us with a tool for studying the density, temperature, and ionization state of the matter in those regions of the accretion flow which produce the lines. These iron lines often appear considerably broadened, apparently as the result of high velocity bulk motions. Evidence of features attributable to cyclotron absorption of X-rays in the energy range above 20 keV has been found in the spectra of both Her X-1 and 4U0155+63, and this implies field strengths of the order of $10^{12}$ gauss in the region of X-ray production.

Although the massive X-ray binaries are in many respects the best understood cosmic X-ray sources, there remain many unresolved questions concerning these sources and the physical processes that go on in them. One important set of questions has to do with the origin and evolution of binary X-ray sources, and where they fit into stellar and galactic evolution. Among the questions one can address with a larger and more complete sample of binary X-ray sources, both from our galaxy and also from other nearby galaxies, are: (1) Can the massive binary X-ray sources be divided into distinct classes, and if so, what are the properties of each class? (2) Following the onset of X-ray emission, how do binary X-ray sources evolve? (3) Precisely which stellar systems evolve into binary X-ray sources, and how does the evolution proceed in detail? (4) What are the populations and distributions of binary

X-ray sources in our own and similar galaxies? (5) How do the populations and distributions of binary X-ray sources vary with type of galaxy, and what does this imply for the galaxy formation and evolution?

### 2.3.2 How AXAF Can Contribute

Many of the observations required for the detailed study of X-ray binaries will require specialized instrumentation such as planned for the temporal X-ray explorer. However, AXAF with its high angular resolution will be able to easily detect and resolve individual X-ray sources in the nearby galaxies. Whole populations of objects can be studied almost simultaneously as has been demonstrated by the Einstein Observatory images of M31. A large fraction of the sources found in M31 ($\sim$ 80) are undoubtedly binary X-ray sources. Thus, one will be able to determine populations and distributions of the X-ray binaries.

Since such measurements will allow one to accurately measure the X-ray luminosity, a useful set of "H-R" diagrams will be determined for these sources. These measurements, which can only be accomplished by the AXAF, will allow one to study the evolution of X-ray sources and compare populations in different galaxies to study the formation of the binary systems and will provide a further tool in the study of evolution of galaxies.

The more refined spectra which can be obtained with both dispersive and non-dispersive instruments on the AXAF will be able to significantly constrain models of X-ray emission from accretion disks around black holes and magnetic neutron stars. These instruments may provide observation of cyclotron features which then measure the neutron star magnetic field strength. The energy range of the AXAF (0.1 to 8 keV) would allow magnetic field strengths in the range of $10^{10}$ to $10^{12}$ gauss to be measured. Observations of X-ray lines (e.g., Fe) will provide information on accretion flows, and in general,

physical processes in high-temperature plasmas. Studies of spectral changes as a function of pulse phase will be used to constrain the geometry of the emission zone on and near the surface of a neutron star. Considering the long life time of the observatory, it will be possible to study spectral changes as a function of orbital phase for a large sample of these systems and thus supply constraints to the distribution of matter within.

The good timing available to all the instruments of high quantum efficiency together with the high signal-to-noise ratio provided by the imaging will allow studies of luminosity-period correlations in the stronger pulsing sources. Such observations are a probe for the understanding of accretion torques, and of the properties of the dense matter comprising the neutron star. Observation and refinement of the shot-noise parameters of Cyg X-1 and other similar sources should provide both impetus to theory and observational constraints on the nature of the physical processes in the vicinity of a black hole.

Finally, polarization measurements of the brighter binary sources which currently are only planned with the AXAF will provide yet another constraint on models of X-ray emission from accretion disks around black holes, from magnetized neutron stars and degenerate dwarfs.

## 2.4 Globular Clusters

### 2.4.1 Context of the Globular Cluster X-ray Source Problem

The study of X-ray sources in globular star clusters has received considerable attention because of its bearing on fundamental problems of stellar evolution and cluster dynamics. The globular clusters are self-gravitating, spherically symmetric assemblages of stars which were born during the epoch of galaxy formation some $10^{10}$ years ago. Containing typically $10^5$ to $10^6$ stars each, the globular clusters are distributed within a spherical halo

about the center of the galaxy. Because of their great age, all their stars with original masses greater than $\sim 0.8\ M_{\odot}$ have completed their nuclear burning lives and collapsed to become white dwarfs, neutron stars or, possibly, black holes. In principle, the latter two kinds of otherwise invisible objects would become high luminosity ($L_x > 10^3\ L_{\odot}$) X-ray sources if they were supplied with material to activate the accretion mechanism known to be responsible for X-ray generation in the heavy mass-transfer X-ray binaries found in the regions of active star formation within the spiral arms. Such binaries, however, are necessarily shortlived, and certainly cannot exist in globular clusters at the present epoch. Moreover, the incidence of binaries in globular clusters is apparently much lower than in the galaxy as a whole. Thus, the discovery of non-pulsing, but variable and therefore compact, high luminosity X-ray sources in five globular clusters was a major surprise from the observations made by Uhuru and the OSO-7 explorer satellites. Moreover, the occurence frequency of these sources among the stars in globular clusters was found to be about one hundred times greater than that of high luminosity X-ray sources among the stars of the whole galaxy. One had to conclude that certain conditions pecular to globular clusters specially favor the formation of high luminosity accretion-powered X-ray sources.

Two hypotheses were put forward to explain the cluster sources. One was that they are old neutron stars which have captured their own supplies of accretion material in the form of nuclear burning companions. Any capture process would obviously be favored by the high star densities that are unique to globular clusters. And the captured companions, being of the low mass typical of the nuclear-burning cluster stars, could last as suppliers of accretion material for times comparable to the age of the clusters themselves.

The other hypothesis was that the sources are massive black holes formed

in the collapse of the cores of centrally condensed clusters. Under this hypothesis the material for accretion is the debris given off as stellar winds in the normal evolution of the other cluster stars. The gravitational wells of the centrally condensed clusters are deep enough to retain some of this debris and feed it to a massive black hole. The fact that the clusters containing X-ray sources are, with one remarkable exception, among the most centrally concentrated of all the clusters is evidently consistent with either hypothesis.

### 2.4.2 Status of the Problem

(1) Pre-Einstein Results. A major development in the problem of the globular cluster sources was the discovery by the ANS and SAS-3 satellites that most and perhaps all of the cluster sources emit, in addition to persistent but variable X-ray fluxes, giant bursts of X-rays in which the luminosity rises in $\lesssim$ 1 second to a peak value near the Eddington limit for a star of 1 or 2 $M_\odot$. The bursts decay over 10 to 100 seconds with changing spectra characteristic of black bodies cooling from temperatures near 30 million degrees. In a given source such bursts may recur at intervals ranging from one to several tens of hours. SAS-3 added to the list of globular cluster sources one more which turned out also to be a burster. But burst sources are not confined to globular clusters. They are also found in the galactic disk outside of globular clusters. Some of these latter "bursters" have been identified with faint blue optical counterparts whose optical luminosities are primarily the result of X-ray heating of gas very near to the sources.

Here again two major hypotheses, one based on neutron stars and the other on black holes, have been advanced to explain the burst phenomena. Detailed numerical calculations have demonstrated that material accumulated on the surface of a non-magnetic neutron star under conditions of accretion that can

occur in a mass transfer binary will undergo explosive thermonuclear burning which heats the surface suddenly to X-ray incandescence. The predicted properties of the resulting burst of X-rays closely resemble the properties of the observed bursts. An alternative model attributes the bursts to instabilities in the accretion flow of material into a black hole.

The occurrence of burst sources outside of globular clusters where there is no adequate supply of accretion material for single black holes makes it unlikely that the phenomenologically similar burst sources inside globular clusters are single black holes fed from gas clouds trapped in the cores. Moreover, the quantitative successes of the thermonuclear flash model of bursts evidently lends strong support to the capture binary idea. And finally, the recent discovery by X-ray and optical observations that 4U1626-67, a seven-second X-ray pulsar, is a low mass binary with a companion to the presumed accreting neutron star of only $\sim 0.1\ M_{\odot}$, demonstrates that such systems actually do exist and can emit high luminosities of X-rays.

Nevertheless, a critical test of the nature of the globular cluster sources is clearly needed. Such a test is made possible by the fact that an object in the core of a dynamically relaxed globular cluster is constrained in its motion by the deep gravitational well of the cluster. A statistical mechanical analysis leads to the conclusion that the expectation value of the radial distance of an object of mass $M_x$ from the cluster center is $R_x = 0.9\ r_c\ (M_*/M_x)^2$ where $M_*$ is the average mass of the cluster stars and $r_c$ is the radius of the cluster core, typically 6 to 10 arcseconds. Thus a low mass binary, say $M_x \sim 3M_*$ is likely to be found at $R_x \gtrsim 0.1\ r_c$ or $\sim 1$ arcsec for typically centrally condensed clusters. On the other hand, a massive black hole with $M > 10$ would almost never be found at a measurable separation from the gravitational center. Much interest has therefore focussed on

measurements of the positions of the cluster sources relative to the optical centers which are presumably also the gravitational centers.

The modulation collimator detectors on the SAS-3 satellite measured the positions of five globular cluster sources with 90% error circle radii in the range from 20 to 30 arcsec. The results demonstrated that the X-ray sources are certainly more concentrated toward the cluster centers than the visible stars. A likelihood analysis of the positional data showed that if the sources all have the same mass, then that mass almost certainly exceeds twice the average mass of the visible cluster stars. However, the error radii of the measured positions were larger than the displacements of the measured positions from the optical centers so that the data did not rule out the possibility that the sources were in fact at the exact centers as would be expected for massive black holes.

(2) Preliminary Einstein Results. A systematic search of other globular clusters by the Einstein Observatory has so far revealed the presence of sources in two or more clusters, bringing the total to 8. The accuracy of the preliminary positions measured for these sources is of the order of 1 arcsec, and in several cases the measured positions are substantially more than 1 arcsec from the center. A likelihood analysis confirms that if the masses are all the same, then that common mass is certainly greater than the average mass of cluster stars. However, with these new data the likelihood function falls off significantly above $M_x = 5\ M_*$, providing strong and direct evidence that the sources are not massive black holes.

Another important result of the Einstein search for additional high luminosity sources in globular clusters is the confirmation of earlier indications that the luminosity function of these sources is cut off below $\sim 3 \times 10^{35}$ erg $s^{-1}$. A question currently under investigation is whether or not there exists

a class of weak sources consisting, perhaps, of white dwarfs in capture binary systems which may resemble the cataclysmic variables found in the galactic disk. Some such systems are known to emit X-rays with luminosities of the order of $10^{33}$ erg $s^{-1}$ and would be detectable if they were in one of the nearest clusters like 47 Tuc, the site of one of the new high-luminosity sources detected in the Einstein observations. Even the Einstein sensitivity is insufficient, however, to extend that search to substantially more distant clusters or fainter sources.

### 2.4.3 Future Work on Globular Clusters with AXAF

The improvement in positional accuracy that would be achieved by AXAF offers the prospect of greatly sharpening the conclusions that can be drawn from a statistical analysis of the radial displacement. One conceivable result could be that the assumption of a common mass is inconsistent with the distribution of observed displacements, e.g., if several sources were found to be within 0.05 $r_c$ of their centers, and the rest were outside of say, 0.5 $r_c$. One might then be led to conclude that some cluster sources are very heavy and are probably heavy black holes, and some are light and something else.

Another major advance in cluster research that AXAF would achieve is the study of the distributions of low-luminosity X-ray sources such as cataclysmic variable type systems and the main sequence M dwarfs which are now known to be remarkably luminous in X-ray with $L_x \sim 0.1\ L_{opt}$. Since these latter stars are very numerous in globular clusters, their combined diffuse emission should be easily detectable and allow important new studies to be conducted of the faint end of the stellar luminosity function for globular clusters. High sensitivity and spatially resolved observations of diffuse X-ray emission from late-type stars in globular clusters would allow the density profile of

these faint stars (not detectable optically against the bright cluster giants) to be measured for the first time. This could provide an important new constraint on the stellar mass function in globular clusters as well as dynamical models of cluster evolution.

Finally, the spectroscopy possible with AXAF would permit sensitive searches for iron line emission. If found (and there is some evidence in HEAO-1 data), then temporal studies of line profiles would be a new and sensitive probe for the accretion wakes expected if the X-ray sources are indeed compact binaries.

## 2.5 Supernova Remnants

It is widely believed that massive stars end their lives as supernovae and that nuclear fusion in the final pre-explosive stages of such stars produce the heavy elements which are then ejected into the interstellar medium (ISM). It is also conjectured that these explosions provide a substantial, perhaps dominant, heat source for the ISM. Since most of the energy in supernova explosions emerges as fast moving ejecta and a high velocity blast wave, interaction with the ISM leads to an expanding remnant of multi-million degree gas. X-ray images and spectra now offer the most direct means of studying such SNR's, providing a detailed and quantitative check on the above beliefs.

The current conception of how a supernova remnant evolves can be summarized in three phases:

(1) Free Expansion Phase. In this phase, the ejected mass exceeds the mass swept up by the blast wave. Interstellar matter entering the shock will be heated to high temperatures ( $\sim 10^8$ °K) and compressed into a thin shell. As the ejecta are decelerated by the interstellar medium, a shock will form on the inside of this shell. In co-ordinates fixed with respect to the

expanding shell this internal shock will propagate inwards and, hence, is often referred to as the "reverse shock wave". SNR models predict that various shells of differing chemical composition in the pre-eruptive star are preserved in the explosion and that when heated by the reverse shock will radiate characteristic X-ray lines.

(2) Adiabatic Phase. In this phase, the swept up mass exceeds the ejected mass but energy is conserved because radiative losses are small compared to the initial explosion energy. Under these circumstances the Sedov similarity solution is assumed to apply for the motion of a blast wave in a medium. Most, if not all, individual SNR's are believed to be in this phase.

(3) Radiative Phase. When energy losses by radiation (mainly in the soft X-ray and UV band) become significant, the pressure behind the shock drops and the shock will decelerate, thereby forming a dense shell of the swept up matter. The SNR shell has thus entered the momentum conserving phase. At this point the SNR may merge with the interstellar medium and "disappear". However, studies of the very late stages of the evolution of SNR's which happen to occur near each other indicate that interconnecting "tunnels" of hot gas may form which could pervade much of the galaxy. The study of features in the diffuse soft X-ray background should establish the reality of this model.

More than 20 remnants of supernova explosions have now been detected in X-rays, including several in the Large Magellanic Cloud. Einstein studies have produced detailed images of many of these with a spatial resolution of 0.1 to 0.01 of the extent of each remnant. This allows a detailed comparison to be made of the X-ray, optical, and radio structure of individual remnants and should clarify the reality of the blast wave model. In addition, improved spectral data from the Einstein solid state spectrometer have allowed

more precise thermal models to be derived for individual remnants. To illustrate the current status of this work, its potential for understanding supernova remnants - and its limitations - three young SNR's will be discussed in more detail, viz. SN1006, the Crab nebula, and Cas A.

(1) SN1006. Figure 2.8 shows the Einstein Imaging Proportional Counter (IPC) image of SN1006 at 0.2 - 4 keV, above a radio contour map.

A gross comparison shows the brightest features of the radio and X-ray maps (on the NE and SW limbs) to coincide, while van den Bergh's optical filament lies just beyond the X-ray extent in the NW gradient. Apparently the X-rays, radio shell, and optical filament delineate the present position of the expanding SN blast wave. Further insight is provided by dividing the X-ray data into its "soft" and "hard" components ( $\sim$ 0.2 - 1.25 and 1.25 - 4 keV) (Figure 2.9). The appearance of SN1006 is now quite different with the hard (or hot) component (kT $\sim$ 1 keV) concentrated at the NE and, to a lesser degree, the SW limbs and the soft (or cooler) component (kT $\sim$ 0.15 keV) filling in the volume of the remnant. Qualitatively, the X-ray appearance of this young supernova remnant is in agreement with current theory for SNR evolution, in which the limb brightening is explained by a thin shell of swept up interstellar gas heated by the SN blast wave, while the cooler interior results from heating by a lower velocity "reverse shock". The analysis also provides an estimate of the temperature and density distribution of material in the remnant, together with its mass. However, substantial errors in such a quantitative treatment are likely, because of assumptions that have to be made, in particular on the degree of equilibrium and the element abundances in different parts of the remnant. These limitations arise directly from the poor spectral resolution of the imaging instruments on Einstein, while the spectrometers have inadequate spatial resolution to map a remnant of this size.

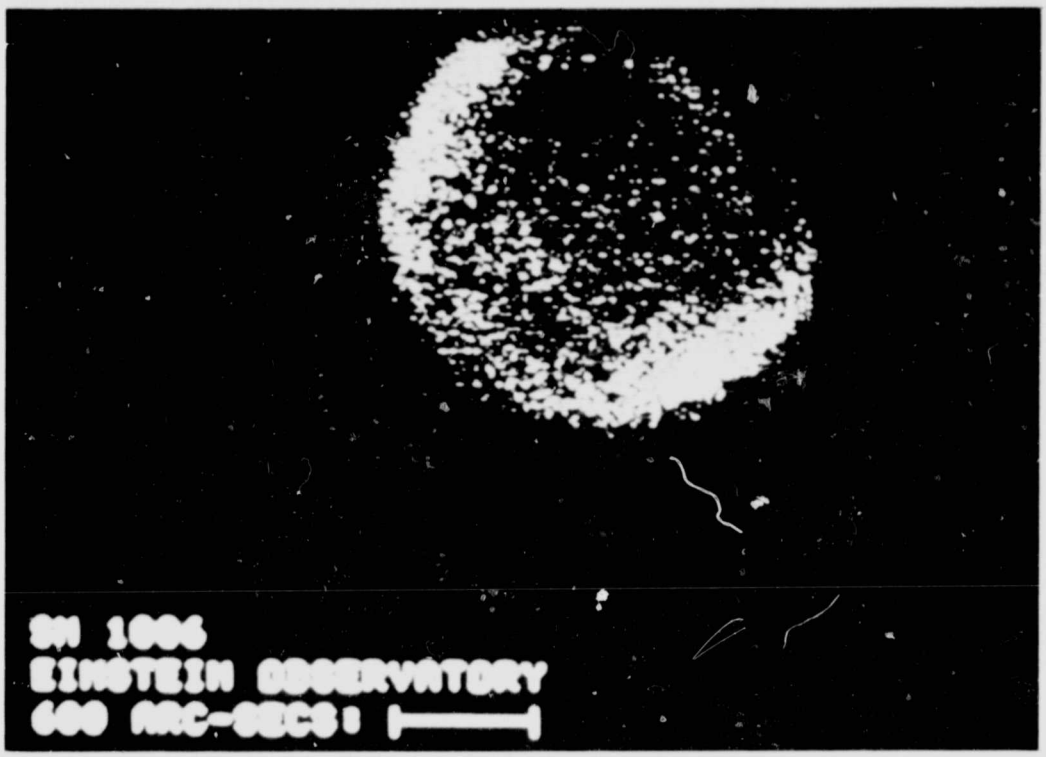


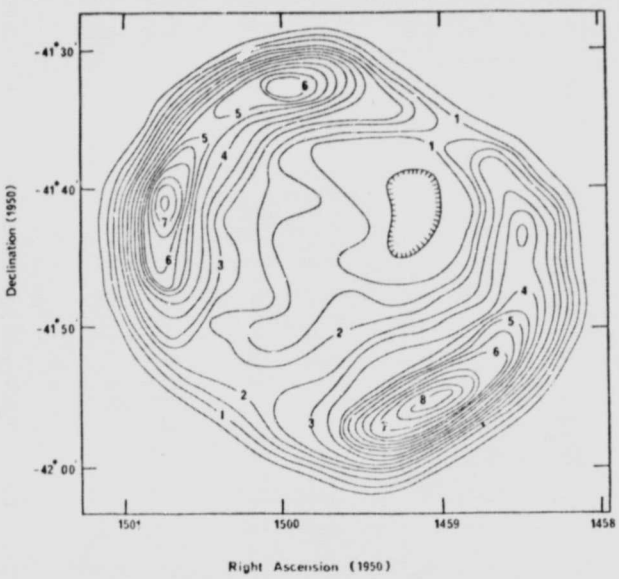


Figure 2.8 - The Einstein Imaging Proportional Counter (IPC) image of SN1006 at 0.2 - 4 keV, above a radio contour map. A gross comparison shows the brightest features of the radio and X-ray maps to coincide, while van den Bergh's optical filament lies just beyond the X-ray extent in the NW gradient.



Figure 2.9 - X-ray image of SN1006 divided into (a) [ 0.2 - 1.25 keV] and (b) [1.25 - 4 keV] components.

(2) Crab Nebula. Although of a very similar age to SN1006, the Crab Nebula has a very different X-ray appearance. There is no obvious shell structure (although one might yet be observable in a higher sensitivity, larger scale image), it is much more luminous and has a hard, non-thermal spectrum. The crucial difference is the presence of the fast pulsar NP0532, providing a copious supply of relativistic electrons. The Einstein HRI image (Figure 2.10) shows the filled-in structure of the Crab at 0.2 - 4 keV, with the pulsar showing clearly and a band of more intense emission visible to the north and west (in the vicinity of the optical wisps).

Specifically in this case, and for other non-thermal SNR's, the most important contribution to be made by the AXAF would lie in its greater bandwidth, extending out to $\sim$ 8 keV, and the spectral/spatial resolution allowing, by comparison with radio maps, the distribution of electron energy and magnetic fields to be obtained. This in turn will allow the diffusion and lifetimes of the relativistic particles to be studied in detail. The inclusion of an X-ray polarimeter in the AXAF payload would provide especially valuable information on the particle and field structure in the Crab and other remnants of its type.

(3) Cas A. The Einstein HRI image (Figure 2.11) of this youngest known galactic SNR shows complex structure, as do the optical and radio maps. A rough correspondence is found between the bright inner ring of X-ray emission ($r \sim 2$ arcmin or 1.7 pc), the radio shell and the main optical filaments. However, the bright radio peak in the NW is relatively faint in X-rays, whereas the optical nebulosity on the east side corresponds to intense X-ray emission. The HRI picture also shows a faint outer ring of X-ray emission ($r \sim 3$ arcmin or 2.4 pc) and an extension to the NE coincident with the fast moving optical knots. A spectrum (Figure 2.12) of the whole remnant obtained with the Solid State Spectrometer (SSS) shows emission lines of Si and S to be particularly

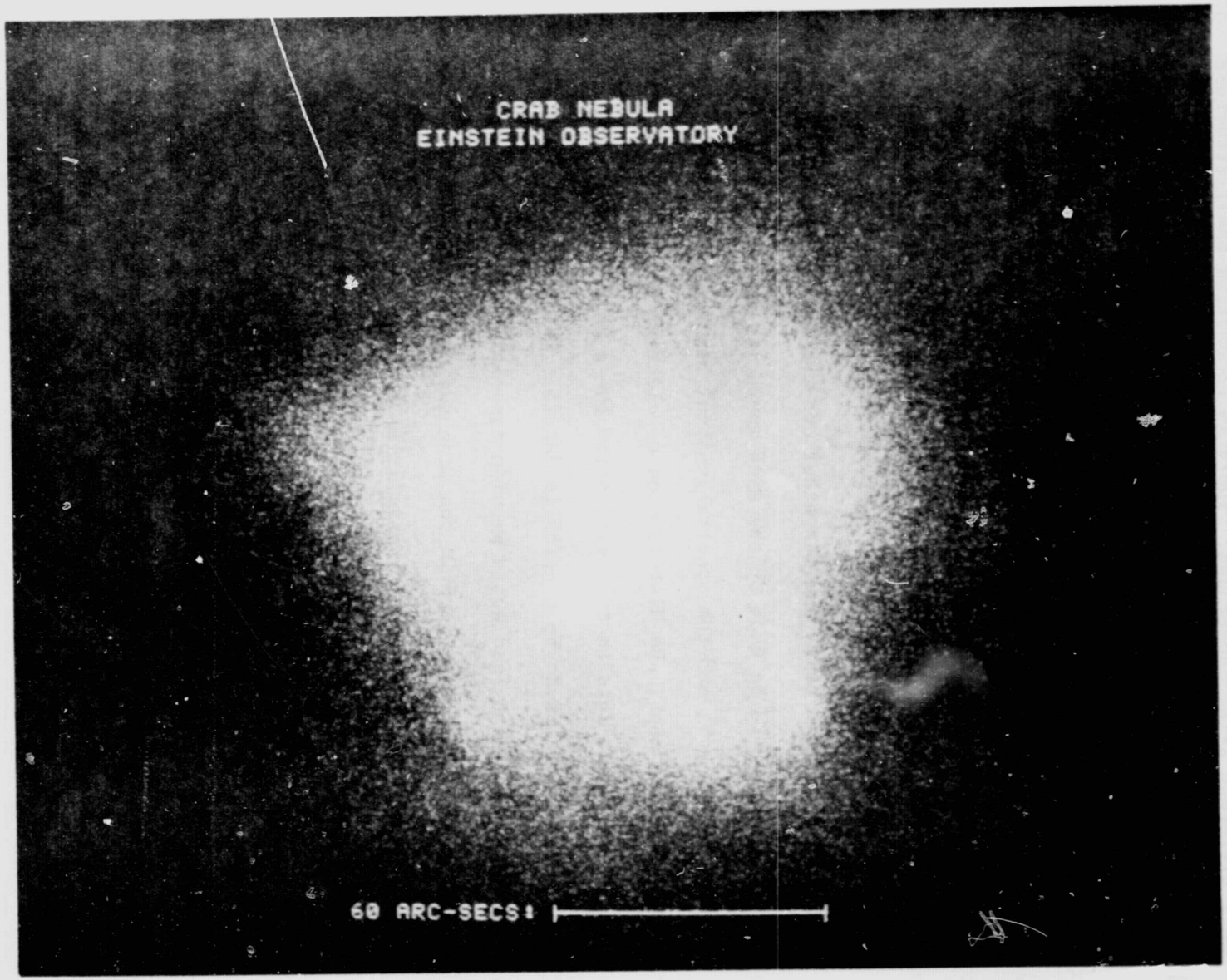


Figure 2.10 - The Einstein High Resolution Imager (HRI) image of the Crab Nebula.

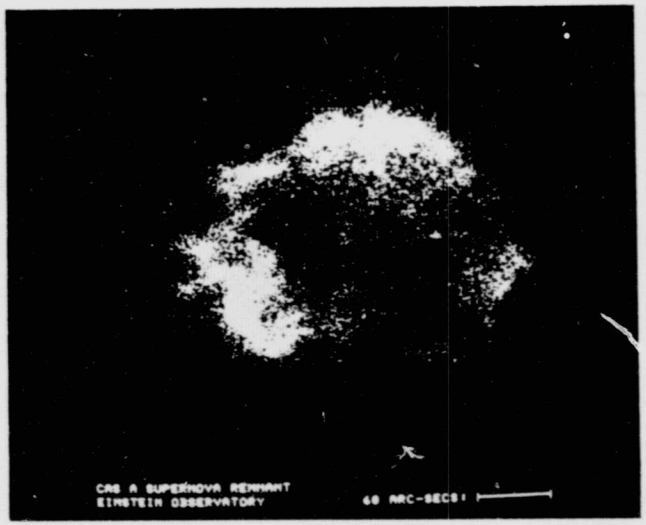


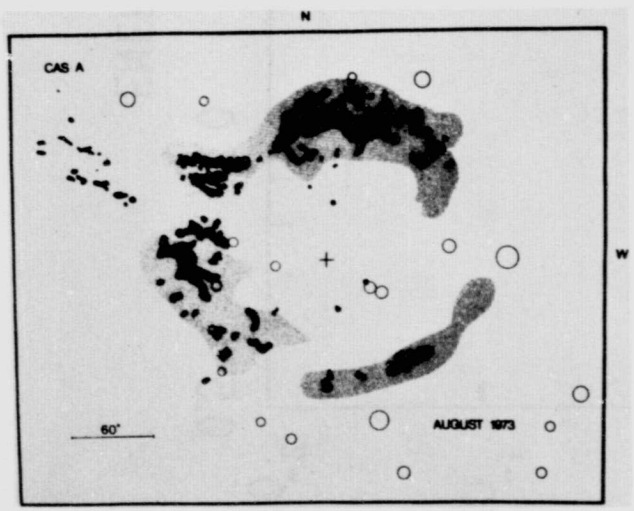


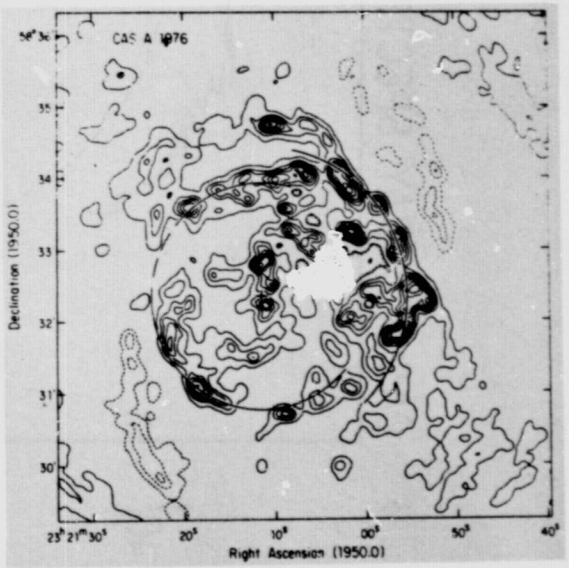


Figure 2.11 - The Einstein HRI image of Cas A. A rough correspondence is found between the bright inner ring of X-ray emission, the radio shell, and the main optical filaments.

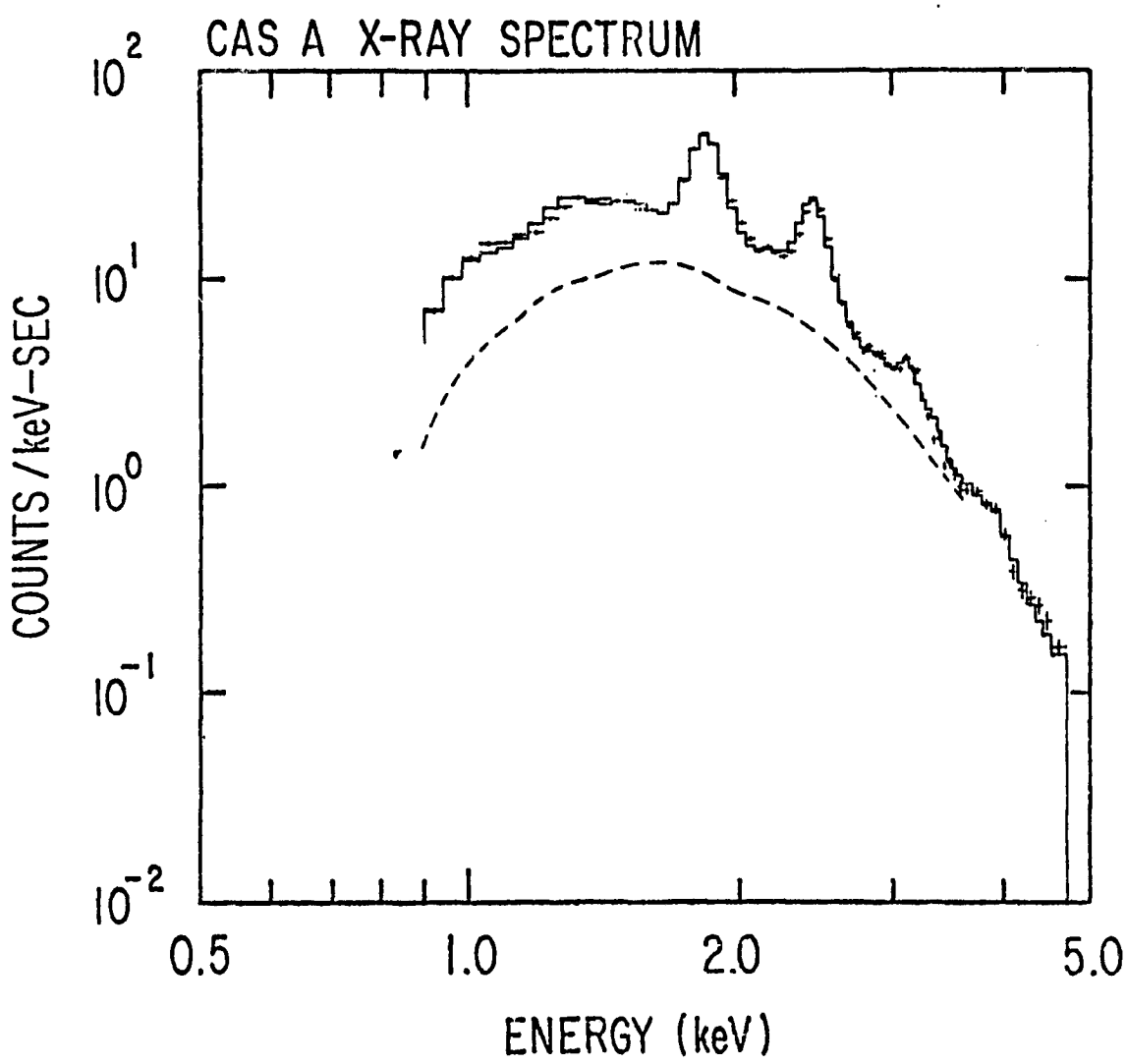


Figure 2.12 - X-ray spectrum of the Cas A supernova remnant as observed by the Einstein Solid State Spectrometer (SSS). Superposed upon the data is the expected response of the SSS to a two-component isothermal model. The lower second trace is the contribution to the spectrum from H, He, C, N, O, and Ne.

strong and an IPC two-color map shows the west limb bright spot (also bright in radio) to be harder than the remnant as a whole. Overall, although the X-ray data offer valuable new information on the distribution of hot gas throughout Cas A, a complete physical analysis, yielding temperature, densities, abundances, mass of ejected and swept up material, etc. cannot be carried out in the absence of resolved spectra on the scale of the spatial features, i.e., a few arcseconds.

In summary, it now seems clear that the X-ray emission delineates the thermal and non-thermal structure of SNR's in a much clearer manner than in any other wavelength band. The Einstein data have provided the first qualitative data on the evolution of many of these remnants. Nevertheless, the limitations - particularly those arising from the lack of combined spectral and spatial resolution - in the present data are important. The AXAF will overcome these limitations and provide, in particular:

- arcsecond images, on the scale of the radio knots, optical flocculi and fast moving ejecta in Cas A, for example, will enable a precise correlation to be made and a determination of the source(s) of the hot gas;

- spectra of solid state spectrometer quality with an imaging detector such as a CCD ( $\Delta E \sim 150$ eV) will allow the main emission lines and continuum to be measured for the individual pixels, providing for a precise determination of non-thermal and thermal components and for the latter, from line intensities, an improved temperature density and chemical composition determination which will provide information on the relative abundances of atomic species in the shells which are reverse shock heated;

- an extended spectral bandwidth, to $\sim$ 8 keV, which will provide sensitivity to the hottest component in the youngest SNR's and cover the important Fe XXV and FeXXVI emission lines;

- the possibility, with a further improvement in spectral resolution

($\Delta E \sim 30$ eV), of resolving X-ray line profiles, yielding ion temperatures and macroscopic velocities;

- the greatly improved sensitivity and resolution of AXAF will also allow more distant SNR's to be detected and resolved, including those in external galaxies out to M31;

- the factor of $\sim 100$ in sensitivity for point sources will push the detectability for black body radiating stellar remnants (neutron stars) close to, or below, the current pion cooling limits.

With little doubt, AXAF will realize the full potential of X-ray observations for the study of supernova remnants, their dynamics and evolution, and indirectly, details of the initial SN explosions, the production of the heavy elements in pre-supernova stars and their dispersal through the interstellar medium.

## 2.6 The Interstellar Medium (ISM)

### 2.6.1 Current Status

Early rocket observations detected a diffuse soft X-ray flux which was highly structured. Analysis of the effects of galactic interstellar absorption and of the results of "shadowing" experiments aimed at detection of absorption by matter in nearby external galaxies showed that the bulk of the diffuse soft X-ray intensity must be of galactic origin. The origin of this diffuse flux has been identified with thermal emission by a hot interstellar medium, since both non-thermal mechanisms for diffuse galactic sources and thermal emission from unresolved discrete galactic sources have been shown to be unable to account for the magnitude of the observed background.

The energy spectrum of the diffuse soft X-radiation places the temperature of the emitting gas in the general region of one million degrees. This general picture of a widely spread hot component of the ISM has been reinforced

by the Copernicus observation that UV absorption lines of O VI, indicating the presence of interstellar gas at temperatures in excess of $3 \times 10^5$ °K, are present in the spectra of hot stars in almost every direction studied. Furthermore, the filling factor associated with this hot gas must be very large. The most direct piece of observational evidence is the high X-ray intensity seen in all directions. X-rays of these low energies can only penetrate with reasonable probability less than 200 or 300 pc of interstellar gas. The emission measure required to account for the observed intensity $n_e^2 \sim 5 \times 10^{-4}$ cm$^{-6}$ pc. If the hot gas is at pressure p, the extent of the emitting region is:

$$d \sim \frac{4T^2 (n_e^2 d)}{(p/k)^2}$$

For (p/k) near its nominal interstellar value of 2000 cm$^{-3}$ K, d is large (hundreds of parsecs) and of the same order or even greater than the nominal distance for one absorption optical length.

In Figures 2.13 and 2.14, our present knowledge of the diffuse soft background, separated into two broad energy bands defined by boron and carbon filters is shown. The spectral as well as spatial resolution of instruments used to date in studies of the diffuse galactic emission has been low. The emission, if thermal, should be dominated by emission lines. Detailed study of the emission spectrum with its rich information content awaits the orbiting of a diffuse spectrometer.

We have so far concerned ourselves with the hot component of the ISM which may well account for more than 90% of the volume of interstellar space, but less than 1% of the mass. The remaining material, much of it concentrated in cool dense clouds or filaments, leaves its signature on every X-ray observation in the form of absorption edge structure and low energy absorption cutoffs.

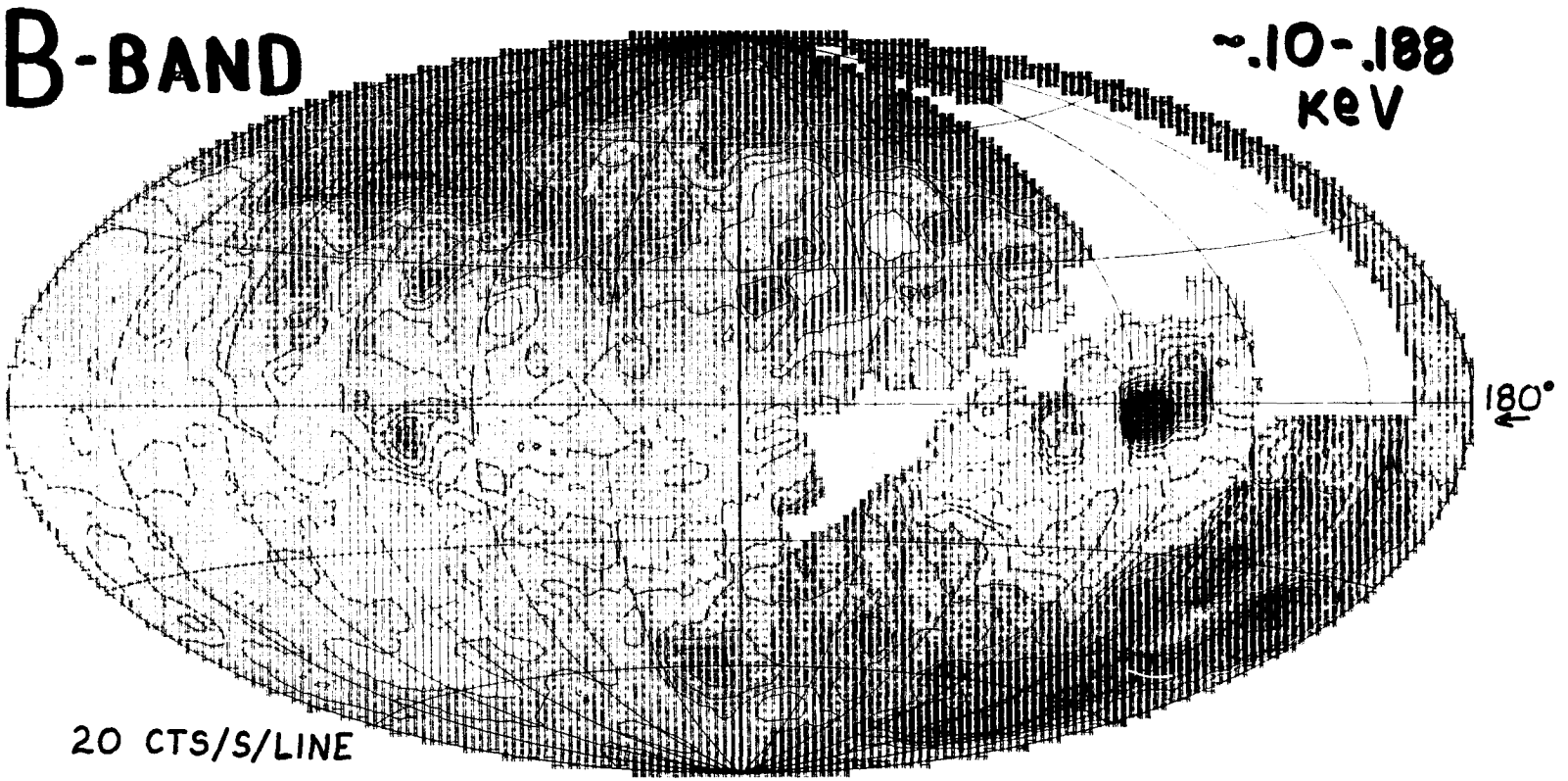


Figure 2.13 - ISM, boron filter.

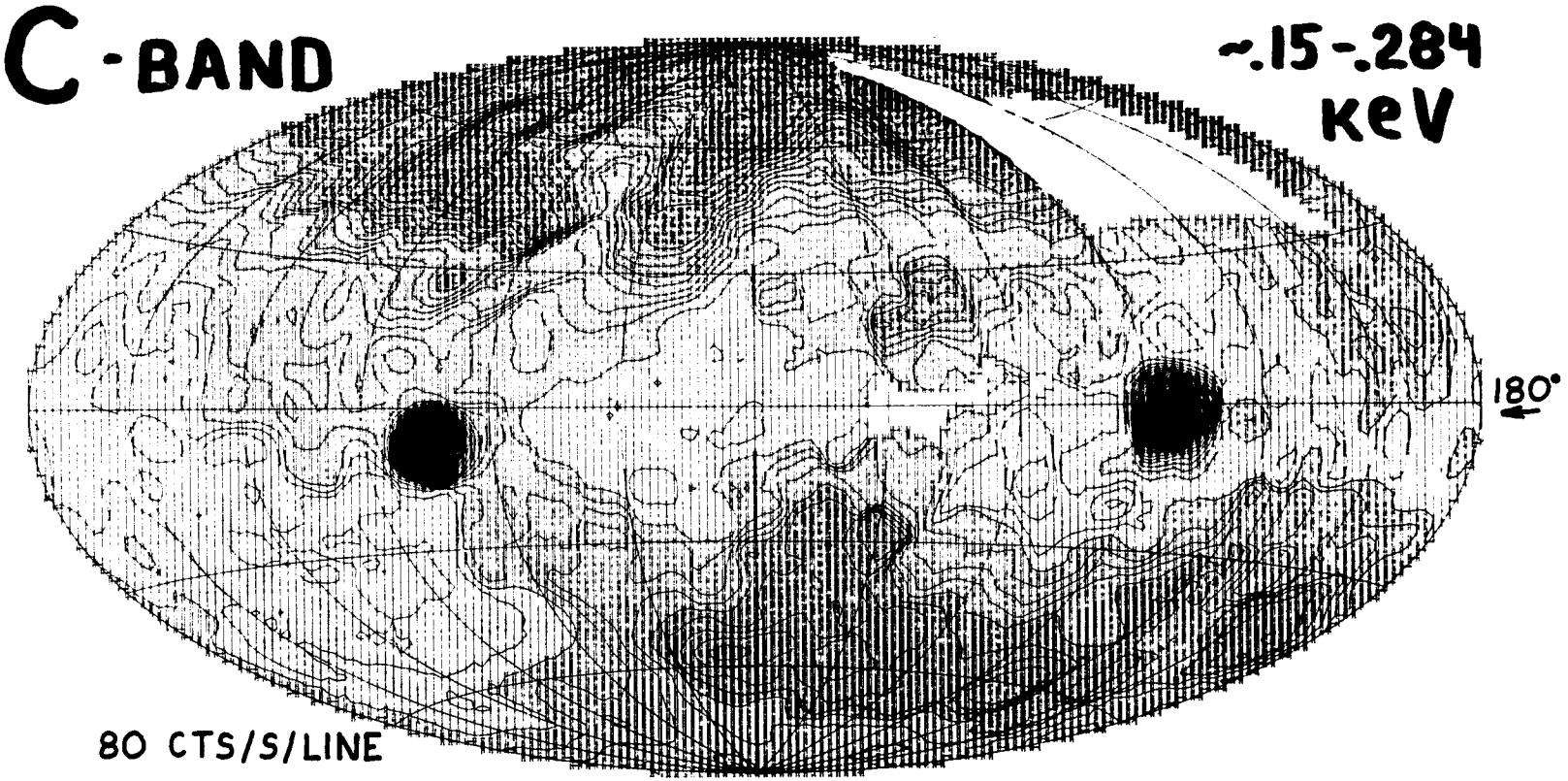


Figure 2.14 - ISM, carbon filter. The large black areas are caused by the Cygnus Loop and the Vela SNR.

With the advent of a spectroscopic observatory of the power of AXAF, this absorption structure will yield data on the ionization structure and composition of the cool gas, and on the composition, size and structure of the interstellar grains, which may have implications as profound as those resulting from the discovery of the hot component of the ISM.

### 2.6.2 Types of Investigations

The new concepts concerning the nature of the ISM which have resulted from X-ray, ultraviolet, and radio observations have led to new models of the structure and dynamics of this important component of our galaxy, and to new insights on important topics such as star formation and the existence of a galactic wind. Observations with the sensitivity and spectral resolution which only AXAF can achieve will be required to provide definitive tests of these new models. AXAF will also provide new insights into such classical problems as the ionization structure of the "warm" component of the interstellar gas, and the composition of the interstellar grains.

(1) The Hot Component of the ISM. It is imperative that the structure of the diffuse background be more accurately determined, and that the spectrum, which is expected to be dominated by emission lines, be measured with higher resolution. It is also important to study the structure of older supernova remnants and of the known enhancements in the background, since it is anticipated that these structures are the source of the hot interstellar gas. It is also likely that the study of diffuse emission in other nearby galaxies will help clarify the structure of the ISM in our own galaxy. The Einstein Observatory has already shown the power of an imaging telescope in the study of the hard X-ray background. The sensitivity of AXAF is required to study the soft background and its spectrum in comparable detail.

(2) The "Warm" Gas, Dust, and Clouds. Absorption spectroscopy for strong

galactic sources provides a unique opportunity to study the composition and structure of the warm ($T \sim 10^4$ °K) gas, of the gas in clouds ($T \sim 10^2$ °K), and of the interstellar dust grains. In the case of the gas, the column density of all important stages of ionization for abundant elements cannot be determined in the ultraviolet due to the absence of suitable lines or due to saturation of line cores for the more abundant elements. X-ray absorption edge spectroscopy on AXAF will not be subject to these limitations. In the case of the grains, X-ray spectroscopy offers unique possibility for the direct determination of grain composition and grain size, which are not possible in the ultraviolet.

A second important technique for the study of the interstellar dust is the study of dust-induced halos of scattered X-rays around strong point sources. The structure of such halos contains information on both the size and composition of the dust.

2.6.3 Scientific Objectives

We summarize the objectives of AXAF studies of the interstellar medium in our galaxy and in other galaxies:

(1) The Hot ISM. a) Determine the density and composition of the "local" hot component of the ISM. b) Determine the energy required to maintain the hot ISM. c) Study the density and composition of the hot ISM in nearby galaxies. d) Search for abundance gradients in the hot ISM in nearby galaxies. e) Search for evidence of galactic winds in our own and in other nearby galaxies.

(2) The Warm Interstellar Gas. a) Determine the composition of the cool interstellar wind. b) Determine the ionization of the gas.

(3) Clouds and Dust. a) Determine the composition of the interstellar dust. b) Determine the size distribution of dust grains. c) Determine the size of typical clouds.

## 2.7 Normal Galaxies

### 2.7.1 Current Status

The study of individual high luminosity galactic sources in the Large and Small Magellanic Clouds first became possible with the Uhuru and SAS-3 class of satellites. Study of such sources is important because one deals with a sample of objects at a known fixed distance, an ideal situation to study the luminosity distribution of a class of objects and one that is not realized in our own galaxy. Sources in the LMC and SMC have higher average luminosities than those in our own galaxy. Models in which the upper end of the X-ray luminosity is limited by the balance between accretion rate and radiation pressure suggests that a higher Eddington limit could be permitted by taking into account a lower average atomic number of the accreting material.

Since the metalicity content of the accreting gas is related to the evolutionary state of the galaxy, extension of these studies to other galaxies may offer us a tool to study metalicity content of galaxies in different evolutionary states. More recently, the Einstein Observatory has provided sufficient sensitivity to image individual high luminosity ($L_x > 8 \times 10^{36}$ ergs $s^{-1}$) sources in M31. Individual galactic X-ray sources, including mass exchange binaries, globular clusters, and supernova remnants have been detected, as shown in Figures 2.15 and 2.16. The most interesting feature of these observations is that it permits us to investigate the distribution in the galaxy of X-ray sources of different types. Particularly striking is the distribution of sources associated with the galactic bulge in M31 which shows a much higher degree of central concentration than in our own galaxy. At least 18 individual sources are found within 2 arcmin or 400 pc of the nucleus of M31. This distribution is narrower than that given by optical objects, but can perhaps be understood by assuming that the formation frequency of X-ray emitting

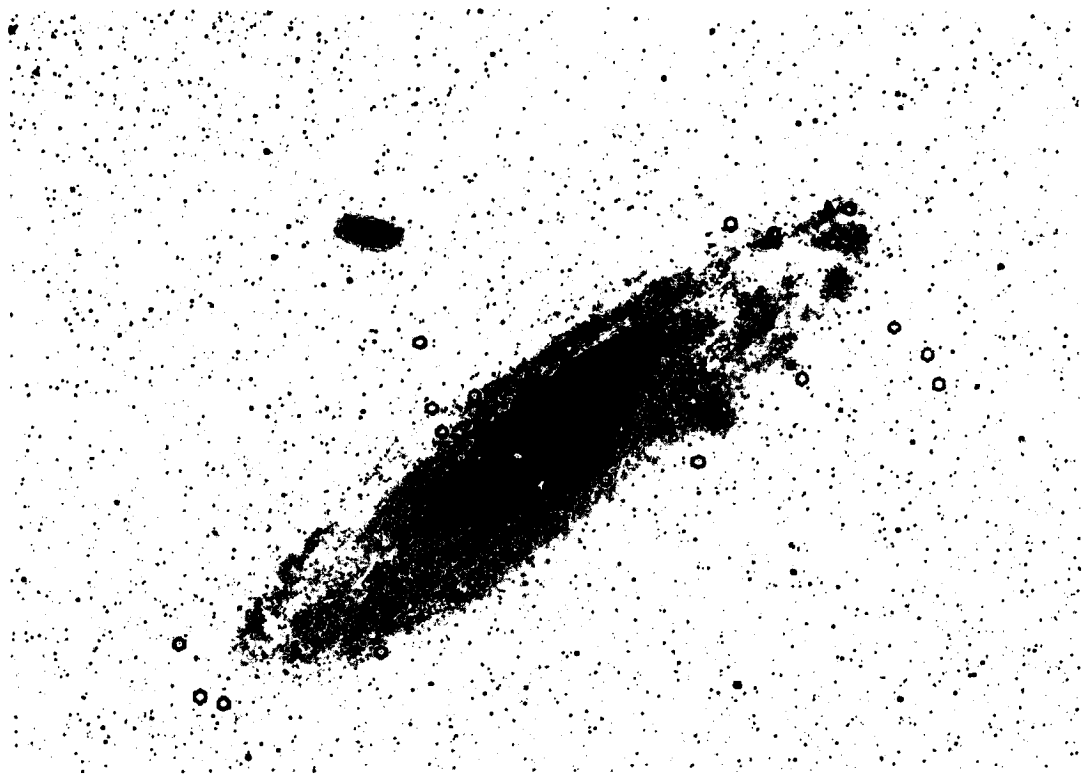

Figure 2.15 - X-ray source positions superposed on an optical photograph of M31. The larger symbols are IPC detections with typical position errors of 1 arcmin. The smaller symbols are HRI detections; most of these are contained in the overexposed central region. The outer sources are associated with spiral-arm features or globular clusters.

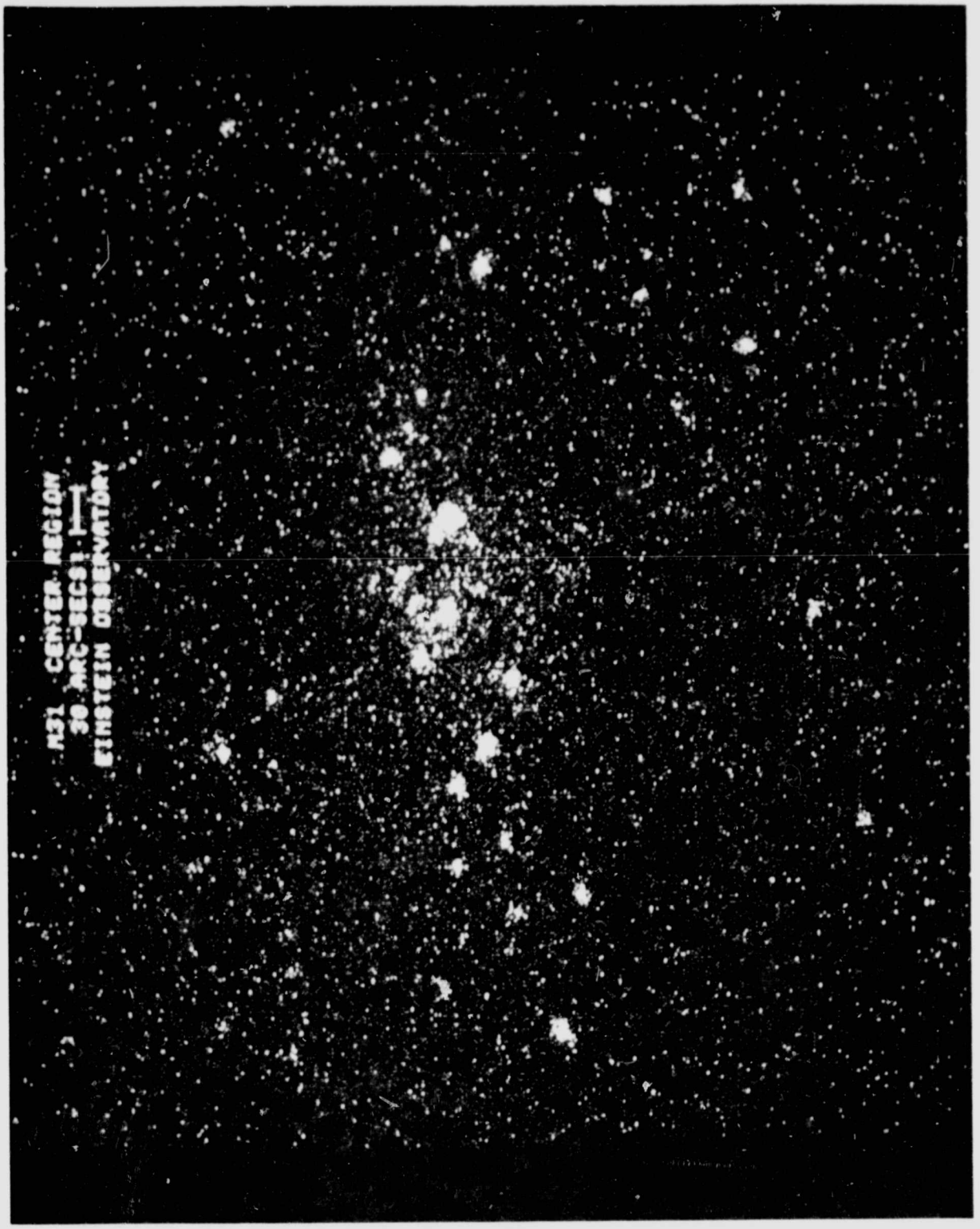


Figure 2.16 - Einstein HRI exposure of the center of M31. North is at the top, and east is at the left. Source 1, which is indicated is near the detection threshold. The nucleus of M31 is coincident with source 14 within the measurement accuracy. The sources classified as the inner-bulge group are contained within 2 arcmin of the nucleus.

systems is proportional to some power of the stellar density as would be predicted from models of X-ray bulge source formation. It is interesting that the distribution of the bulge sources in our own galaxy spans a region as much as 10 times larger. No immediate theoretical interpretation for this difference has been advanced, although this is certainly a large effect: in M31 a central region that contains only about 1.5% of the total mass appears to be responsible for $\sim$ 1/3 of the total X-ray emission from discrete sources.

The fraction of globular clusters luminous in X-rays turns out, on the other hand, to be very similar to that found in our galaxy. Of the 237 globular clusters known to exist in the observed M31 fields, 9 are estimated to be X-ray sources of luminosity greater than $\sim 10^{37}$ ergs $s^{-1}$. In our own galaxy, 7 out of 150 clusters attain similar luminosity.

The correspondence between population I source locations and other indicators of population I activity, such as OB associations, HI, HII, CO, and dust is striking. A study of the more detailed correspondence between location of X-ray sources and the boundaries of dust lanes is in progress. Such studies are not feasible in our own galaxy.

The sensitivity of Einstein has also permitted the study of the integrated emission of stellar sources from normal galaxies to distances of 20 Mpc. In Figure 2.17 the error circle of one of the deep survey sources in Draco is shown. The candidate object is a blue Sb galaxy at Z = 0.0039, with a luminosity of $5 \times 10^{38}$ erg $s^{-1}$. Several individual galaxies in the Virgo Cluster, including M84, M86, and NGC4472 have also been detected in addition to the giant elliptical M87. It is not clear in this case, however, how much of the flux we detect is due to the galaxy itself and how much is due to the gas surrounding it. The detection of diffuse emission around M86 and M84 points to the large role played by the surrounding gas.

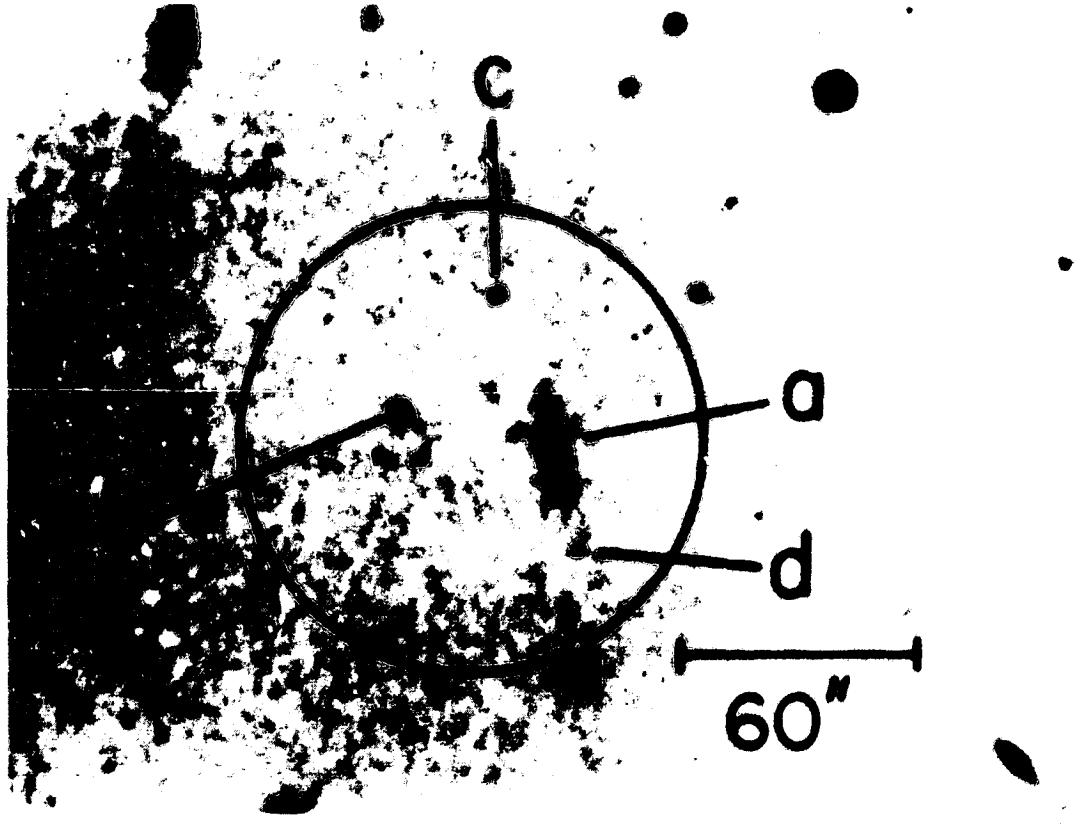


Figure 2.17 - Error circle of one of the deep survey sources in Draco. The candidate object is a blue Sb galaxy at Z - 0.0039, with a luminosity of $5 \times 10^{38}$ ergs $s^{-1}$, object (a).

Current observing plans for the Einstein Observatory call for additional exploratory investigations of a large number of nearby elliptical, S0, spiral, and irregular galaxies exhibiting a wide variety of morphological types, colors, and luminosity. This investigation will be carried out both on field galaxies and on galaxies in the Virgo Cluster.

Finally, the detection of copious X-ray emission from the coronas of normal stars from O to M gives us a tool to help us study the distribution of the stellar content of a galaxy among different spectral types. In order to relate stellar content to galactic morphology, it has been customary to model such distributions and to derive observed integral spectra to be compared with the observed spectrum of the galaxies in the visible. Such investigations often suffer from a lack of definition and the uniqueness of their solution can be challenged. In particular, the total stellar content due to low mass late stars is largely undetermined.

Yet, it is precisely these late low mass stars which have given us some of the most surprising results in stellar surveys conducted with the Einstein Observatory. K and M stars have been found to have some of the largest ratios between X-ray and optical emission of all stellar classes and therefore the integral X-ray emission from a galaxy can be used to establish severe upper bounds on the number of late stars one can associate with it. To be more specific, the predicted X-ray emission from elliptical galaxies containing $10^{11}$ - $10^{12}$ M type stars should be of order $10^{38}$ - $10^{40}$ erg $s^{-1}$ from their contribution alone. Particularly interesting may be the detection of low mass stars in dark halos surrounding such galaxies which could be accomplished through their X-ray emission. In a more general vein, the study of the X-ray source luminosity functions in different galaxies may be directly related to Class I and Class II population contents.

### 2.7.2 Future Developments

The AXAF observational capabilities will permit us to greatly extend these studies beyond the exploratory phase of Einstein.

The sample of galaxies for which the integrated emission will be detectable will increase enormously. While with Einstein we detect one normal galaxy in a 1° field, we will detect as many as 1000 at the 100-fold increased sensitivity of the AXAF.

AXAF sensitivity will allow detection and study of individual high luminosity galactic sources in galaxies closer than 20 Mpc. This means that the type of results obtained with Einstein on only one object, M31, can be extended by AXAF to a large number of galaxies; for instance, to all the 2500 galaxies in the Virgo Cluster.

AXAF will permit us to study lower luminosity individual sources in the nearest galaxies, $L_x > 5 \times 10^{34}$ erg $s^{-1}$ in M31 and $L_x > 5 \times 10^{32}$ erg $s^{-1}$ in the Large and Small Magellanic Clouds. This means, for instance, that coronas of O and B stars will be detectable in the Magellanic Clouds. The study of lower luminosity individual sources in the nearest galaxies will permit us to establish luminosity functions for X-ray sources in different galaxies, a quantity related to the metalicity content, the evolutionary state and the morphology of the individual galaxies.

These investigations may be particularly applicable to the study of young galaxies just forming. Models have been developed suggesting an early phase with much gas, many massive stars, and frequent supernova explosions which lead to a prediction of copious X-ray emission from these young galaxies. Deep X-ray surveys with AXAF might well detect them and determine the epoch at which this activity took place.

The relationship of normal galaxies to active galaxies may also be

probed by studying the X-ray luminosity function for nuclei of normal galaxies. Is high luminosity nuclear activity confined to a small fraction of all galaxies, or do all galaxies spend a small fraction of their life in a highly active state? The X-ray data from AXAF can be used to probe questions such as this by providing the inputs needed to develop luminosity functions at various epochs.

The objectives of these studies can be summarized as follows:

- extend the observation of individual galactic sources in nearby galaxies to lower luminosity ($L_x = 5 \times 10^{34}$ erg $s^{-1}$ in M31);

- extend the observation of high luminosity individual sources ($L_x \geq 10^{37}$ erg $s^{-1}$) to galaxies at 20 Mpc ( $\sim$ Virgo Cluster);

- study the spatial and luminosity distributions of stellar sources distinguishing between bulge and disk components and nucleus;

- correlate these distributions to the galaxy morphology, color, luminosity, group environment, radio emission, and other pecularities for early and late type galaxies;

- obtain an X-ray luminosity function for normal galaxies as a function of morphological type;

- investigate the stellar content of different morphological types using models derived from optical studies and the constraints of X-ray observations.

## 2.8 Active Galactic Nuclei

Within the last three years or so, active galaxies have been established as a class of extragalactic X-ray emitter whose number and range of luminosity now exceed those for clusters of galaxies. The continuing Einstein observations are likely to widen this gap since considerations of the X-ray background imply than an increasing fraction of faint extragalactic sources will be active

galaxies.

From the X-ray data there appears to be a continuous distribution of X-ray luminosities, extending from the most luminous, high redshift QSO's (at $L_x \sim 10^{47}$ erg $s^{-1}$) down through the BL Lacertids ($L_x = 10^{46.5}$ to $10^{43.5}$ erg $s^{-1}$) and type I Seyferts ($L_x \sim 10^{45}$ to $10^{42}$ erg $s^{-1}$) to the type II Syeferts and narrow emission line galaxies ($L_x \sim 10^{43}$ to $10^{40}$ erg $s^{-1}$).

Further, the frequent detection of X-ray variability on timescales of weeks, days, or even shorter, imply that this powerful emission arises from the core of the galactic nucleus. The X-ray variability is the first evidence for such a nuclear core to occur in the narrow emission line objects. The qualitative similarity of the X-ray emission from this wide range of active galaxies [which may, indeed, extend further to the nuclei of "normal galaxies such as M31 ($L_x \sim 10^{38}$ ergs $s^{-1}$) and our own galactic center ($L_x \sim 10^{35}$ ergs $s^{-1}$)] is particularly intriguing in the light of current views on the physical nature of the "powerhouse" in active nuclei. An early proposal suggested that the enormous energy involved in QSO's, radio galaxies, etc. arose from the accretion of matter by a massive ($10^6$ - $10^8$ $M_\odot$) black hole lying in the nuclear cores of such objects. Optical data on the rotation curves of the cores of active galaxies give support to a massive central object. The recent X-ray data strongly suggests that this strange phenomenon may be a very common property of galaxies. Figure 2.18 summarizes the great variety of ways, both thermal and non-thermal, in which kilovolt X-rays might be produced in the vicinity of such a power source.

In summary, observations to date reveal the following X-ray properties of active galaxies:

(a) X-ray luminosities in the range $10^{42.}$ - $10^{47}$ ergs $s^{-1}$;

(b) correlation between $L_x$ and both the nuclear V magnitude and the width of

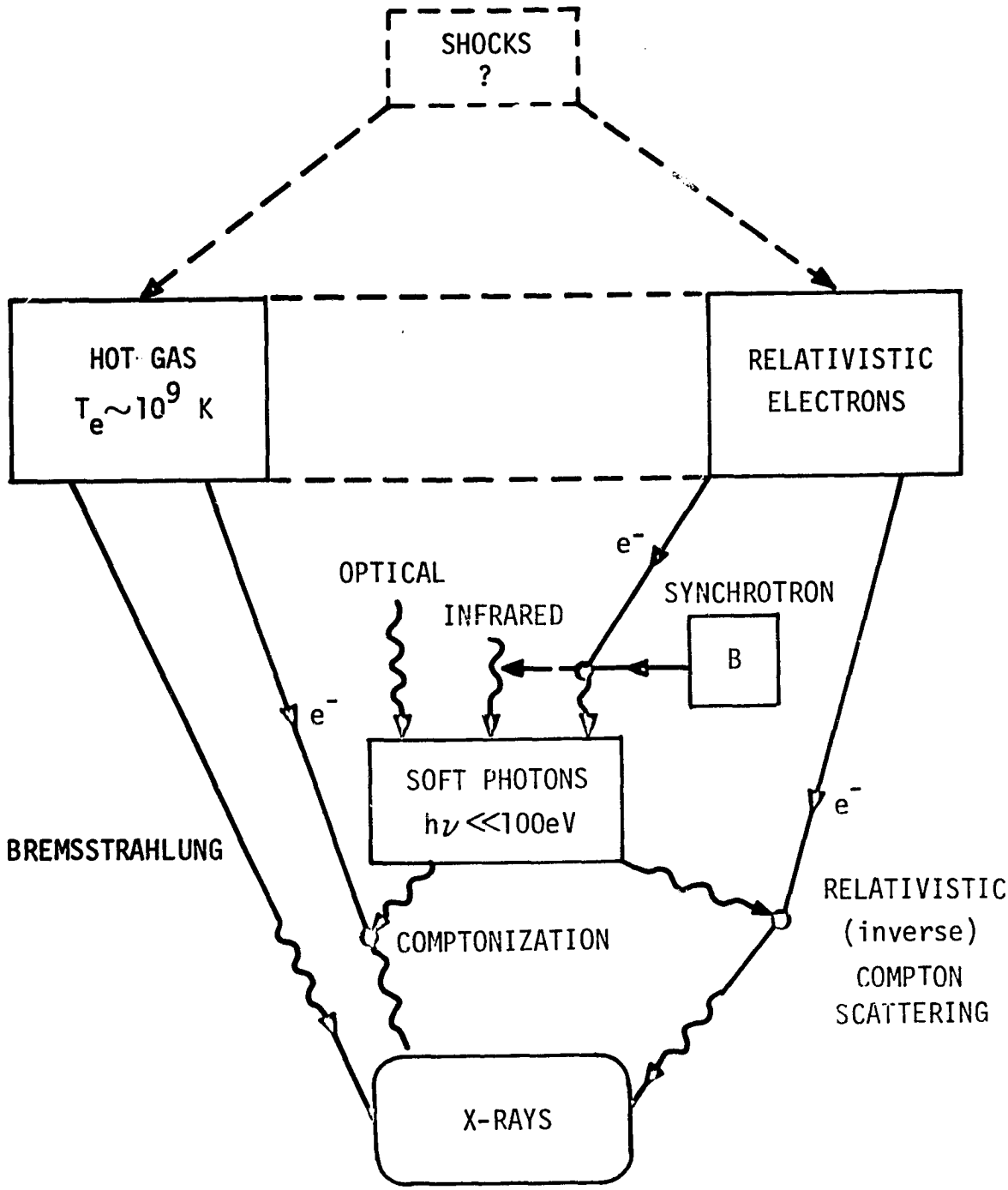


**Figure 2.18** - A schematic diagram of emission mechanisms is shown. The two major reservoirs of energy that can be directly radiated are hot gas and relativistic electrons, both of which may be supplied by shocks, etc. These can radiate by various pathways, the dominant X-ray mechanism being decided by the relative emission timescales. Processes such as shocks, supernovae, etc. produce hot gas with a higher energy efficiency than they create relativistic electrons. This tends to imply that the dominant radiation observed is due to thermal processes. It is difficult to attribute all the X-rays and $\gamma$-rays in Cen A to non-thermal processes (involving relativistic electrons, for example) without questioning the efficiency with which those particles have been produced. The thermal particles may, of course, have put most of their energy into adiabatic expansion, or have been accreted into a massive black hole, but the cooling timescale for thermal electrons is expected to be very short. (After Fabian and Rees).

the permitted optical emission lines;

(c) variability on timescales of weeks, days, or less, implying a nuclear component with r < 0.1 pc;

(d) power law (non-thermal or multi-temperature) spectra.

The most significant new information expected from Einstein observations relates to the detection of rapid time-variability, resulting from its essentially noise-free sampling of a point source, and to the resolution of structure on a larger scale than the < 0.1 pc nuclear core. As an example, Figure 2.19 shows the Einstein HRI image of NGC 5128 (Cen A), in which X-ray emission can be seen not only from the known variable galaxy nucleus, but also from a several arcmin extended region about the nucleus, and from an X-ray jet between the nucleus and the NE inner radio lobe. The newly discovered X-ray jet provides strong evidence for the continuous resupply of energy to the lobes from the nucleus, and contributes to our understanding of the relation between active galactic nucleii and the formation of giant radio lobes in some galaxies.

A second exciting example of structure in an X-ray active galaxy is shown in Figure 2.20, where an extension to the (variable) point source coincident with the nucleus of the QSO 3C273 is seen projecting some 20 arcsec to the SW. The near coincidence of this feature to the well-known optical jet suggests a physical connection. The "X-ray jet" contains only $\sim$ 0.4% of the 0.1 - 4.5 keV emission of 3C273, but its existence together now with the detection of similar features in Cen A and M87 offers a good prospect for further studies with the Einstein Observatory and, even more with AXAF, given its greater sensitivity and angular resolution.

Finally, several examples of time variability, also from Einstein, are

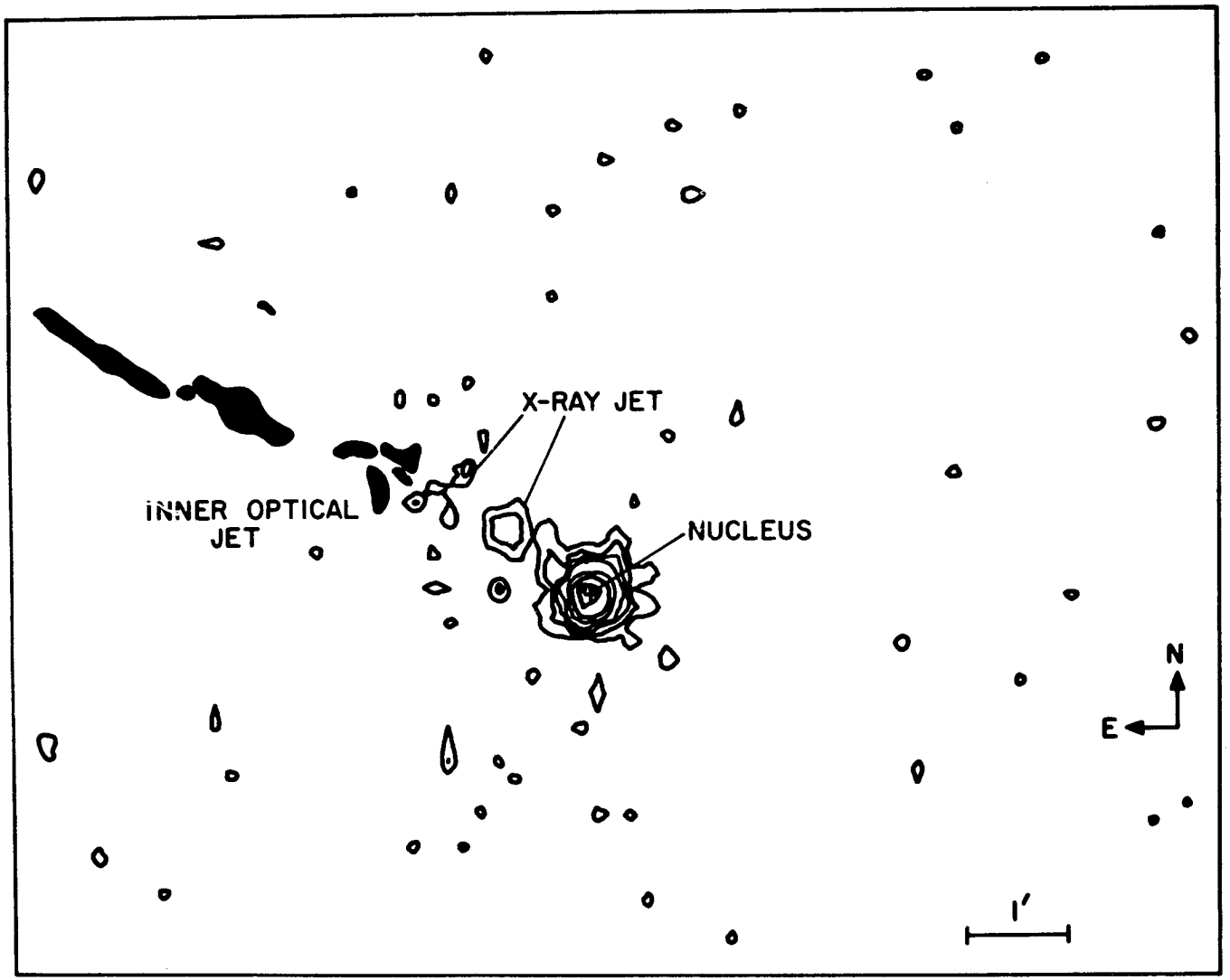


Figure 2.19 - Iso-intensity contour map of the HRI image around the nucleus of Centaurus A. The X-ray jet to the NE is clearly seen. The dark shapes to the NE show the positions of diffuse features in the optical jet discovered by Dufour and van den Bergh.

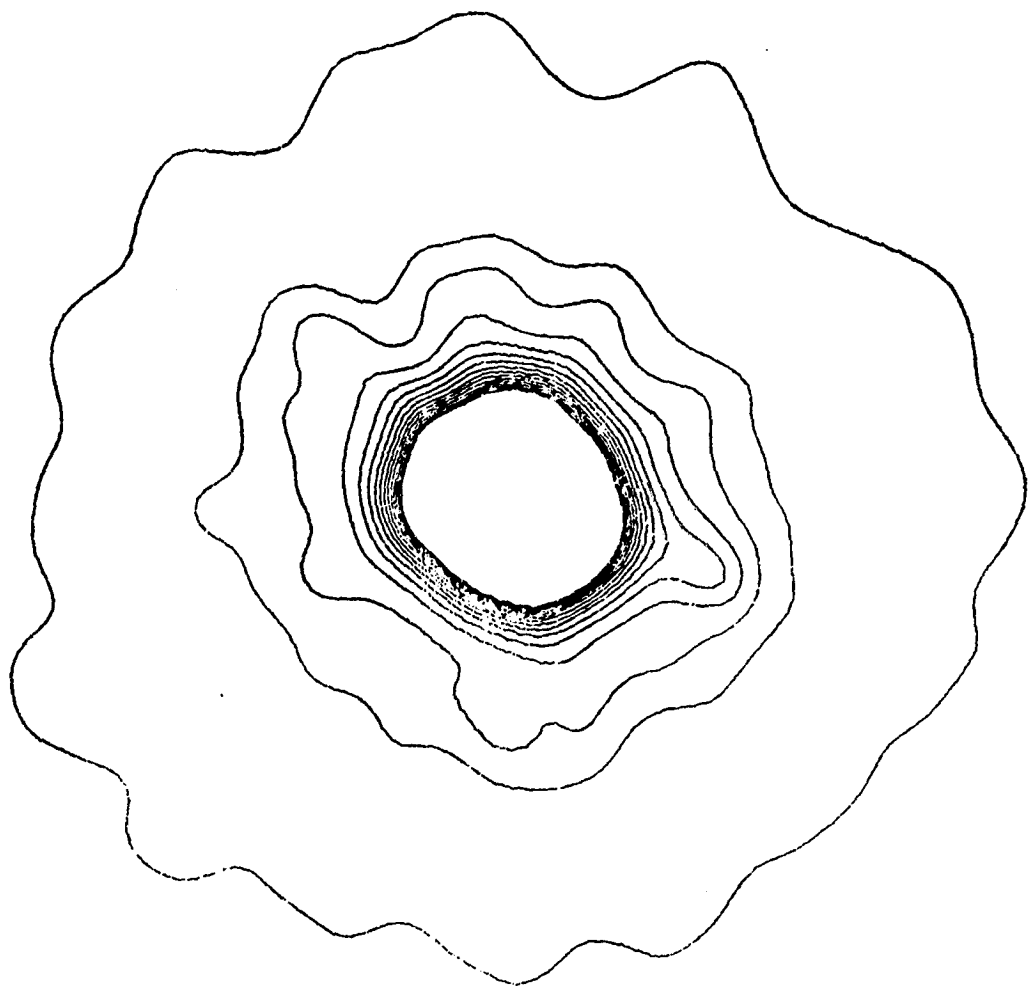

**Figure 2.20 - An example of structure in an X-ray active galaxy, where an extension to the (variable) point source coincident with the nucleus of the QSO 3C273 is seen projecting some 20 arcsec to the SW. The near coincidence of this feature to the well-known optical jet suggests a physical connection.**

shown in Figure 2.21.

Figure 2.21a shows the light curve of NGC6814, a nearby, low luminosity Seyfert type I galaxy, binned in 10,000 sec bins. There is clearly a large scatter of points about the mean and a chi-square test gives a probability of less than $10^{-3}$ that the source is constant. The error bars on the background have been made very small by using a large part of the $\sim 1$ deg$^2$ field of the IPC. The event around 50 ksec into the observation stands out clearly and can be seen at other binnings. NGC6814 clearly varies by factors $\gtrsim 2$ on timescales $\lesssim$ 20,000 sec ($\sim$ 1/4 day). We know from NGC4151 that the low energy spectral cut-off seen in some Seyfert galaxies can be variable. Observations of changing low-energy absorption would be valuable to make estimates of the size, density, and geometry of the clouds believed to exist in the broad line emitting region. We can use the spectral data provided by the IPC on Einstein to look for such changes in NGC6814. However, no correlation of total count rate with spectral "hardness" is present. It seems that this event is due to a change in the underlying continuum source.

The light curve of the quasar OX169 (Figure 2.21b) also shows a rapid intensity decrease over $\lesssim$ 20,000 seconds. Such fast variations can be used to investigate the radiation mechanism. For instance, if we assume that thermal bremsstrahlung is operating, then the cooling timescale is

$$t \approx \frac{2 \times 10^{11} T^{1/2}}{n_e} \text{ seconds}$$

where t is the temperature and $n_e$ is the electron density ($cm^{-3}$).

So for a typical active galaxy temperature $\gtrsim 10^9$ °K, we find $n_e \sim 10^{11}$ $cm^{-3}$. In this case, comptonization would become the dominant loss mechanism leading to an inconsistency. Thus, the data can be used to rule out bremsstrahlung as the mechanism causing the rapidly variable emission seen in OX169.

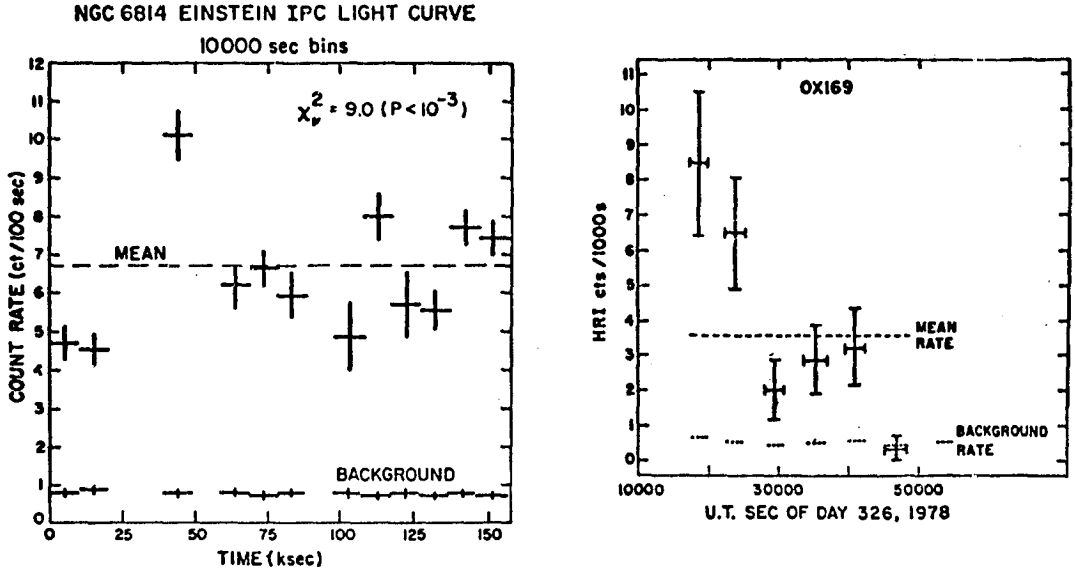


(a) (b)

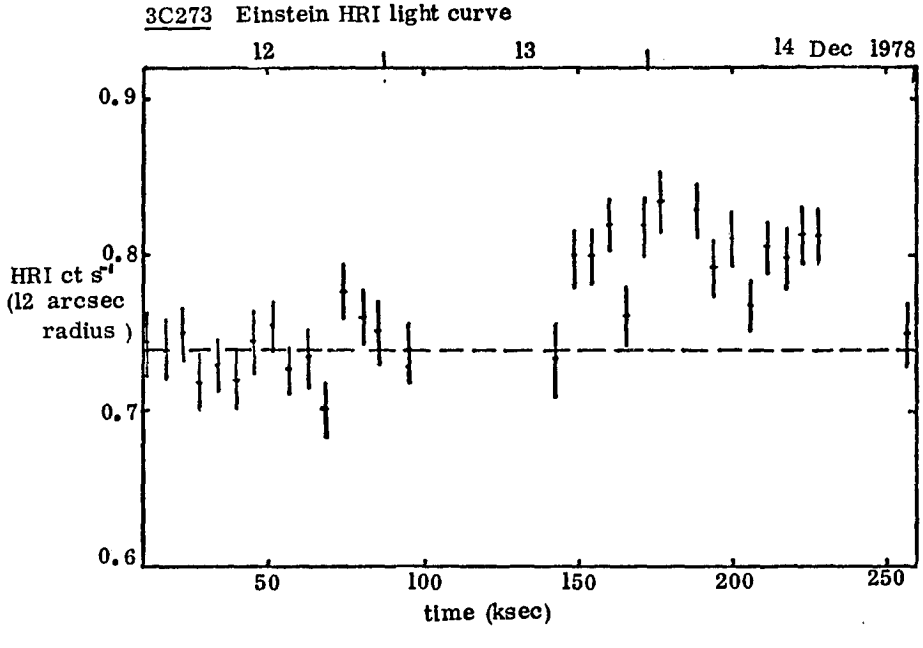


(c)

Figure 2.21 - (a) The light curve of NGC 6814, a nearby low luminosity Seyfert type I galaxy.
(b) The light curve of the quasar OX169.
(c) The light curve of 3C273.

3C273 has been seen to increase its flux by $\sim$ 10% over $\sim$ 50,000 seconds (Figure 2.21c) between the first and second halves of the observation. Since 3C273 is a high luminosity quasar ($L_x \sim 2 \times 10^{46}$ erg $s^{-1}$, 0.1 - 4.5 keV), even a small percentage increase in its output corresponds to a large change in luminosity. In the absence of relativistic expansion effects, one can derive: a minimum efficiency, $\eta$, for energy release from the matter involved in the emission by using the electron scattering optical depth of the emitting matter itself:

$$\eta \gtrsim \frac{5\ \Delta L_{43}}{\Delta t} \text{ , where}$$

$\Delta L_{43}$ is the change in luminosity, in units of $10^{43}$ erg $s^{-1}$, in a time $\Delta t$ seconds. Applying this to 3C273, we have $\eta \gtrsim 0.02$. If we assume the whole X- to $\gamma$-ray spectrum of 3C273 was involved in this outburst, then $\eta \geq 0.1$. These efficiencies provide a strong constraint on assumed emission processes.

AXAF will allow such intriguing observations as noted above to be clarified and extended to many other active galaxies. In this respect, both the improved sensitivity and angular resolution of AXAF will be crucial. For example, the possibility will exist for resolving the narrow emission line region of an active galaxy, which may well be an additional X-ray source arising from collisions of gas clouds moving at several 100 km $s^{-1}$. With a linear extent of 500 pc, the 0.5 arcsec capability of AXAF may resolve such regions in active galaxies out to $\sim$ 100 Mpc. X-ray spectra of this region would then yield, in principle, the mass, density, composition, and velocity distribution of the shocked gas.

The spectral capability of AXAF will mark a significant step forward for the study of active galaxies in general. In particular, such data will provide the most direct evidence as to the thermal or non-thermal nature of the

individual components in a given source/nucleus, jet, etc.

Finally, the 100-fold increase in sensitivity of AXAF will allow complete samples of active galaxies of differing optical and radio classes to be detected, yielding precise luminosity functions, measuring the evolution of more distant objects (a type I Seyfert of $L_x \sim 10^{44}$ erg $s^{-1}$ will be visible at $Z \gtrsim 1$) and, more important, clarifying the apparently fundamental nature of the nuclear X-ray emission and the information it contains on the source of power in these nuclei. In this context, it is finally worth recalling that current X-ray observations already point strongly, from both the short timescales and implied source efficiencies, to a massive accreting black hole as the most likely energy source to power the nuclear activity.

## 2.9 Active Galaxies at High Redshifts (QSO's)

Einstein observations have opened a new chapter in the study of X-ray emission from QSO's. Prior to the launch of this observatory, only three quasars had been detected as X-ray sources, all at redshifts less than Z = 0.158.

Einstein's imaging capabilities have extended the observation of QSO's to the most distant known objects at Z = 3.5, and the overall observation plans include a few hundred objects. More than 20 new QSO quasars have been discovered with redshifts ranging from 0.03 to 2.1 as a result of deep X-ray surveys and serendipitous discoveries of sources in shorter exposures coupled with optical follow-ups. The ease with which quasars at the most distant redshifts can be observed is illustrated by Figure 2.22 showing an image of the field containing QSO 0537-28 which was obtained with a 10,000 second exposure of the Imaging Proportional Counter. The quasar has an estimated luminosity of $10^{47}$ erg $s^{-1}$ in the 0.5 to 4.5 keV band (at the source and assuming $H_o$ = 50 km $s^{-1}$ $Mpc^{-1}$ and $q_o$ = 0). Other sources in the field include main sequence stars as well as yet


Figure 2.22 - Einstein IPC image of field containing QSO 0537-28 which was obtained with a 10,000 second exposure.

unidentified objects fainter than 15th magnitude. The ease with which these observations can be made indicates that even with the Einstein Observatory the intriguing cosmological question of the formation epoch for QSO's may be within reach of our study. Fast time variability of the order of days has been observed in different sources with some indications of variability in times as short as one hour.

The luminosity of the observed quasars, now including several tens of objects from redshifts of 0.1 to 3.5, extends from $10^{43}$ to $10^{47}$ ergs $s^{-1}$. In the early phase of the observing program, in the absence of any preliminary knowledge on the X-ray emission of QSO's, particular emphasis was given to radio bright QSO's. The observation of radio quiet quasars now reveals a definite correlation between X-ray and radio properties.

The ratio between X-ray and visible light luminosity is also correlated and probably changes somewhat as a function of redshift. In the absence of statistically complete samples in the X-ray band, these facts can be used to evaluate the quasar contribution to the X-ray background utilizing the known evolution found in the optical source counts. When this is done, it can be shown that the source counts have to flatten somewhat above 20th magnitude if the X-ray background is not to be exceeded. This appears to be in accord with recent work on quasar number counts in the optical domain. With more detailed studies, the X-ray background rate together with a carefully determined X-ray luminosity function which takes into account evolutionary effects can be used to set strong constraints on the density evolution of quasars at very early epochs. Also, the constraint of the X-ray background rules out most models in which quasars are local, rather than at the distances indicated by their redshifts. Of course, Einstein observations are hampered by the current inability to determine redshifts for faint X-ray QSO's in the X-ray domain

directly and by the inability to study the faintest QSO's due to limited sensitivity. On the other hand, efforts are underway to obtain an intensity limited, statistically complete sample of QSO's based on X-ray detections and the study of the redshift distribution of such a sample promises to yield important insights into the behavior of QSO's as a function of epoch.

The use of the higher sensitivity and greater observing time which will be provided by AXAF will have important implications in the continuation of these studies. In particular, the ability to obtain even modest resolution spectra for some of the objects at the current limit of sensitivity for Einstein offers the possibility of observing emission or absorption lines in QSO's with the implications that the redshifts of QSO's at distances greater than Z = 3.5 could be measured although no spectral features have yet been observed in any of these objects. If such features are discovered, the most distant QSO's could be selected by X-ray observation up to redshift 4 - 10, and used to establish the epoch at which the quasars first formed or at least became luminous objects.

With respect to the study of the underlying source, detailed studies of intensity, variability, spectra, and polarization will give direct information on the processes occurring at the source. For instance, if the X-ray emission process is inverse Compton scattering of soft photons from a hot electron cloud, the measurement of an energy dependent lifetime during flaring activity would yield a complete description of the input spectrum as well as of the scattering region. Polarization measurements could be used to establish the synchrotron nature of the source and specific models such as accretion onto a central black hole could be severely constrained.

AXAF will be used to obtain much larger complete X-ray samples of quasars which can be compared with optically-selected and radio-selected samples. The

study of optically-selected and radio-selected samples can be extended to significantly fainter quasars by the more sensitive AXAF observations. Magnitude, redshift, and intrinsic luminosity distributions can be developed and compared for samples obtained at different wavelengths. Luminosity functions including density and luminosity evolution can be constructed from the X-ray data (to do so requires many quasars at different redshifts and therefore the AXAF data). These can be compared with bi-variate and tri-variate luminosity functions to look for similarities and differences. Since the X-ray observations may be subject to fewer biases and less confusion than optical selection techniques, the AXAF results may well be the most important in studying evolution.

## 2.10 Clusters of Galaxies

The discovery from Uhuru of spatially extended X-ray emission from nearby clusters of galaxies was the first direct evidence for the existence of diffuse intracluster gas. Subsequent observations showed powerful X-radiation to be a characteristic property of most clusters with the following characteristics:

(a) $L_x$ in the range $10^{43}$ to $10^{45.5}$ ergs $s^{-1}$ and correlated with the richness and the central condensation of the cluster;

(b) $L_x$ and the derived ram pressure both inversely correlated with the fraction of spiral galaxies;

(c) thermal emission dominant below 10 keV, with kT in the range 2 to 12 keV and correlated with the velocity dispersion (implying the virial mass is real);

(d) spectra of cool clusters ( $\sim$ 2 keV temperature) often have a hot ( $\sim$ 10 keV) component which may be evidence of inverse Compton emission;

(e) strong line emission from FeXXV and FeXXVI, corresponding to a typical abundance for the cluster gas within a factor of 2 of the solar value.

The major outstanding questions from these observations were the origin of the gas and the heating mechanism. From (e) it is apparent that a

substantial fraction of the gas has been processed in the individual galaxies (or that there was a stellar population III preceding the galaxy formation) and (b) suggests one way in which this processed material has been removed from the galaxies.

The Einstein Observatory has now provided qualitatively new information on the distribution of the X-ray emitting gas. A great variety of morphologies are found, but with two extreme types, as illustrated in Figure 2.23. Figure 2.23a, an IPC map of A1367, shows an irregular X-ray appearance, with the brightest X-ray emission occurring in clumps, some centered in individual cluster galaxies and some not. This has been interpreted as a cluster in its early phases of dynamic evolution in which the gas is cool and primarily associated with individual galaxies. In contrast, the cD cluster A85 (Figure 2.23b) exhibits a smooth, centrally condensed X-ray profile, suggestive of it being a more highly evolved system.

Although X-ray emission is a common characteristic of rich clusters, cluster emission also has been found to be associated with compact groups, or poor clusters, of galaxies. Although not all groups are strong X-ray sources, several (which contain dominant galaxies) have extended X-ray emission with luminosities from $10^{42}$ to $10^{44}$ ergs $s^{-1}$.

Undoubtedly, the Einstein data will add greatly to current knowledge on the distribution of hot intracluster gas in clusters of different types. Comparison with optical and radio maps should provide important clues as to the nature and origin of this gas. These data will uniquely map the gravitational potential of the cluster, while the emission from individual galaxies will relate to their total mass. However, it seems unlikely that a detailed analysis of any individual cluster will be possible until X-ray spectra are available throughout the cluster. Only then can the temperature, density, and abundance

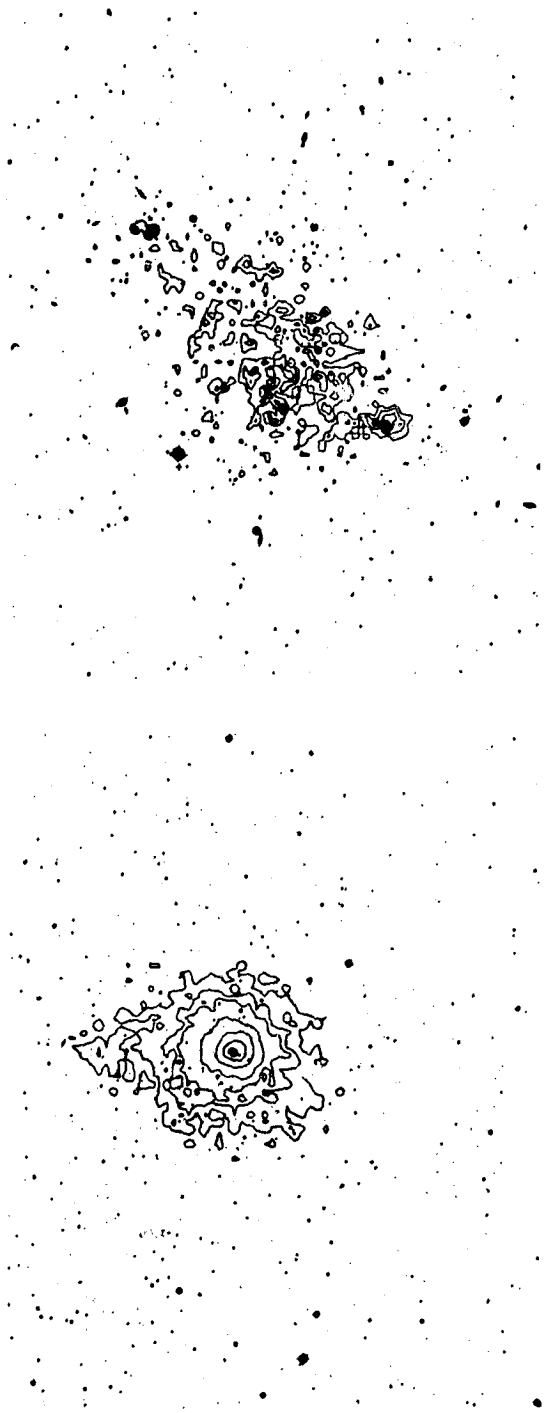

**Figure 2.23 - (a) An IPC map of A1367, showing an irregular X-ray appearance, with the brightest X-ray emission occurring in clumps, some centered in individual cluster galaxies and some not. (b) In contrast, the cD cluster A85 exhibits a smooth, centrally condensed X-ray profile, suggestive of it being a more highly evolved system.**

profiles be determined, showing directly the origin of the gas and how it has been heated. Further, the limited bandwidth of the Einstein telescope ($E < 4$ keV) preferentially detects the cooler gas. The extended AXAF bandwidth is better matched to the hotter gas ( $\sim$ 10 keV) detected in previous whole-cluster spectra and also covers the intense Fe K-shell lines at $\sim$ 7 keV. Any significant non-thermal component also would be more apparent at the higher energies and would be expected to correlate with the radio structure.

Perhaps the most important question relating to clusters is the nature of their early evolution. Optical and radio observations provide few clues and it remains uncertain even as to whether the clustering occurred before or after the formation of the component galaxies. Current Einstein observations of distant clusters ($Z \sim 0.5$) may provide indications as to the nature of the evolution of cosmologically young clusters. Of particular interest is whether galaxy formation efficiently depletes the intracluster gas so that young clusters would not be bright X-ray sources, and thus there would be marked luminosity increases as the galaxies are stripped of their gas, or if substantial intergalactic gas remains after galaxies are formed which would imply initially bright X-ray clusters. However, a proper study of this question requires an instrument with the power resolution, and spectral capabilities of AXAF.

In particular, AXAF will:

(a) detect and spatially resolve clusters to $Z \gtrsim 3$, depending on their epoch of formation and early evolution;

(b) allow detailed mapping and spectroscopy of clusters to $Z \sim 0.5$ to 1, yielding abundances, densities, temperatures, masses, and directly, the redshift;

(c) determine the nature of cluster evolution, showing, in particular, whether clusters originated via cooling and fragmentation of protoclusters, or via the aggregation of galaxies. The evolution in the latter case depends on the

balance between primordial gas supply and galaxy mass loss and the deepening of the cluster potential.

## 2.11 Cosmological Tests Using X-ray Observations of Clusters

The investigation of standard cosmologies reduces to the observational determination of the Hubble constant $H_o$ and the deceleration parameter $q_o$, which together specify the density and size of the universe; $q_o > 1/2$ for a closed universe and $q_o < 1/2$ for an open universe.

Measurement of $q_o$ according to the classical test of galaxy magnitude vs. redshift has encountered difficulties because of selection effects and the lack of understanding of galaxy evolution. The test is unlikely to provide conclusive evidence for the case of a closed or open universe, at least in the foreseeable future.

A second classical test for $q_o$ is to measure the angular diameter of clusters as a function of redshift. Major uncertainties in applying this test, which include lack of knowledge about the evolution of the core radii of clusters and the mass distribution of the universe, also preclude this test from resolving the question of the correct cosmological model.

A new test for $q_o$ using clusters of galaxies as the observational object has been suggested. By using the theoretical relation for the differential number of objects at a given redshift instead of the relations for apparent magnitude or apparent size, many of the difficulties encountered with the classical measurements of $q_o$ can be avoided. Homogeneity is required only on distance scales encompassing many clusters, at least tens of Mpc.

The observational method consists of counting the number of X-ray emitting clusters of galaxies per unit redshift as a function of redshift. At a Z of 1, the ratio between the differential number of counts for $q_o = 0$ and $q_o = 1$ is

about 4. For the same $q_o$ values, the ratio is 2.3 for the apparent magnitude, 1.5 for the angular diameter, and 2.8 for the integrated number of objects at redshift Z = 1. This last ratio is misleading since one would have the same number of objects whether the differential or integral form of the test was used. The differential test is much more sensitive since a chi-square test with many degrees of freedom can be used to compare with predicted curves.

The AXAF sensitivity is such that for an observation time of $10^5$ seconds, objects of $1 \times 10^{44}$ ergs $s^{-1}$ could be seen to Z = 1.1 for $q_o = 0$ (Z = 1.7 for $q_o = 1$). Assuming a density of cluster sources of $10^{-6}$ $Mpc^{-3}$ (luminosities $\geq$ $10^{44}$ ergs $s^{-1}$) about 800 clusters would be detected for 100 $deg^2$ surveyed ($10^7$ seconds of observing time).

The properties of the AXAF high resolution imager will permit the determination of the cluster redshifts, at least for the stronger sources. The 6.7 keV Fe line probably appears strongly in all clusters with temperatures in the 4 to 10 keV range, and for a Perseus type cluster source with a line of $\sim$ 500 eV, equivalent continuum width, the redshift could be determined to Z $\sim$ 1.

X-ray and microwave observations of the hot gas in rich clusters have also been proposed to give a direct and model-free measurement of the angular diameter distance to clusters. The observations provide an evolution-independent global method for the determination of both $H_o$ and $q_o$. In principle, the determination could be carried out by using joint X-ray and microwave measurements of one nearby rich cluster and one cluster at Z $\sim$ 1.

The AXAF will be capable of detecting luminous galaxy clusters and measuring spectral and spatial parameters out to Z $\sim$ 1. For example, a remote rich cluster with the luminosity of the Coma cluster ($8 \times 10^{44}$ ergs $s^{-1}$) could be detected to $10\sigma$ at a redshift of 1 by observing for $10^5$ seconds. AXAF would be able to determine the X-ray flux, the central gas temperature, the gas core radius, the spatial distribution of the X-ray surface brightness and temperature, and the

abundances of Fe, A, S, Si, and Ca.

The microwave observations are required in order to determine the diminution in intensity of the cosmic microwave background caused by Compton scattering on intervening hot cluster gas, and to determine the microwave diminution core radius. The combination of the X-ray measurements of the cluster central temperature, the surface brightness, and the core radius with the microwave measurements of the diminution intensity and diminution core radius yields $q_o$ independent of detailed modeling of the intracluster gas or of the cluster itself.

## 2.12 The Extragalactic X-ray Background

The origin of the diffuse background has been an important question in X-ray astronomy starting from the earliest measurements. When it was recognized that the X-ray background above 2 keV was isotropic and hence extragalactic, it became evident that understanding its origin would have cosmological implications. Two general explanations representing opposite points of view have received the most attention. One is that the background is composed of faint unresolved objects which are of the same classes as, but perhaps in earlier phases than, the objects which can be detected directly and identified. If this explanation is correct, then the luminosities and/or proper densities of the objects must be larger at earlier times in the universe, and the magnitude and graininess of the background can be used to place important constraints upon the evolution of the objects. The other explanation is that the background is truly diffuse. The most probable explanation of this type is a hot plasma that pervades the intergalactic medium. If it accounted for only 10% of the background, the mass that could be attributed to such a plasma would represent more matter in the universe than has been detected so far by all other means. Such a large mass would be important dynamically, and in determining the deceleration parameter,

although it would not "close" the universe. Furthermore, the density of such a plasma would place constraints upon determining the epoch of galaxy formation.

The differences between the Einstein Observatory and all preceeding X-ray astronomy satellites are its ability to detect sources several hundred times fainter and to obtain positions with extremely fine precision. This represents a significant qualitative as well as a large quantitative improvement upon previous investigations of the background because the sensitivity and resolution of the Einstein Observatory permits us to resolve and study sources which are $10^4$ more numerous per unit solid angle and to obtain their optical counterparts. Previous work on the source counts was based upon the interpretation of relatively small fluctuations among fields of several square degrees. With the Einstein Observatory, we are in position to resolve a significant part of the background into identifiable sources.

Two lines of investigation of the Einstein Observatory converge in their conclusion on the origin of the background. The first is the study of the X-ray luminosity of quasars. The conclusion of the Einstein quasar investigation is that it is possible to account for essentially all of the X-ray background with QSO's if we assume that their ratio of X-ray luminosity to optical luminosity, $L_x/L_{opt}$, is like that of the Einstein quasar sample. Although this result is very suggestive, the quasar study by itself is not conclusive. Because of the large spread in the ratio $L_x/L_{opt}$, there are systematic uncertainties in determining its effective value even for the objects studied. Also, there are real uncertainties in the density of QSO's,

particularly those fainter than 19th magnitude, so that even with the correct effective value for $L_x/L_{opt}$, it is difficult to make a precise prediction of their integrated contribution to the X-ray background. Finally, we must assume that the X-ray spectra of QSO's (or any other objects for that matter) have the composite spectral shape $dN/dE \propto E^{-1.4}$ necessary to match the 2 - 20 keV background.

The other line of investigation of the Einstein Observatory that is relevant to understanding the X-ray background is the "Deep Survey". Because the sensitivity and angular resolution are so much superior to previous surveys (several hundred times better), we have the opportunity, a priori, to resolve a significant part of the background into possible discrete source components. On the other hand, because of the nature of focusing optics, the nominal energy band is 1 - 3 keV which is below the 2 - 20 keV regime where the extragalactic component is known to be predominant. (Because the energy resolution of the Einstein detectors is finite, there is a non-negligible contribution from even lower energies.) Therefore, the galactic contribution both in terms of discrete sources and diffuse emission may be very important, and we do not necessarily expect that all, or even most, of the actual X-ray background in the Einstein detectors is due to the discrete extragalactic sources which may account for the 2 - 20 keV background. Nevertheless, by detecting and identifying discrete sources, we can determine if extragalactic sources are appearing in Einstein fields at a rate that is consistent with a discrete source hypothesis for the 2 - 20 keV background. If the sources are QSO's and their $L_x/L_{opt}$ is consistent with the Einstein quasar study, then the explanation for the background would be nearly settled. In fact, the preliminary results of the Einstein survey show that discrete sources provide a significant fraction of the extragalactic background. Several of the discrete sources are identified with QSO's (Figures 2.24 and 2.25), while many remain unidentified. For the

Figure 2.24 - A deep survey exposure with the Einstein HRI detector to a previously empty X-ray field in Eridanus. North is up, east is to the left, and the exposure time is 43000 sec. Three sources should be apparent in the photo. The northern most source corresponds to a previously unknown $19.8^{m}$ quasar with Z=0.5. The westernmost source corresponds to a previously unknown $17.8^{m}$ quasar with Z= 1.96. The easternmost source corresponds to a $13.1^{m}$ GO star.

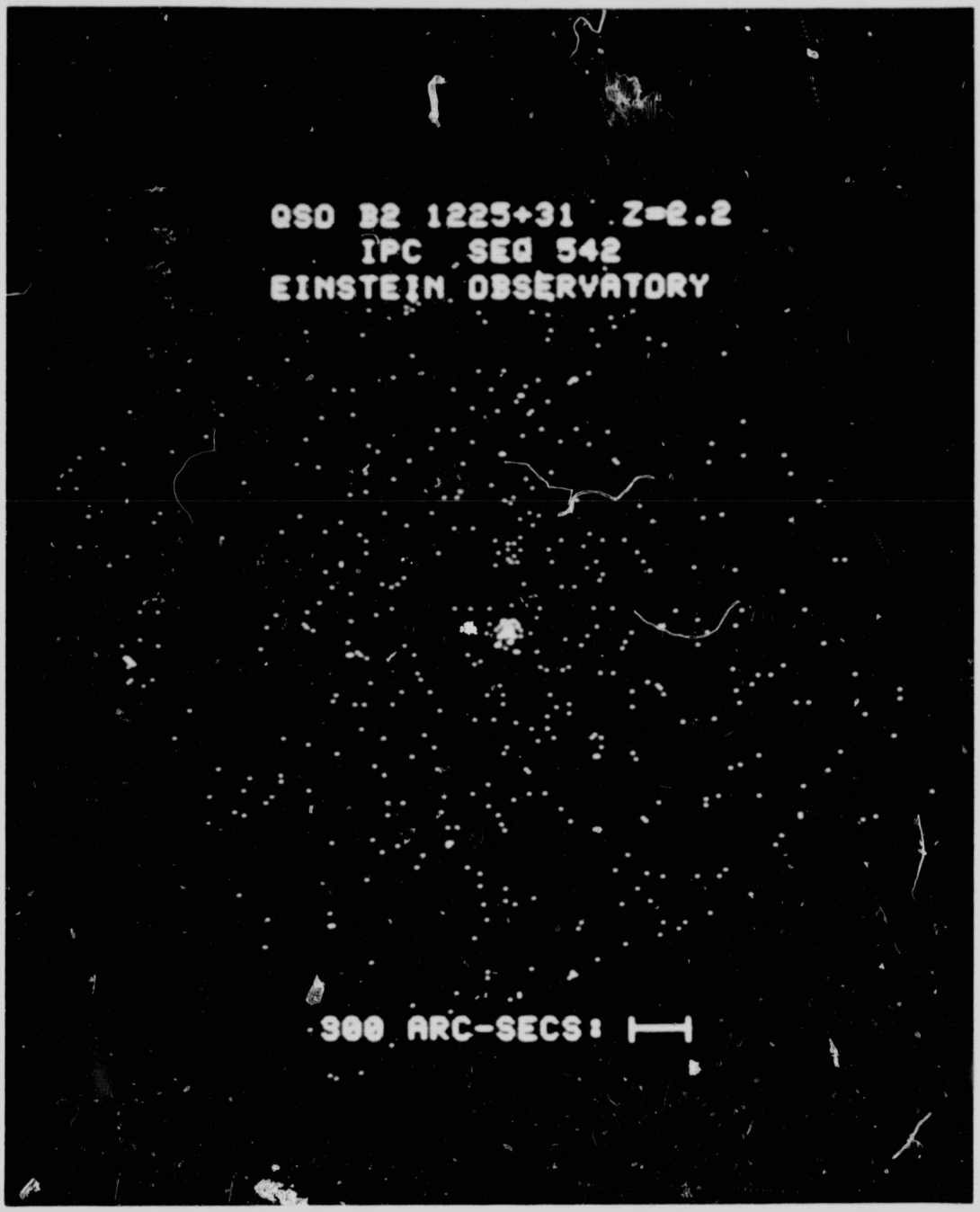


Figure 2.25 - A 6000 second X-ray exposure with the Einstein IPC showing the detection of the quasar B2 1225+31 at a redshift of 2.2. The source is clearly seen in the center of the detector. The 0.5 - 4.5 keV X-ray luminosity is $5 \times 10^{46}$ ergs $s^{-1}$.

latter, the large $L_x/L_{opt}$ ratio is consistent with their being QSO's.

The current result is that the Einstein Deep Survey and quasar investigations converge to the conclusion that the X-ray background is composed principally of unresolved sources and that they are probably QSO's. Sources of the type seen in the Deep Survey themselves account for about 1/3 of the background. With the assumption of QSO evolution models suggested by optical observations, the remainder of the X-ray background could easily be accounted for. This apparently leaves little room to observe a possible residual intergalactic source of X-rays that is truly diffuse. However, uncertainties in the X-ray flux and spectrum of QSO's and their evolution will probably always make it impossible to exclude a contribution of up to about 10% from an intergalactic plasma, and even larger contributions can not be rigorously excluded at the present time. Yet the existence of such a plasma at a level that produces only a small fraction of the X-ray background would still represent more mass than has been found previously in the universe. How could one detect such a plasma if it is not possible to observe it directly in the face of the overwhelming contribution by the unresolved QSO's? The answer may lie in the study of the X-ray structure of clusters of galaxies. The spatial distribution of hot gas near the outer boundaries of a cluster of galaxies may be affected by the pressure exerted by a gas in the intergalactic medium that may be even hotter. External pressure will be manifested in subtle but possibly detectable effects upon the shape of the X-ray surface brightness distribution.

Study of the sources of the background with AXAF's increased sensitivity, positional accuracy, and spectral coverage will provide definite conclusions to the question of their origin and will account for a large fraction of the overall background over a broader energy range. It will also provide information on their evolution at a very early epoch which will be of fundamental importance to

cosmology.

In addition, AXAF is necessary to provide a qualitative improvement in the measurement of the isotropy of the background in the 2 - 8 keV range. All non-focusing experiments are limited by source confusion noise to a precision $\delta I/I \approx 1\%$. Because AXAF can individually pick out, and discard point sources at the level of $10^{-5}$ UFU, and still integrate the remaining background within its field of view, it can improve the isotropy measurements by an order of magnitude. This will allow, for example, a search for a small component due to our galactic halo, or to the local supercluster, and for the 24-hour anisotropy due to the peculiar motion of our galaxy (Compton-Getting effect).

## 3.0 THE AXAF

The Einstein Observatory (HEAO-2), launched in November 1978, is the first observatory capable of high resolution imaging of cosmic X-ray sources. In a period of fifteen years, X-ray astronomy progressed from a dependence upon rocket-borne detectors (Geiger counters with 20 $cm^2$ collecting area and source location to about 10°) to a true astronomical quality observatory with arcsecond spatial resolution, 500 $cm^2$ of collecting area, and a life of 1-1/2 to 3 years. Because of its imaging capability, the Einstein Observatory has achieved a spectacular increase in sensitivity and angular resolution over all previous rocket and satellite experiments. Einstein has already discovered and investigated over a thousand X-ray sources of galactic and extragalactic origin, and the total number of sources that could be detected, given sufficient time in orbit, exceeds $10^5$. Figures 3.1 through 3.3 are illustrations of this imaging capability. Prior to Einstein each field shown was thought to contain only a single source.

Given the capabilities of the observatory, one might ask why we have undertaken the study of the AXAF mission. One of the primary reasons is the finite lifetime of the Einstein Observatory. The nominal Einstein Observatory lifetime was 1 year, due to the finite amount of gas available. Attitude control is maintained through reaction wheels which have their momentum dumped by expending reaction control control gas. The Einstein consortium has worked with NASA to extend this lifetime to almost 3 years by active momentum management. The use of such techniques will only extend the useful life somewhat, and there will come a time in 1981 when the observatory will no longer be operational. At this time the Einstein Observatory deep surveys will have covered some 10 $deg^2$ at the ultimate sensitivity limit and the moderate sensitivity surveys will have covered an additional few hundred square degrees (or less than 1% of the sky). Thousands of new objects will have been discovered


Figure 3.1 - Region observed during the first exposure to the X-ray sky with the Imaging Proportional Counter on Einstein. North is up and east is to the left in each portion of the plate. (a) Arcmin resolution X-ray image; the gray scale is approximately logarithmic, with denser and darker regions corresponding to higher 0.2 - 4 keV X-ray intensity. The bright source at the lower right is Cyg X-3. The composite image containing $10^4$s of data, is a superposition of 11 separate exposures of a region which fortuitously includes an OB star association. (b) Reproduction of the Palomar Sky Survey red print, with the X-ray locations (labelled A through E and Cyg X-3) superposed as 1 arcmin radius circles; the scale is indicated at the lower right. The large trapezium of stars (A-D) consists of the four most luminous stars of the VI Cygni OB association.

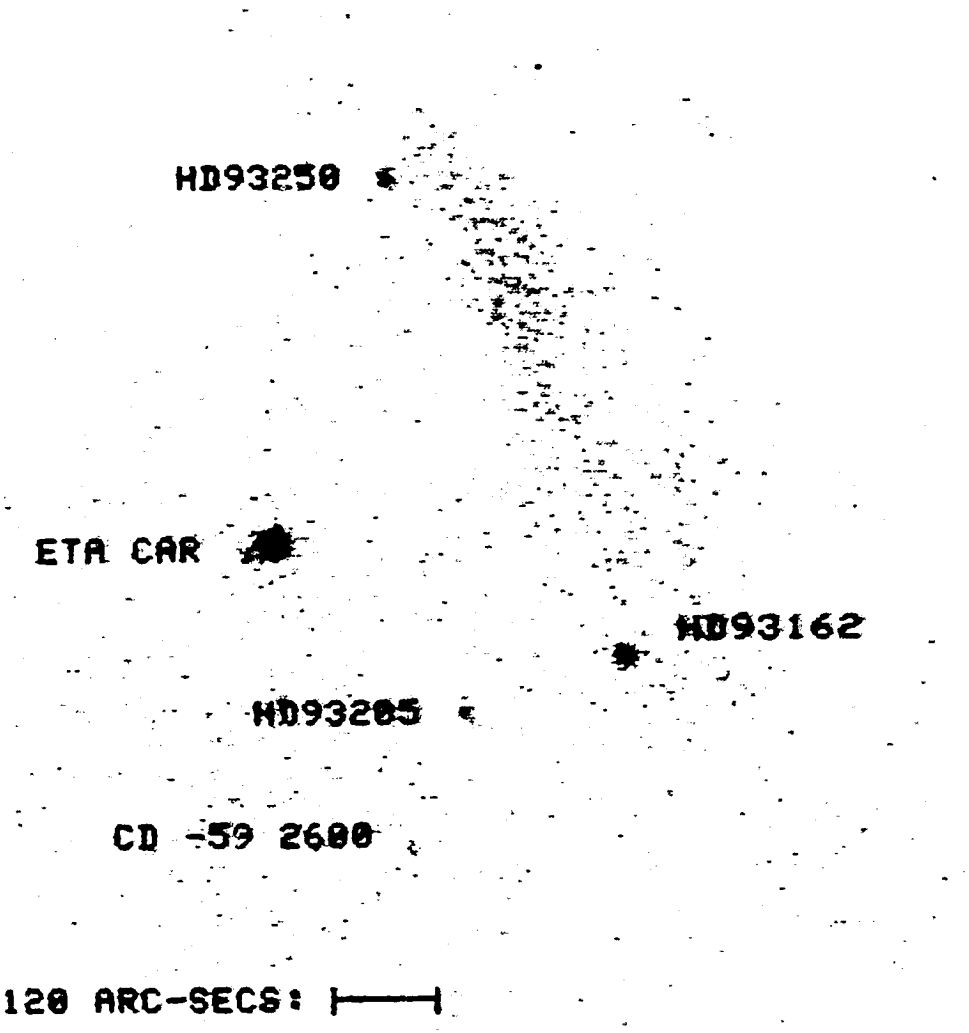


Figure 3.2 - An HRI picture centered on Car showing that Car itself is an extended source. Four stars are also seen. The diffuse feature in the NW is an instrumental effect (in the HRI only).

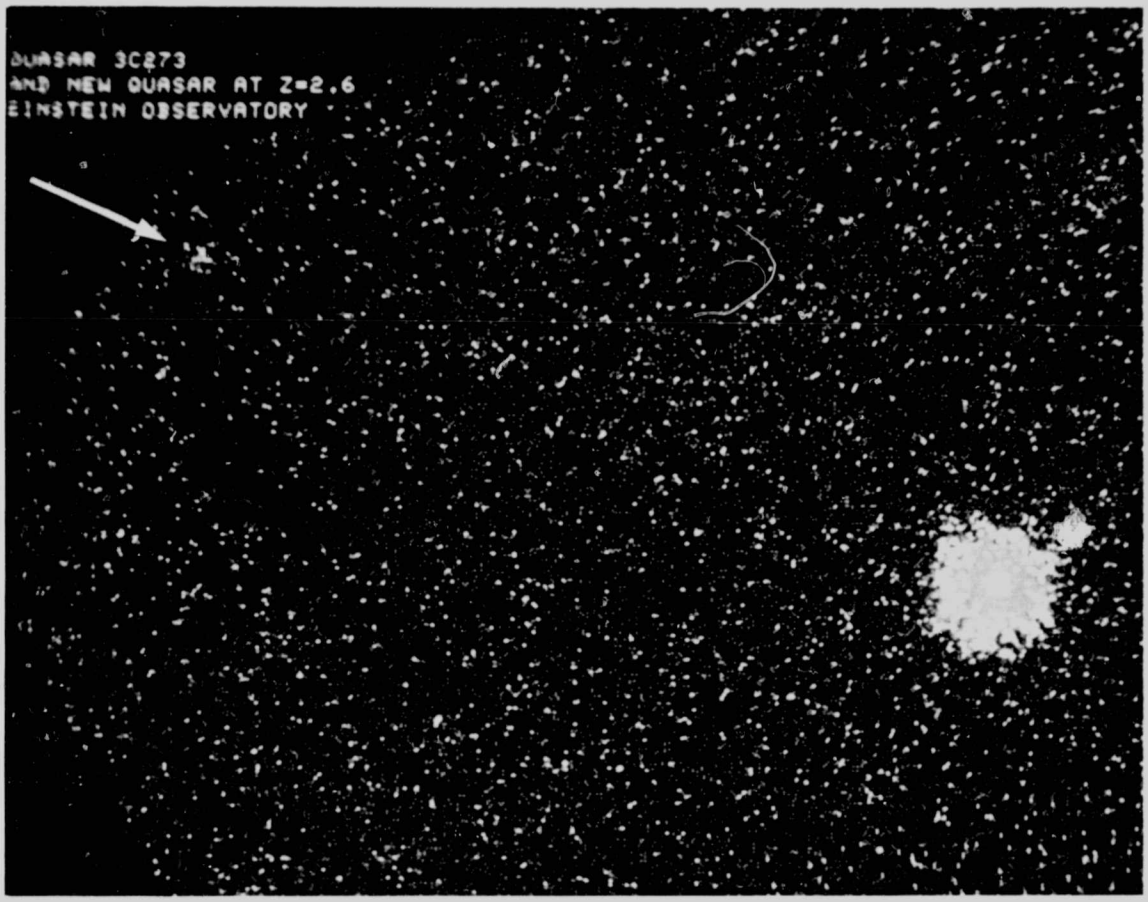


Figure 3.3 - HRI deep survey showing an over-exposed view of the nearby quasar 3C273 (bright source to the right), and the new distant quasar discovered in the observation. The new quasar is to the upper left (just below the "E" in observatory). Optical data give a redshift of 2.6.

by Einstein, but more sensitive exposures will be needed to study their structure, spectra, time variability, and polarization. With AXAF's projected increase in mirror resolution (a factor of 8 over Einstein) and with its increase in mirror area and detector efficiency, a factor of 100 increase in sensitivity over Einstein is expected. The AXAF observatory will be designed for revisitation at selected time intervals for orbit reboost and repair or replacement of instrument and support subsystems components, and retrievable for major refurbishment on the ground. This capability, for the first time, permits development of a "permanent" national facility for X-ray astronomy, much as astronomers at other wavelengths now utilize.

In the following sections, the AXAF high resolution mirror and representative focal plane and non-focal plane instrumentation will be described. The AXAF elements are shown in Figure 3.4.

## 3.1 High Resolution Mirror Assembly

The design of the mirror assembly for the AXAF has benefited to a very large degree from the fabrication, assembly, and X-ray test experience with the Einstein mirror assembly. This experience established that the optical measurements made during mirror manufacture and final assembly and alignment, if properly made and interpreted, can provide a high degree of confidence in predicted X-ray performance. A key point established was that while in-process X-ray testing is certainly desirable, it is not absolutely necessary for the manufacture and assembly of a properly figured and aligned mirror at the 5 - 10 arcsecond resolution level.

The second point established was the need for full aperture testing of the mirror assembly in X-rays. This is necessary to establish resolution and total energy response and to provide boresight information for use in the on-orbit

# ELEMENTS OF THE AXAF

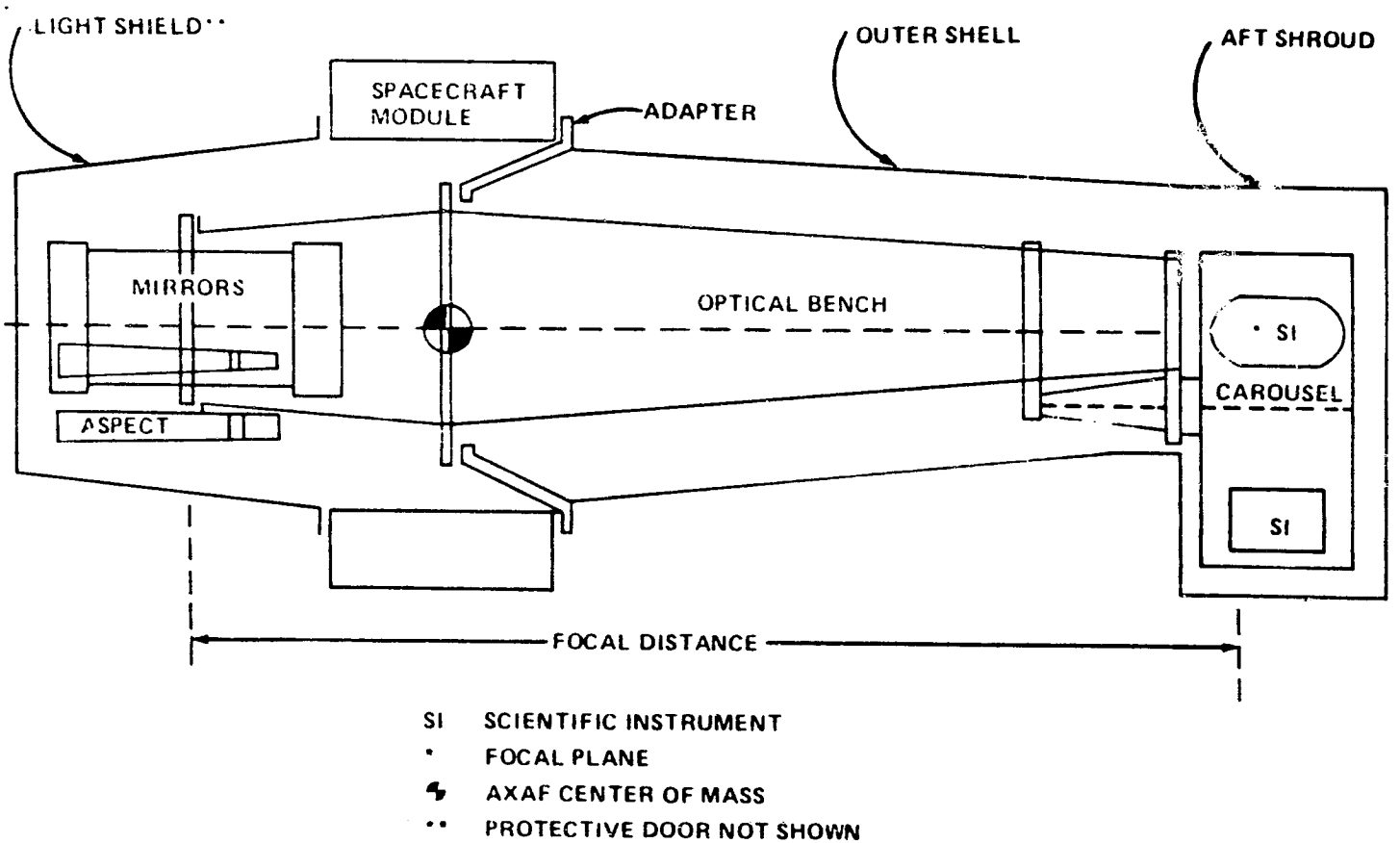


Figure 3.4 - Elements of the AXAF

alignment of the X-ray axis to the aspect sensor axis. The test experience at MSFC established the difficulty of deriving total mirror response from computations based on sub-aperture testing.

The third and probably most important point which emerged from the Einstein mirror test and analysis activity was that the mirror assembly performed very well and that limitations on performance due to surface roughness, thermal effects during assembly, etc. were quantitatively understood. Given the Einstein mirror results, performance limits can be established primarily by local slope tolerances and surface finish rather than by alignment and figure tolerances. However, in achieving the AXAF goal of an eight times improvement in resolution, and the increased effective area provided by six nested mirror pairs, alignment, and particularly alignment maintenance requirements, must be re-examined. Based upon the Einstein mirror fabrication and test experience, and recent AXAF mirror sensitivity and preliminary error budget analysis, the AXAF mirror assembly resolution goal of 0.5 arcseconds, while demanding, is entirely feasible.

### 3.1.1 Optical Design

We have reviewed a number of candidate mirror designs for the AXAF that were studied by the SAO/MSFC team. The approximate size of the optics is limited both by the length of a shuttle payload and by engineering constraints; the latter limits are based upon preliminary mechanical calculations and upon a desire not to depart excessively from experience with the Einstein mirrors. The candidate designs reviewed thus span relatively small ranges (typically of order $\pm$ 25% about a base design) of the parameters which define a mirror.

We chose to emphasize the effective area in the few keV region and also to obtain a useful response at the energy of the K$\alpha$ line of single electron iron ($\sim$ 7 keV). We have selected a provisional design based on these criteria which we believe is suitable for planning purposes at this stage of the program. The

design has not been "fine-tuned" to optimize any specific performance specification. The final design will accommodate mechanical requirements as these become known quantitatively, and also, minor variations which will slightly improve projected performance.

The telescopes studied are all based upon two-mirror surfaces of revolution. This was done for fundamental reasons. The minimum number of reflections is desired because of reflection and scattering losses, and two is the minimum number of surfaces which will form an image over an extended field at the small grazing angles required for efficient X-ray reflection.

The effective area for this telescope design is approximately proportional to the product of the reflection efficiency squared, the grazing angle squared, the focal length, and the mirror segment length. The efficiency enters twice because of the two surfaces (the grazing angles at both surfaces, and therefore, the efficiencies are approximately the same because this also maximizes the collecting area for a given amount of surface to be polished). The projected area is approximately proportional to the segment length times the grazing angle, and to the radius, which is proportional to the focal length times the grazing angle, thus accounting for the remaining factors. It was useful, therefore, to examine the product (efficiency grazing angle) squared as a function of grazing angle for various mirror coatings. As a result of the examination, nickel was chosen as the most suitable surface material in the mid-atomic number region, yielding superior reflection efficiencies in the few keV region. Gold was selected to represent the high atomic number materials which will give better reflection efficiencies at higher energies. It is probable that platimum will be substituted for gold in the final mirror because of superior evaporation properties.

We chose, as a base design, a Wolter type I mirror assembly having 6

nested paraboloid-hyperboloid pairs, an outer optical diameter of 1.2 meters, a focal length of 10 meters, segment lengths (paraboloid and hyperboloid) of 84 cm, and an optical surface separation sufficient to avoid vignetting rays within 20 arcminutes of the optical axis (Figure 3.5). This results in grazing angles for the inner and outer mirror of 27 and 51 arcminutes, respectively. The inner mirror grazing angle thus is suitable for the 7 - 8 keV region, whereas the outer mirror is optimum at about 3 keV. A larger diameter outer mirror would be useful for lower energies, but 1.2m was chosen as a reasonable extension of the Einstein value of 0.6m. Similarly, a nest of 6 pairs is a modest extension of the 4 pair Einstein design. The focal length of 10m was somewhat less than we originally thought could be accommodated, but is about the maximum length which is allowed by the Shuttle configuration. Finally, a wall thickness allowance of 3.8 cm was based on the Einstein experience, and seems reasonable after preliminary mechanical calculations, but must be subjected to further engineering analysis.

Figure 3.6 shows the theoretical rms blur circle radius as a function of the field angle of a point source for the baseline design with a flat focal surface assuming a perfect set of mirror elements. The distribution of the photons in the image is not completely described by the rms radius. The FWHM of the central peak of the point response function varies slowly with field angle, but the fraction of the photons within the FWHM decreases more rapidly with field angle. The practical consequences of this is that high contrast features can be readily resolved out to the edge of the field, but the sensitivity to point sources falls off with field angle.

The effective collecting area of the telescope as a function of incident energy was calculated for various degrees of mirror surface roughness. The Beckmann treatment of the scattering distribution was extended to the two reflec-

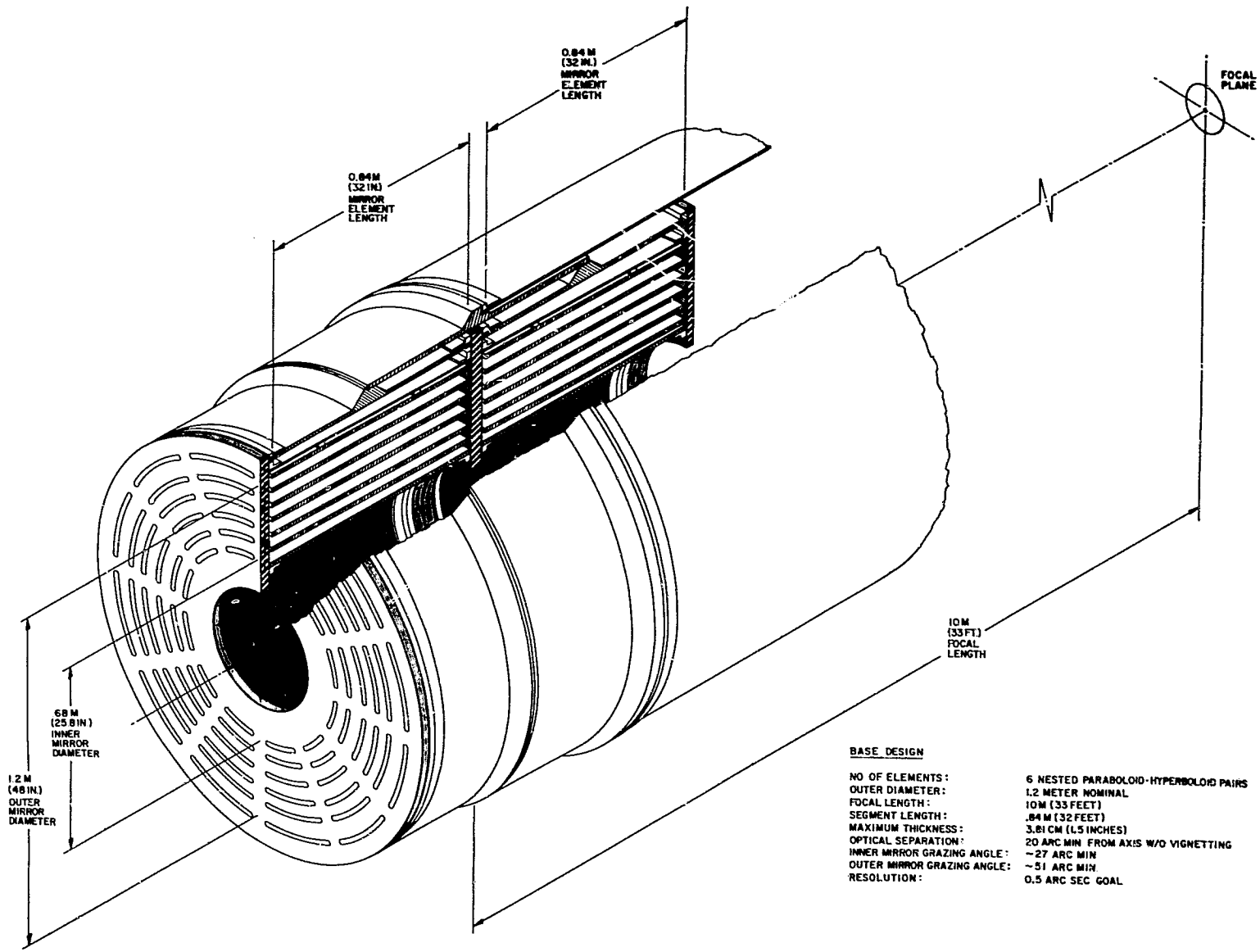


Figure 3.5 - Baseline optical design - high resolution mirror assembly.

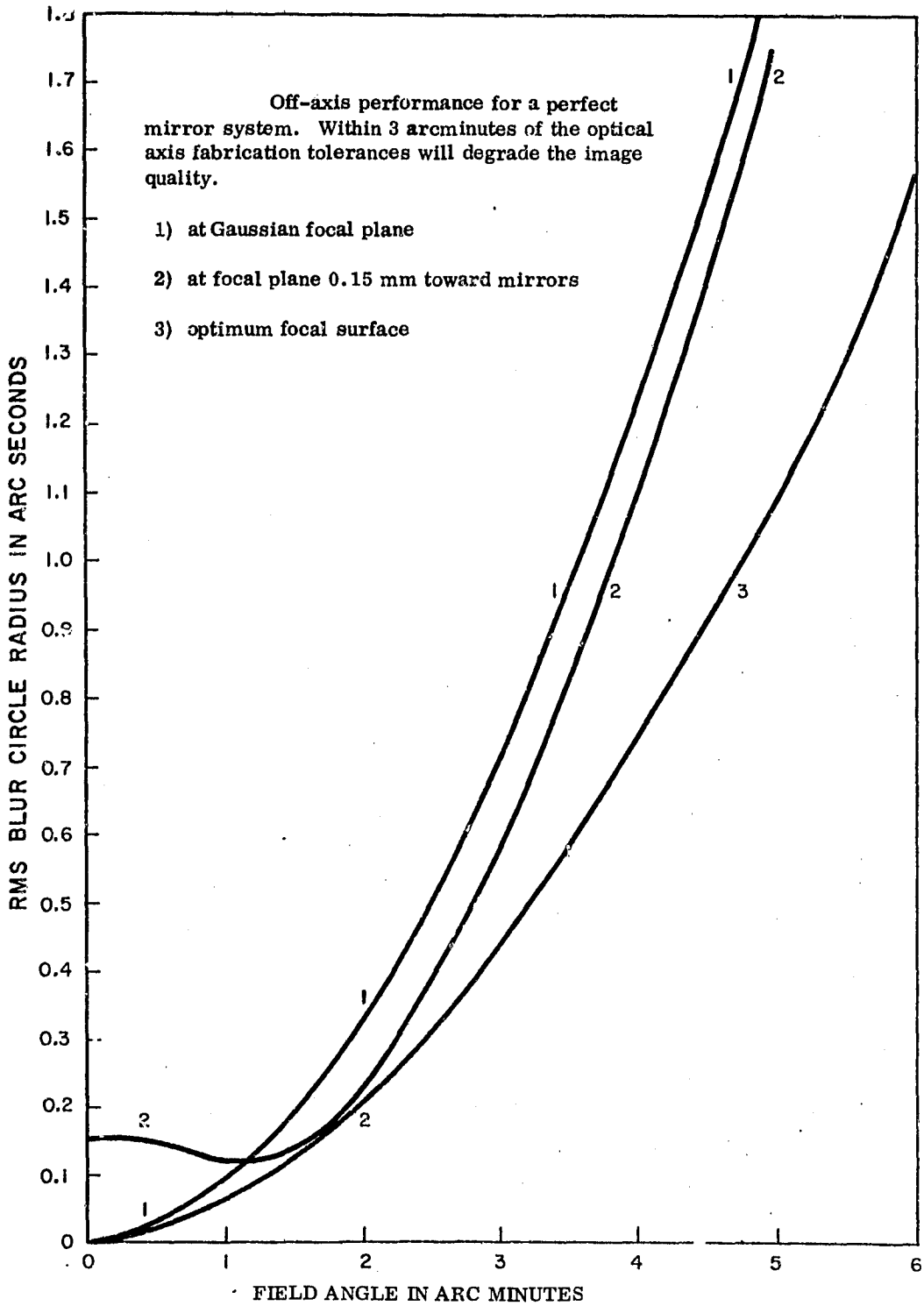


Figure 3.6 - Off-axis performance for a geometrically perfect mirror system. (Within 3 arcminutes of the optical axis, fabrication tolerances will degrade the image quality.)

tion conical geometry typical of X-ray telescopes assuming a Gaussian auto-correlation function. (Fits to Einstein test data, using measured values of roughness and an estimated value of 0.05mm for the correlation length, agreed qualitatively with the scattering which was observed.) The scattering model can be improved by making a more realistic approximation to the auto-correlation function, but is useful in its present form to indicate the scale of scattering effects to be expected for AXAF.

The results of the calculations (Figure 3.7) show that a 15 Å surface, which is a conservative expectation, will have less than 24% effective area loss from the central image for E < 2 keV, but only about 20% remaining in the central image at 7 keV. The angular scale of the scattering is small, however, and for most observations much of the energy will not be lost; for example, about 50% of the energy at 7 keV will be within 10 arcseconds of the image center.

Figure 3.8 is a comparison of the energy response of the AXAF and Einstein mirrors. The total effective areas are shown. For Einstein at 3 keV, 50% of the photons incident on the focal plane are imaged in a circle of 17 arcsecond diameter; for AXAF, it is expected that 50% of the photons would be imaged into a 1 arcsecond diameter circle at this energy.

A more complete description of the high resolution mirror assembly can be found in the report SAO-AXAF-79-003.

### 3.1.3 Mechanical Design

The success of the Einstein Observatory mirrors in terms of optical/X-ray tests, mechanical and thermal tests, and subsequent on-orbit performance provides an excellent basis for the development of the AXAF mirror assembly design. It also creates a temptation to merely "scale up" the Einstein design directly and concentrate on other aspects of the studies. This is not as straight forward as it appears initially when both the improved resolution

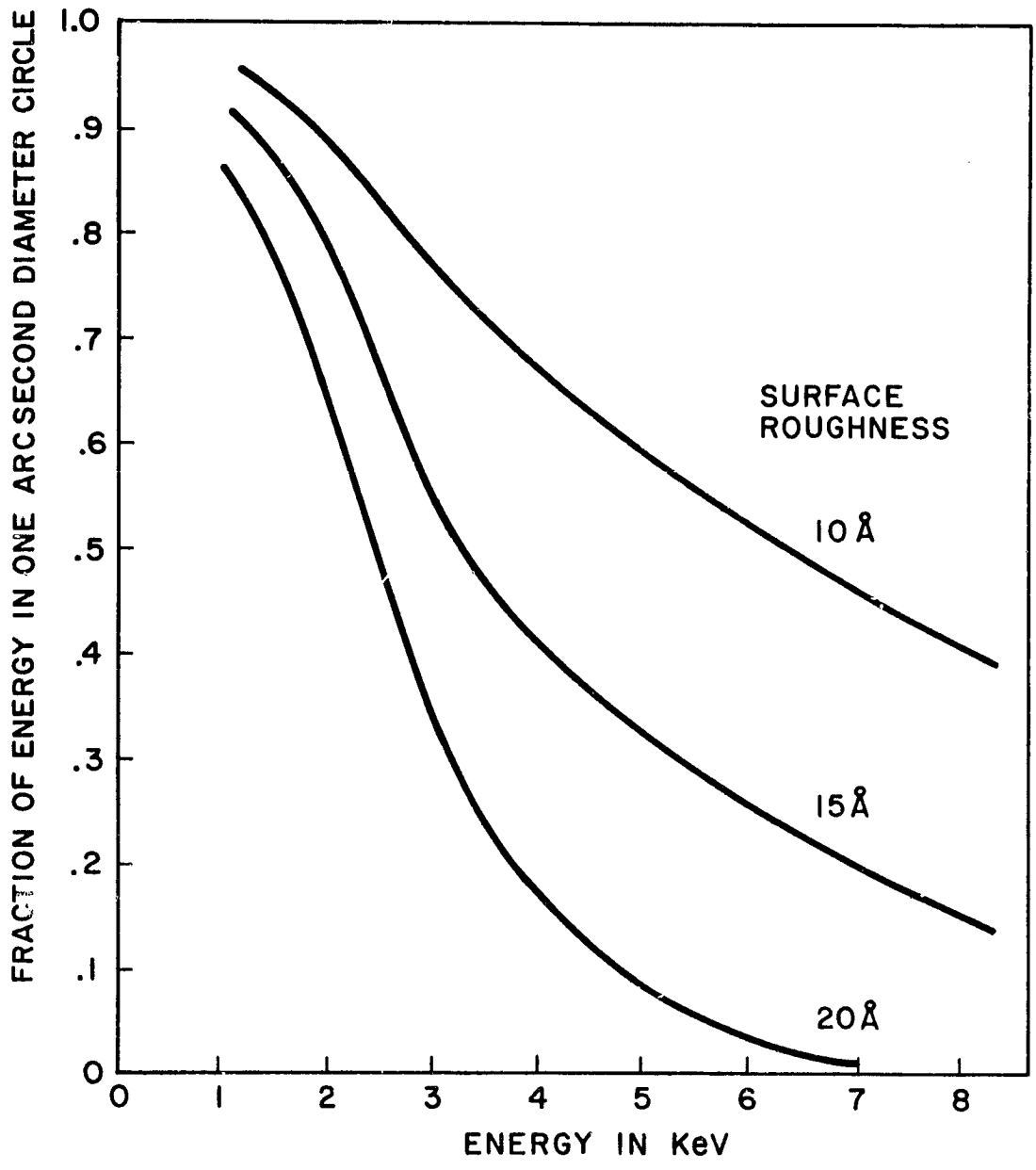


Figure 3.7 - Calculated fraction of the encircled energy in a 1 arcsecond diameter circle for an on-axis point source as a function of X-ray energy and rms surface roughness for the AXAF mirror assembly.

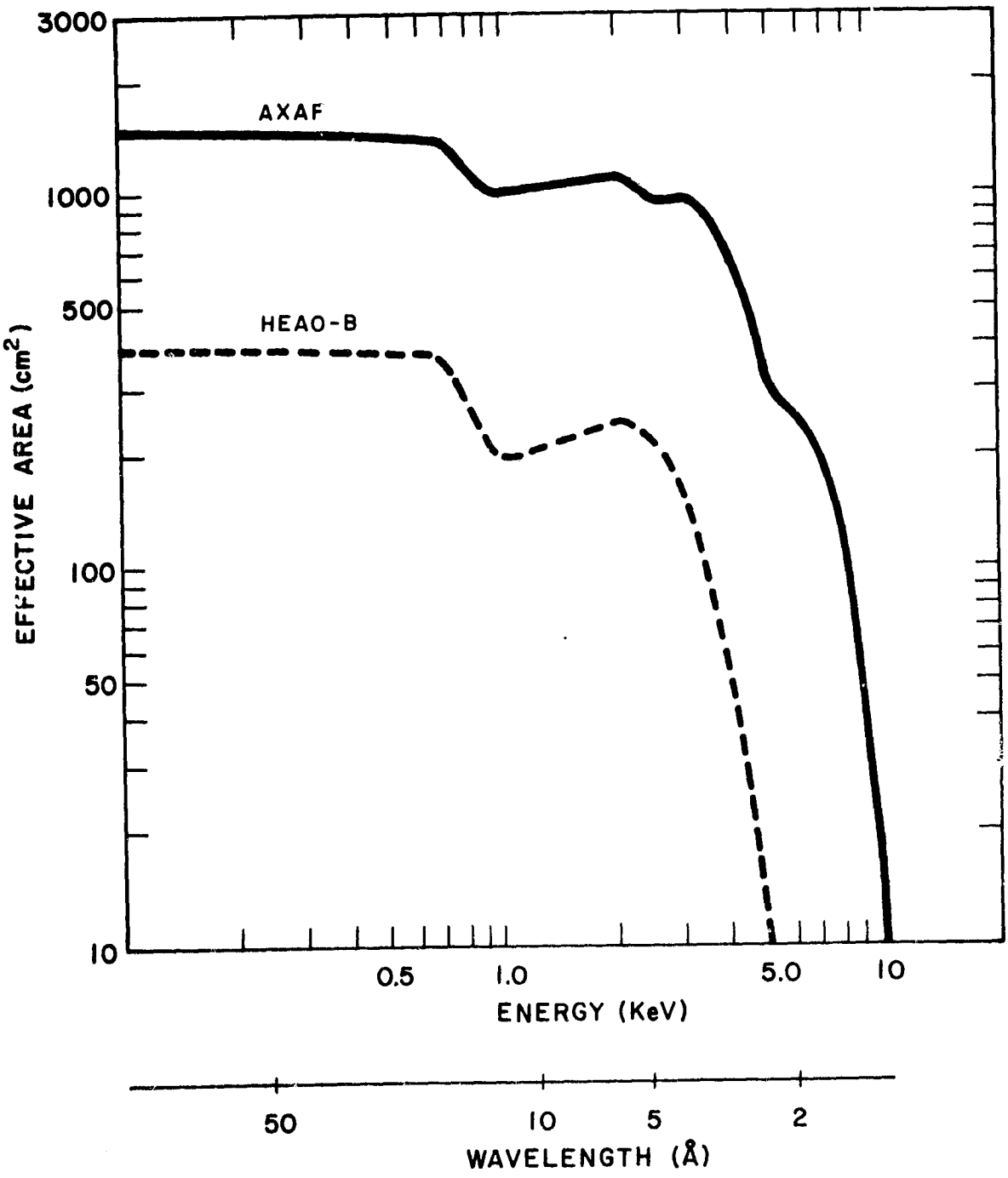


EFFECTIVE AREA VS. ENERGY

Figure 3.8 - A comparison of the energy response of the AXAF and Einstein mirrors. The total effective areas are shown.

and increased size of the AXAF as compared with Einstein are considered. A comparison of the relative sizes of AXAF and Einstein is shown graphically in Figure 3.9.

There are four principal criteria to be satisfied in developing the mechanical design of the AXAF telescope:

(a) Will the mirrors survive mechanical and thermal loads during launch, re-entry, relaunch, and orbital operations, and maintain its alignment?

(b) Can telescope performance be tested horizontally and on the ground with X-rays in a meaningful way?

(c) Is the design such that support fixturing during alignment, assembly, and horizontal test permits reliable prediction of 0g performance?

(d) Does the design permit assembly and alignment to the desired level of precision?

In this section three basic support concepts are presented which illustrate the classes of mirror assembly systems under study by SAO/MSFC. A detailed discussion of the mirror assembly structural analysis can be found in the report SAO-AXAF-79-003.

Figure 3.10 shows cantilever, cluster, and modified cantilever designs. The cantilever design is an extension of the Einstein mirror design. The major difference between the present designs and the Einstein design is the addition of a support sleeve for each mirror. A common center support plate rigidly controls the coaxial alignment of the elements. The cantilevered approach has the disadvantage of an inherent 1g sag and some uncertainty in the load path which may impair our ability to predict 0g performance.

The cluster design overcomes some of the disadvantages of the cantilever approach. It has reduced 1g sag (essentially only a decentering without any tilt) and more control of the load paths. Its disadvantages include complexity

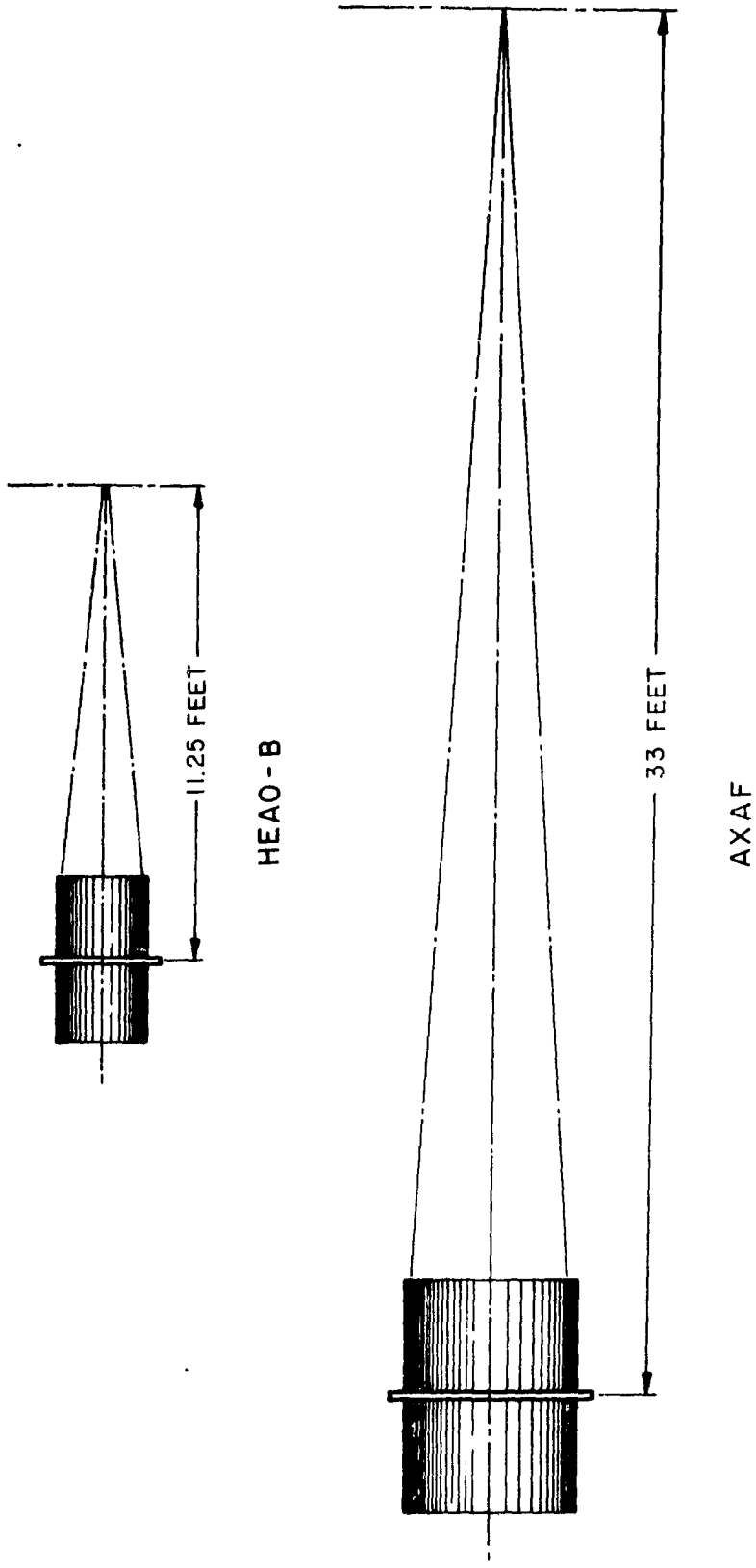


Figure 3.9 - A comparison of the relative sizes of the AXAF and Einstein.

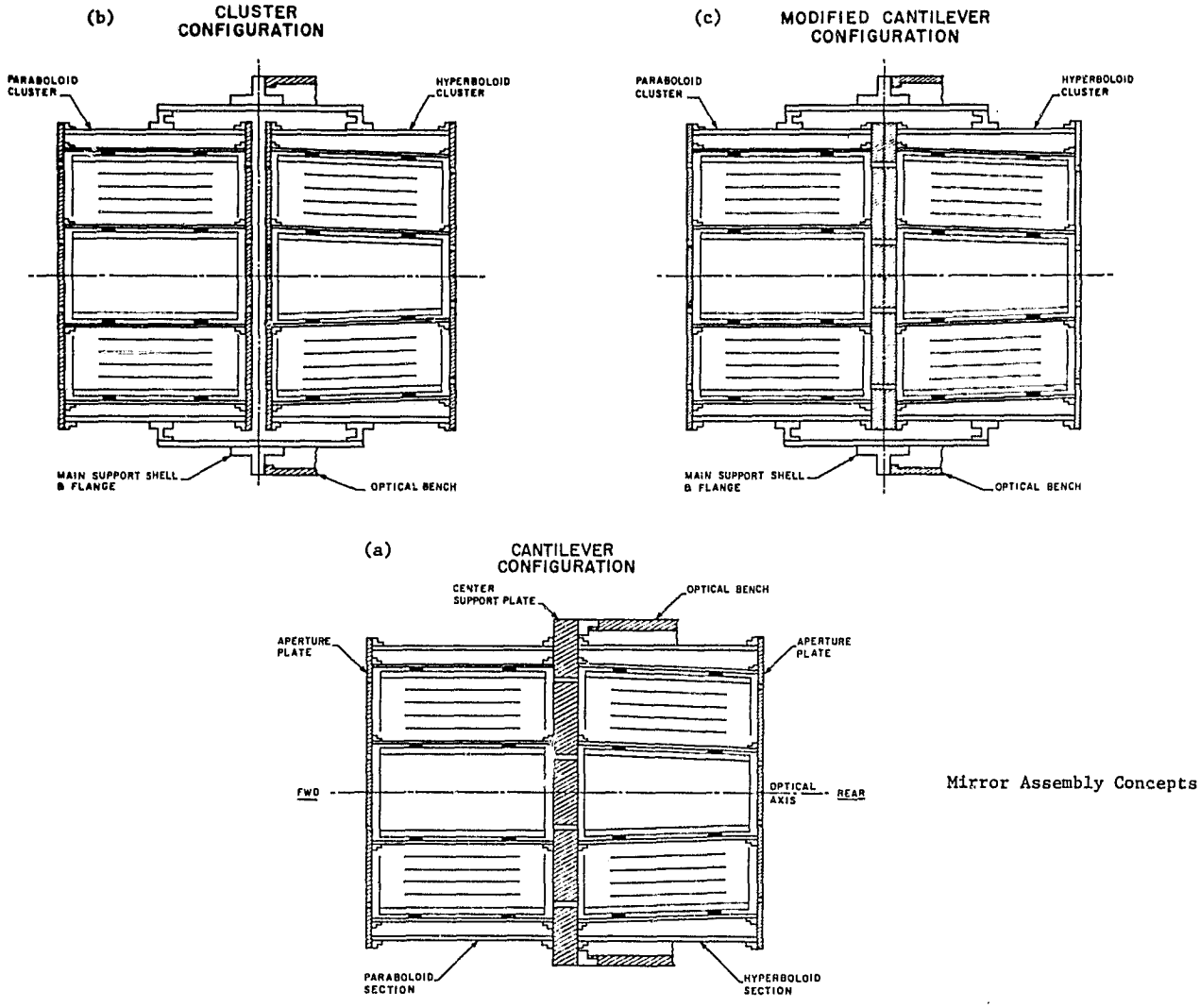


Mirror Assembly Concepts

Figure 3.10 - The cantilever, cluster, and modified cantilever mirror assembly concepts.

in the assembly and alignment process due to less direct coupling of the paraboloids and hyperboloids. More elaborate fixturing may be required in assembly, and the telescope may have a lower natural frequency in the lateral direction.

The third design, the modified cantilever, is a combination of the preceeding two which should prove to combine the advantages of both while minimizing the disadvantaged.

It should be noted that all three designs incorporate a significant design improvement resulting from the work to date: namely, the use of a graphite/epoxy (or similar material) support sleeve to connect the individual mirror elements to the aperture plate. This method of support, as opposed to the Einstein method where the mirror elements are bonded directly to the flanges, has the advantage of reducing lg effects in the element itself to very small levels. It also permits isolating the mirror elements from global lg effects.

The twin goals of 0.5 arcsecond telescope and post facto relative aspect determination to better than 0.5 arcsecond require the optical bench to be considered together with the mirror assembly, the aspect determination system, and the focal plane assembly as an integrated X-ray Telescope Assembly (XTA) system. Optical bench studies have been concentrated on analysis of allowable thermal and mechanical deformations. The results indicate that the required static tolerances can be met with realizable configurations. Additionally, concerns relative to dynamic response considerations have been identified and indicate the need to perform dynamic analyses of all candidate configurations.

Temperature control of the mirror assembly is required in the fine sense to maintain optical figure and alignment tolerances and in the coarse sense to preclude excessive local stress levels due to differential thermal expansion. The basic concept examined is shown in Figure

3.11. The objective is to establish a benign thermal environment for the mirror assembly and to isolate the X-ray Telescope Assembly from the outer thermal shroud and the support system module. In the figure "active" is taken to mean either controlled heaters or variable surface properties (louvres, etc.). The emphasis has been on the use of heaters alone to establish isothermal surfaces.

The requirement for control of the optical bench temperature along its entire length is strongly dependent upon the material selected and is not firmly established. However, the design of a wide variety of instruments over the life of the AXAF will be greatly simplified by a standard, uniform environment. Although Figure 3.11 shows the bench establishing the focal plane environment only for the front assembly, the detailed design certainly could be extended to provide control for the entire focal plane assembly.

## 3.2 Focal Plane Assembly

Modularization of the AXAF focal plane instruments is a concept that was developed in the initial AXAF conceptual design studies. Some of the primary advantages associated with modularization are the standardized instrument volumes for both the first flight and replacement focal plane instruments. The electrical and mechanical interfaces as well as ground handling and transport can also be standardized. The modules provide a common instrument level verification test vehicle and standardize the instrument/facility integration requirements. The on-orbit handling, integration, and removal as well as Shuttle/instrument return interfaces are the same for all instrument modules.

Modularization also allows an instrument to provide for its own special requirements within the module, such as gas supply, adjustable focus mechanisms, etc., without placing the burden for unique instrument services on the AXAF facility.

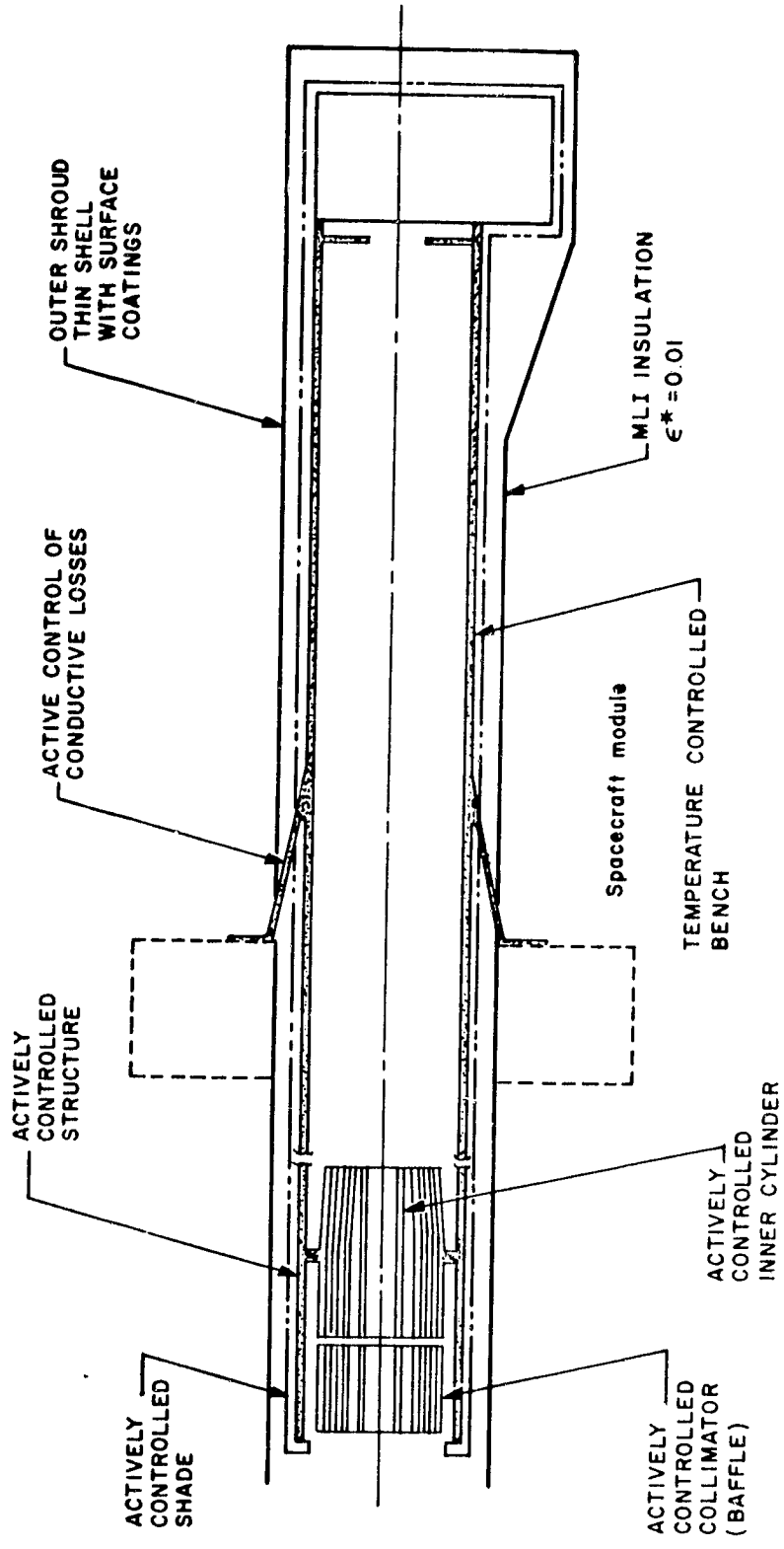


Figure 3.11 - Temperature control of the mirror assembly.

In fact, the prime purpose of mounting a complete AXAF focal plane instrument within a module is to accommodate on-orbit instrument maintenance with a minimum of complexity. The on-orbit maintenance concept is a primary requirement of the AXAF facility, necessary for the extension of observational capability beyond 10 years, with a variety of focal plane instruments.

Two major types of focal plane assembly concepts have been studied for use on the AXAF program: the rotating carousel and the fixed focal plane assemblies. A third concept, the radial track focal plane assembly was reviewed but discarded because of inherent complexities of the system.

The carousel focal plane assembly concept is a cylinder which rotates about a central shaft to place a radially-mounted focal plane instrument into the mirror focus position of a fixed axis mirror assembly (Figure 3.12).

The fixed focal plane assembly concept can be as simple as a fixed plate or nonmovable mount to which the focal plane instruments are mounted. Here the mirror assembly is moved to position the mirror focus on each focal plane instrument (Figure 3.13).

Figure 3.14 depicts the concept of a modularized AXAF carousel focal plane assembly utilizing the strawman instrument and instrument module sizes. This figure combines in one illustration, the estimated size, weight, and power requirements of each modularized strawman AXAF focal plane instrument. The anticipated larger detectors, the low and high resolution imagers, occupy the 90 degree modules, while the others are assigned the smaller 30 degree modules. Also illustrated are the positions of the electronics assemblies and gas reservoirs, where applicable. These assemblies are positioned forward of the detector to minimize the length of the focal plane assembly aft of the mirror focus and to allow the detector to grow along both the Y (lateral) and Z (vertical) axes to the maximum that the particular module will allow.

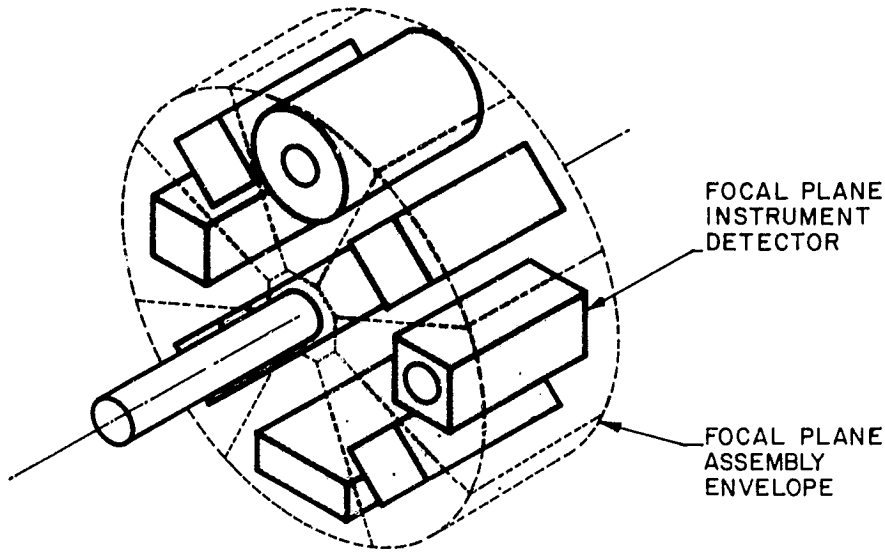


1A - CAROUSEL FOCAL PLANE ASSEMBLY

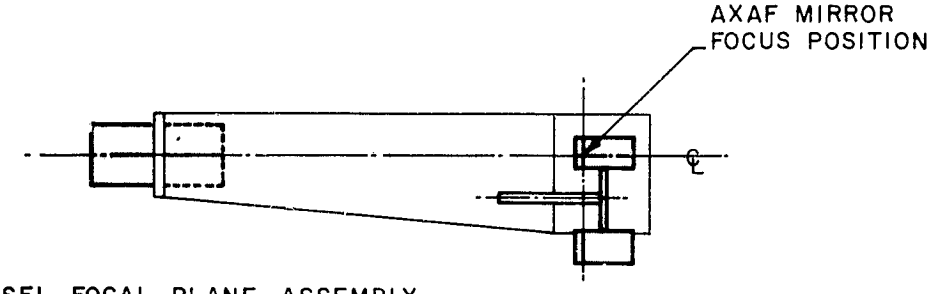


1B - CAROUSEL FOCAL PLANE ASSEMBLY
WITH FIXED AXIS MIRROR ASSEMBLY

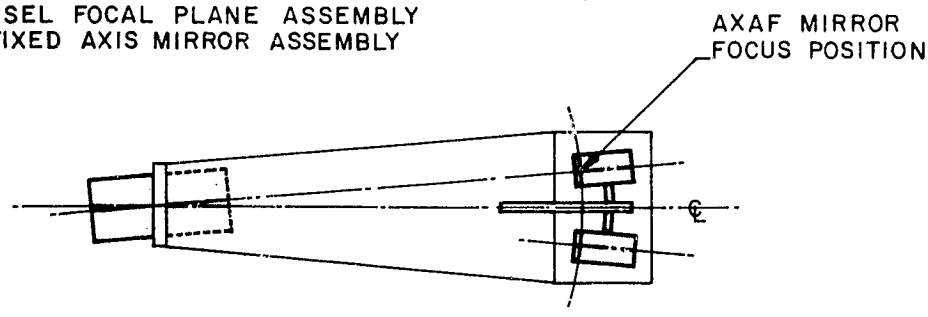


1C - CAROUSEL FOCAL PLANE ASSEMBLY
WITH FIXED AXIS ANGULAR OFFSET
MIRROR ASSEMBLY

## CAROUSEL FOCAL PLANE ASSEMBLY

Figure 3.12 - The carousel focal plane assembly concept.

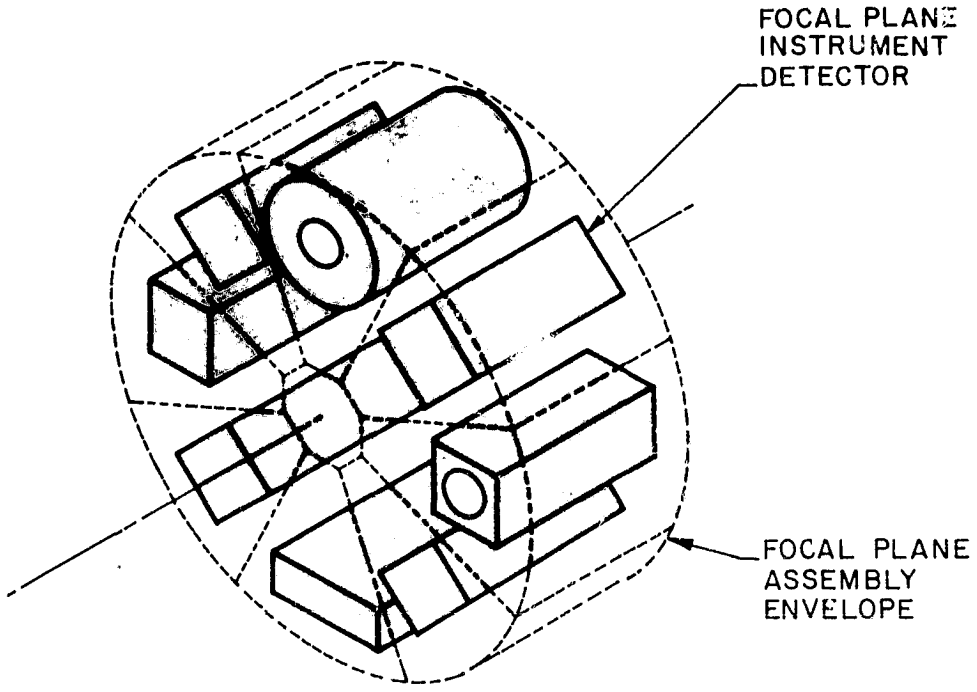


FIXED FOCAL PLANE ASSEMBLY

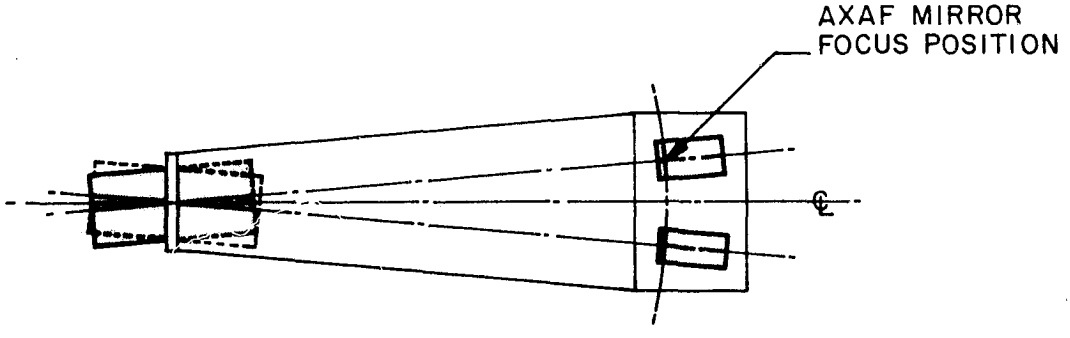


FIXED FOCAL PLANE ASSEMBLY WITH
MOVEABLE AXIS MIRROR ASSEMBLY

Figure 3.13 - The fixed focal plane assembly concept.

Figure 3.14 - A modularized AXAF carousel focal plane assembly utilizing the strawman instrument and instrument module sizes.

Figure 3.15 illustrates the facility provided instrument interfaces for a modularized instrument. All interfaces would be connected automatically upon insertion of the module. Fastening of the modularized instrument to the instrument support structure would be accomplished utilizing a GSE flexible drive unit.

A more detailed description of the AXAF focal plane assembly concepts can be found in the report SAO-AXAF-79-004.

## 3.3 Facility Cooling System

A facility cooling system to support the low temperature cooling requirements of the aspect system and focal plane instruments represents an extension of the modularization effort and also maximizes the transfer of Einstein past and on-going experience.

AXAF must accommodate a wide variety of focal plane instruments. It is always desirable to provide a benign thermal environment to these instruments as well as the AXAF mirror and aspect system. An on-board cooling system could be provided with capabilities to satisfy the cooling requirements of solid state aspect detectors and to provide some level of cooling for the focal plane instruments.

Four basic types of cooling systems were reviewed in determining a candidate AXAF facility cooling system. These were the closed cycle, open cycle, solid state, and passive radiator systems.

Based upon a preliminary examination, an attractive approach appears to be the passive radiator type system. This type cooling system offers the longest operational life, highest reliability, and greatest design flexibility for heat loads greater than 10 watts in the temperature range of 100 to 200 °K of all the systems reviewed. A diode heat pipe radiator and variable conductance heat pipes and heat sinks could be coupled together to provide a stable heat

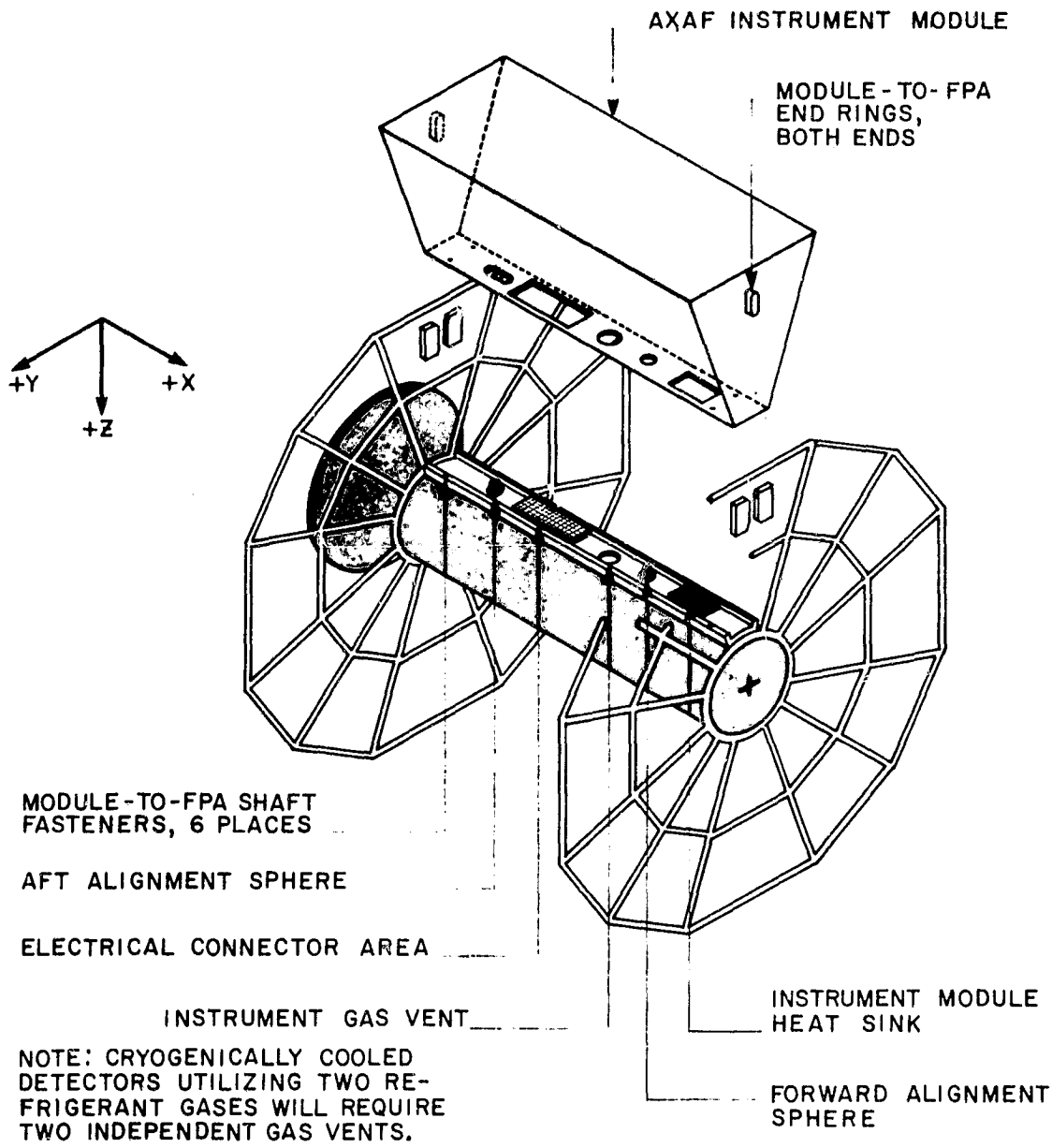


## FOCAL PLANE INSTRUMENT MODULE INTERFACES

Figure 3.15 - AXAF provided instrument interfaces for carousel or fixed focal plane assemblies.

sink temperature during the low orbit, low inclination mission planned for AXAF. The function of the variable conductance heat pipes (VCHP) would be to maintain a near constant heat sink temperature with varying heat input from the various focal plane instruments. The function of the diode heat pipes would be to thermally disconnect a radiator from the cooling system during periods when the external environment does not permit heat rejection to space. For a focal plane open cycle (cryogen) cooled detector, the combination of increased volume of cryogen plus diode heat pipe to reduce the parasitic heat load could possibly extend the life of the cryogen to meet or exceed the AXAF three-year on-orbit lifetime requirement.

A representative AXAF cooling system might be configured as follows:

Three or more passive radiators, $\sim$ 3 square meters each are positioned about the AXAF facility (Figure 3.16). To maximize heat rejection, the radiators are connected to both a heat sink or plenum located within the central shaft area of the focal plane assembly by diode and variable conductance heat pipes or fluid loop. At six of the focal plane instrument pallet positions, an aluminum heat sink would be located as a heat rejection point for the modularized instrument. (Instruments not requiring cooling could be required to add a heater at this location to balance the system if necessary.) Within the module a fluid loop heat pipe or bus bar is utilized to transport the heat load of the cold plate. As an application to a high resolution CCD imager, a thermoelectric cooler at the detector could be thermally connected to the heat sink using the fluid loop method. The thermoelectric cooler in this case is used to remove the conductive, convective, and power dissipative loads of the detector mosaic and lower its temperature to about 160°K from the 180 - 190°K heat sink temperature provided by the AXAF cooling system. Similar lines also run from the radiators to a forward heat sink, which in turn, is connected to each aspect sensor detector.

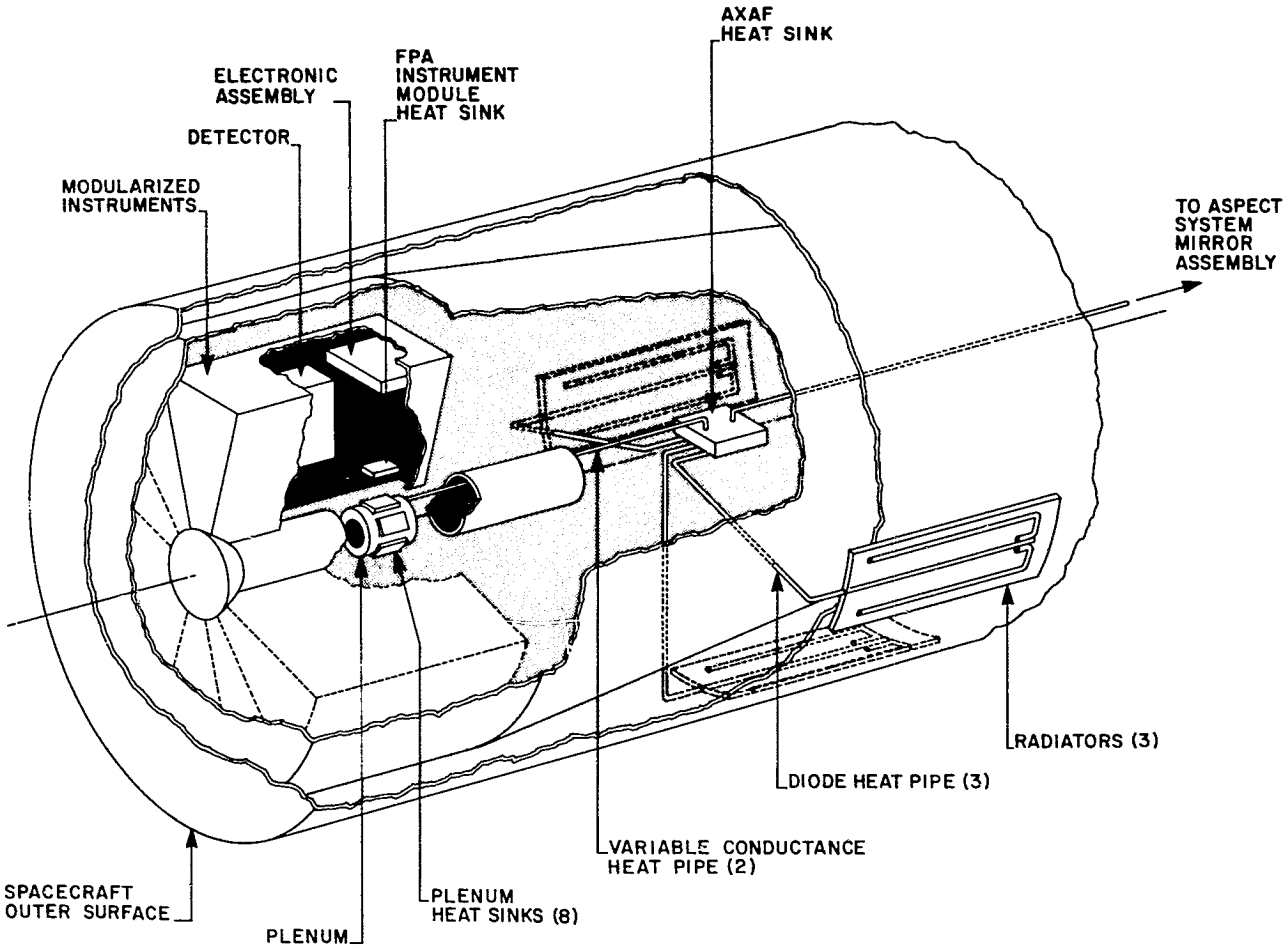


## AXAF COOLING SYSTEM

DIODE HEAT PIPE
RADIATOR CONCEPT

Figure 3.16 - Diode heat pipe radiator concept.

The passive radiator cooling system has no moving parts, hence, its reliability and operational lifetime are better than with other systems. The system can be designed to provide the low temperature cooling in the range of 180°K in non-sun-synchronous low earth orbits (350 - 500 km and inclinations of 28 degrees), where radiative cooling was never before considered.

## 3.4 Aspect Determination System

X-ray imaging of weak sources will require long observations over many orbits during which changes of up to 30 arcseconds in the AXAF optical axis pointing vector can occur (by the present strawman specification). Thus, even though the source is fixed in celestial coordinates, the detected events will be spread over the image plane due to the vehicle motion during the observations. In order to reconstruct an X-ray image it is necessary to refer the point in the image plane at which the event was detected to an apparent source position in celestial coordinates. The instantaneous optical axis must be reconstructed in roll, pitch, and yaw. Therefore, aspect data which references the position of the X-ray image to the celestial sphere are truly part of the scientific data. A key point is that image reconstruction will, at least in general, be performed on the ground. The aspect solution can therefore also be post facto. Figure 3.17 illustrates the principles of the AXAF aspect system.

The ultimate quality of the reconstructed image will be determined principally by the resolution of the X-ray mirror assembly, the uncorrectable effect of system motions, the resolution of the X-ray detector used, and the relative accuracy of the total aspect determination system. The present goal is to ensure an aspect solution of relative accuracy 0.5 arcsecond. Such accuracy approaches state of the art capability. The aspect determination system is, therefore, along with the mirror assembly, the major system driver and an area

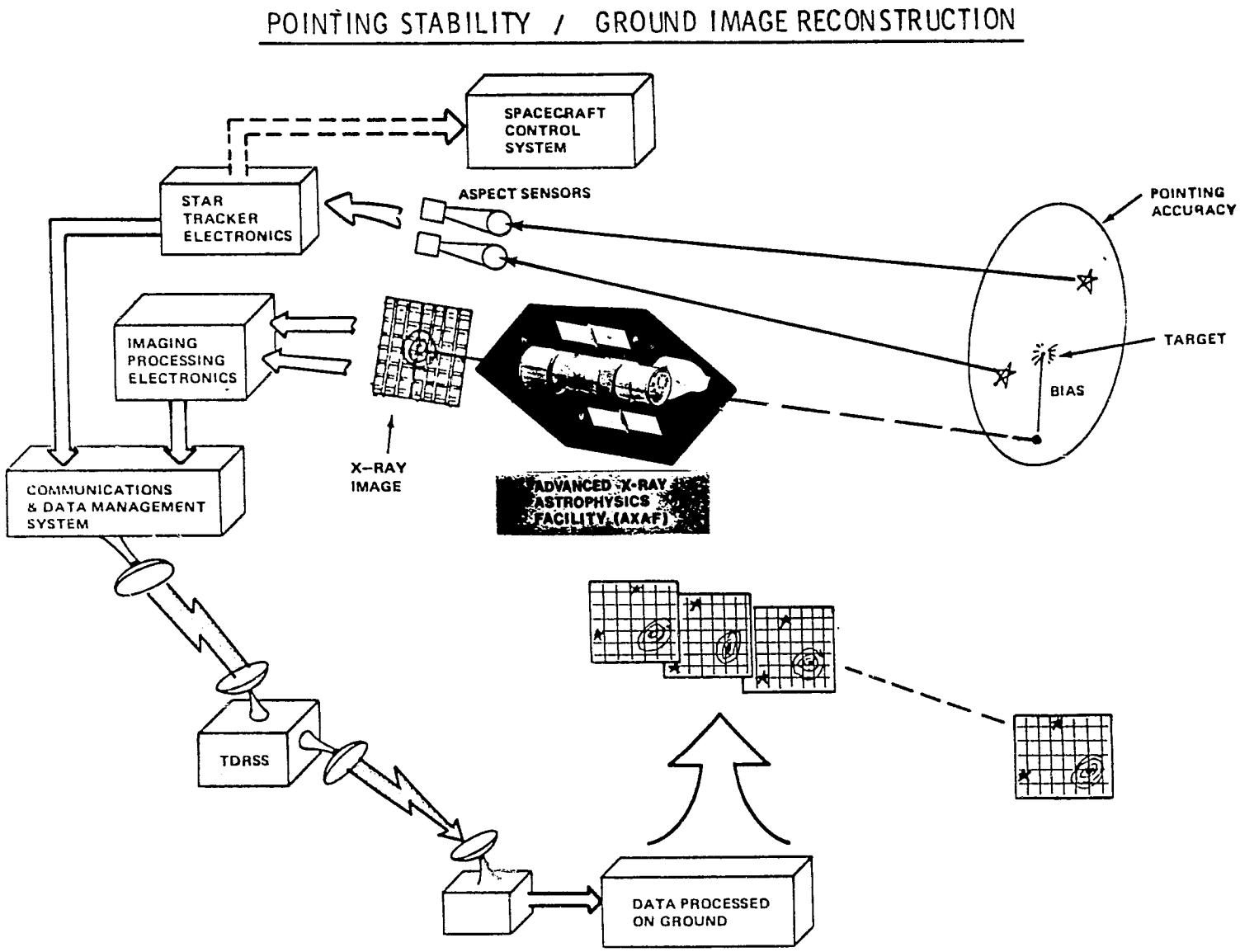


Figure 3.17 - The principle of the AXAF aspect system.

requiring considerable study.

The basic aspect determination system requires:

(1) Appropriate fine aspect sensors mounted in a stable and well-defined way (relative to the mirror assembly) which view both the sky and focal plane fiducial lights.

(2) Fiducial lights and associated optics which refer radial position of the focal plane to the axes of the fine sensors.

(3) On-orbit system absolute alignment calibration provided by viewing known X-ray sources having well-defined and known optical positions.

A preliminary error budget has been established as follows:

| | |
|---|---|
| Fine Aspect Sensor | 0.3 arcsecond |
| Fiducial System and Structural Stability | 0.2 arcsecond |
| Effect of "Fast Motions" and Sampling Error Due to Spacecraft Motion | 0.1 arcsecond |
| Root Sum of Squares | < 0.4 arcsecond |

The above error budget deals with relative accuracy. This is the precision with which the image can be reconstructed. Absolute accuracy requires knowledge of the relation between the X-ray telescope instantaneous axis and fixed stars whose positions are well established. In practice, this will be done by viewing an X-ray source which is also an accurately located optical source. This will determine the alignment of the X-ray telescope axis to the aspect system axis. (The fiducial light system will permit tracking of temperal variations in alignment between "boresightings".) The Einstein Observatory has significantly increased the number of available "boresight" X-ray sources. The absolute position or aspect accuracy will be determined by the absolute accuracy of optical position determinations ($\sim$ 1 arcsecond). Thus, at present, system studies are proceeding with aspect

determination goals of 0.5 arcsecond post facto relative accuracy and 1.0 arcsecond post facto absolute accuracy.

Preliminary study has shown that the image dissector tube (IDT) sensors of the type used in Einstein will not meet AXAF objectives. Improvements in the aspect sensor accuracy may be obtained by using solid state detectors. The study is directed not towards the detailed design of a specific sensor, but towards an in-depth understanding of aspect system performance specifications affecting AXAF scientific capability. This analysis and the Einstein experience will provide the basis for specification of an AXAF fine aspect sensor.

Table 3.1 gives a comparison of the AXAF, Einstein, and Space Telescope aspect/attitude control systems.

## 3.5 Instruments

The following discussion is meant to provide a representative list of instruments which can exploit the capabilities of the AXAF. This is intended for the purposes of stimulating instrument development and of providing a basis for engineering studies of AXAF requirements.

### 3.5.1 Imaging

The design of suitable imaging detectors for AXAF is driven by the parameters of the mirror system:

| | |
|---|---|
| focal plane scale | 1 arcsecond = 50 μm |
| high resolution field of view | 1 arcsecond resolution within 10 arcminute field (diam.) |
| linear scale for 10 arcminute diameter field | 30 mm diameter |
| total field of view | 1° = 180 mm diameter field |
| energy range | 0.1 - 8 keV |

Table 3.1

| Pointing (arcsec) | AXAF | Einstein† | Space Telescope |
|---|---|---|---|
| Accuracy | 30 | 15 | 0.01* |
| Short Term Stability | 0.1 arcsec/10 sec+ | 1 arcsec/sec | 0.007* |
| Long Term Stability (in 1 orbit) | 30 | 15 | 0.007* |
| Aspect Sensor | 0.3 | 1.5 | Fine Guidance |

† Achieved in orbit.

* Accuracy and stability to these levels are obtained by using Space Telescope optics and extremely accurate fine guidance sensor rather than externally mounted aspect star trackers.

+ Stability to be such that the contribution to the size of the image of a point source due to all motions is to be less than 0.1 arcsec ($1\sigma$) for periods no less than 10 seconds.

and the need for high quantum efficiency ( > 50%), adequate time resolution ($\Delta T \lesssim 0.1$ ms), and moderate spectral resolution ($E/\Delta E \gtrsim 2\sqrt{E/1\ keV}$ ).

At present there is no single device that can achieve all of the imaging objectives which are of central importance to the AXAF mission. Several highly effective techniques have been demonstrated and several promising new ones are in various stages of development. Each of these can achieve one or several of the AXAF imaging objectives. These techniques will be discussed below.

As a point of departure, Table 3.2 gives the basic characteristics of the Einstein imaging detectors.

The following devices are likely candidates for imaging detectors for AXAF and will be discussed in more detail:

Charge Coupled Device (CCD)

Negative Electron Affinity Detector (NEAD)

Microchannel Plate Detector (MCP)

Imaging Proportional Counter (IPC)

Imaging Gas Scintillation Proportional Counter (IGSPC)

(1) Charge Coupled Device (CCD). CCD's are attractive for single photon X-ray imaging because of their broad energy response, high quantum efficiency, relatively high spatial resolution, low readout noise, high charge conversion, small size and weight, low power, and low voltage requirements. Their main disadvantages are that they must be cooled and that they are not yet available in large formats. Development of the CCD as a single photon X-ray detector is being carried out at several institutions, although at a low level of effort.

A CCD is a two-dimensional array of metal-oxide-semiconductor (MOS) capacitors fabricated by depositing electrodes on a silicon wafer (Figure 3.18). The silicon substrate is the sensitive layer in which photons are converted to electron-hole pairs. Localized potential wells at the Si-$SiO_2$ interface generated

Table 3.2 - Characteristics of the Einstein Imaging Detectors

| Einstein Imaging Detector | Quantum Efficiency | Spatial Resolution | Spectral Resolution | Field of View |
|---|---|---|---|---|
| HRI (Multichannel Plate Detector) | Moderate (< 5% above 3 keV) | High (15 μm) | None | 25 mm diameter |
| IPC (Imaging Proportional Counter | High | Moderate (1 mm) | Moderate ($E/\Delta E \sim 1.5 \sqrt{E}$ (keV) | 60 x 60 mm |

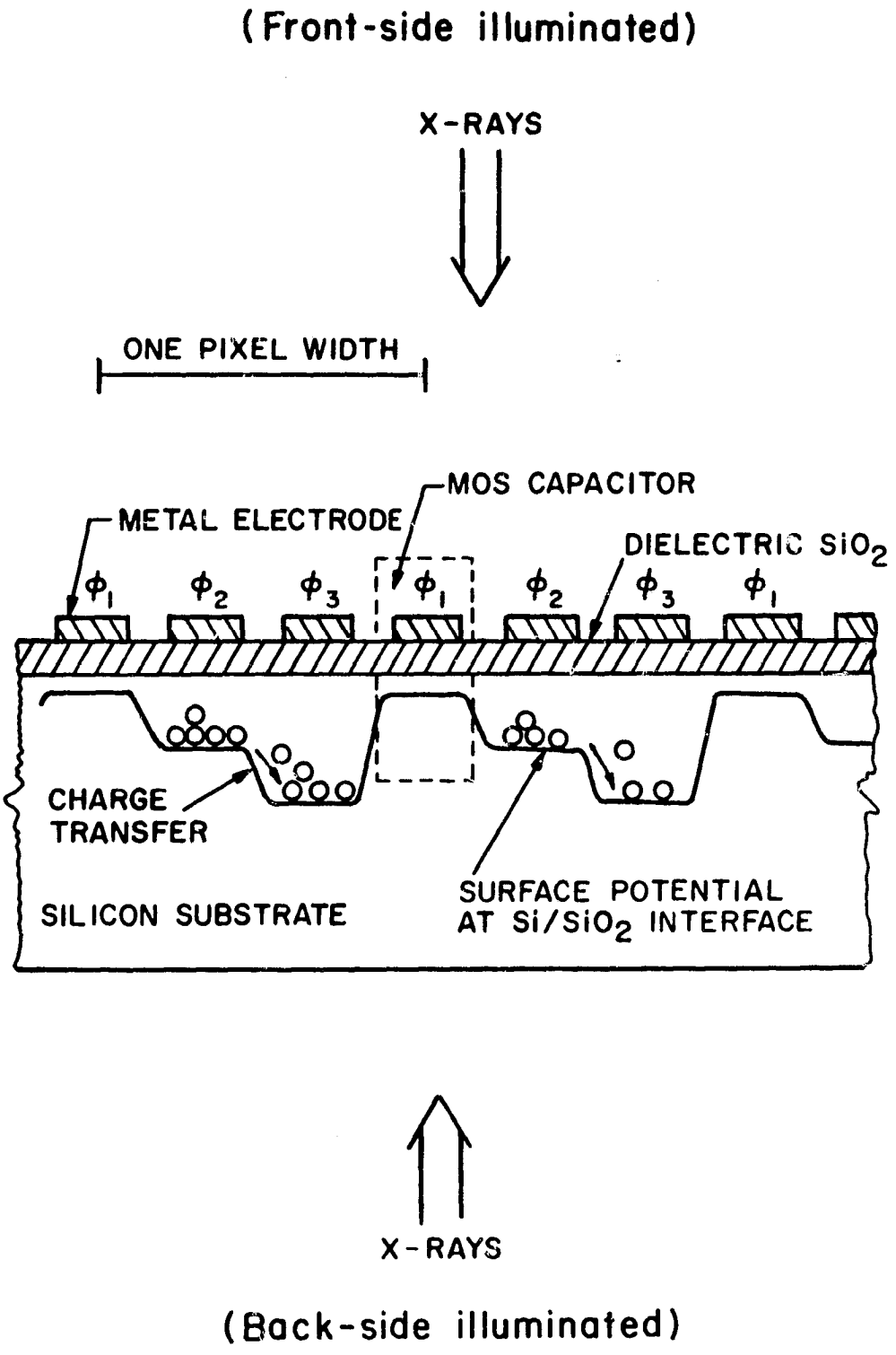


Figure 3.18 - Three-phase CCD illustrating the principle of charge transfer. The depth of the potential well varies with the voltage applied to the electrode.

by biasing the electrodes collect and store minority carrier charges. The charge packets subsequently can be transferred synchronously through the array by manipulation of the electrode voltages which control the potential wells. Typically, the cell or pixel size is 15 - 40 μm.

The CCD, with optimization of its architecture, can provide 50% quantum efficiency over the energy range 0.25 - 7 keV. The low energy response is limited by "dead" layers above the bulk silicon for back-side illuminated devices or by the relatively thick gate structures for the front-side illuminated devices. The high energy response is limited by the thickness of the silicon substrate or the minority carrier diffusion length.

Figure 3.19 shows calculated quantum efficiencies for representative devices. The model for the quantum efficiency takes into account the transmission of the dead layer or dielectric-electrode structures and the absorption by the substrate. All electron-hole pairs created within a depth of 70 μm (the minority carrier diffusion length in silicon varies between 50 and 100 μm) are assumed to be collected.

The number of electron-hole pairs formed within a CCD is proportional to the absorbed X-ray energy. Therefore, the CCD when operated as a single photon detector acts as an array of solid-state spectrometers. The energy resolution is given by the following expression:

$$(\Delta E)_{FWHM} = 2.35 \left[ (\Delta E)^2_{system} + (\Delta E)^2_{CCD} + e_p F E \right]^{1/2} \text{ keV}$$

$(\Delta E)_{system}$: ↑ amplifier (rms)

$(\Delta E)_{CCD}$: ↑ dark current (rms)

$e_p$ = mean energy required to produce one electron-hole pair (0.0036 keV for silicon)

F = Fano factor ($\sim$ 0.15)

E = energy of incident photon

| Device | "Dead Layer" | Substrate |
|---|---|---|
| "A" | 0.5 micron Si | 200 micron Si |
| "B" | 0.25 micron Si | 30 micron Si |

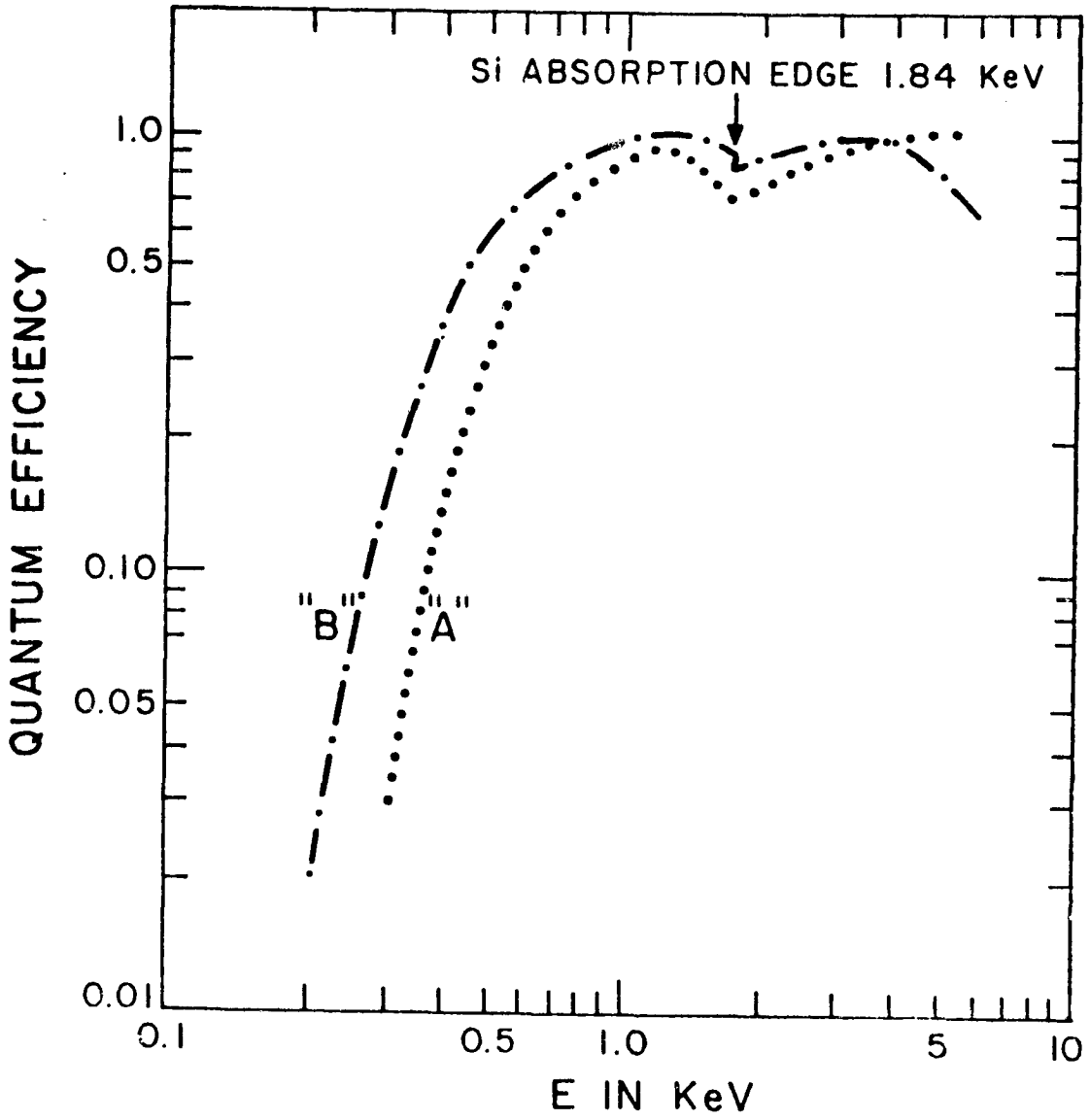


Figure 3.19 Expected quantum efficiency (defined as the probability that an incident X-ray photon is detected as an "event") vs. energy. The calculations consider only the interactions of X-rays in Si, for two hypothetical CCD's whose dead-layer and substrate thicknesses are separately within the range spanned by real devices. There will be a low energy cutoff (not shown) depending on the minimum signal which can be discriminated against the system noise.

Figure 3.20 shows the predicted energy response of the CCD assuming a system plus dark current noise of 0.3 keV (rms noise equivalent signal of 90 electrons). Noise levels one-third of this appear achievable.

As a comparison Figure 3.20 also shows the energy resolution of a conventional gas proportional counter. Since a proportional counter has internal gain, the system noise can be neglected and the energy resolution is:

$$(\Delta E)_{FWHM} = 2.35 \left[ (F + f)WE \right]^{1/2} \text{ keV}$$

where:

F = Fano factor

f = a factor to account for variance in the gas gain

W = mean energy to form an ion pair

As an example, for methane gas:

F = 0.26

f = 0.75

W = 0.027 keV

so that for a proportional counter:

$$\frac{E}{(\Delta E)_{FWHM}} = 2.6\ E^{1/2} \quad \text{(with E in keV)}$$

If the overall noise could be reduced to 10-15 electrons rms, the CCD would compete with the solid state spectrometer in energy resolution, besides simultaneously providing high spatial resolution and high quantum efficiency photon detection.

(2) Negative Electron Affinity Detector (NEAD). The NEAD is an X-ray to optical converter with high quantum efficiency, high spatial resolution, and moderate energy resolution capability. An NEAD would have a quantum efficiency greater than 90% over most of the AXAF energy range and spatial resolution of 15 μm (0.3 arcsecond at the focus of AXAF). The spectral resolution is expected

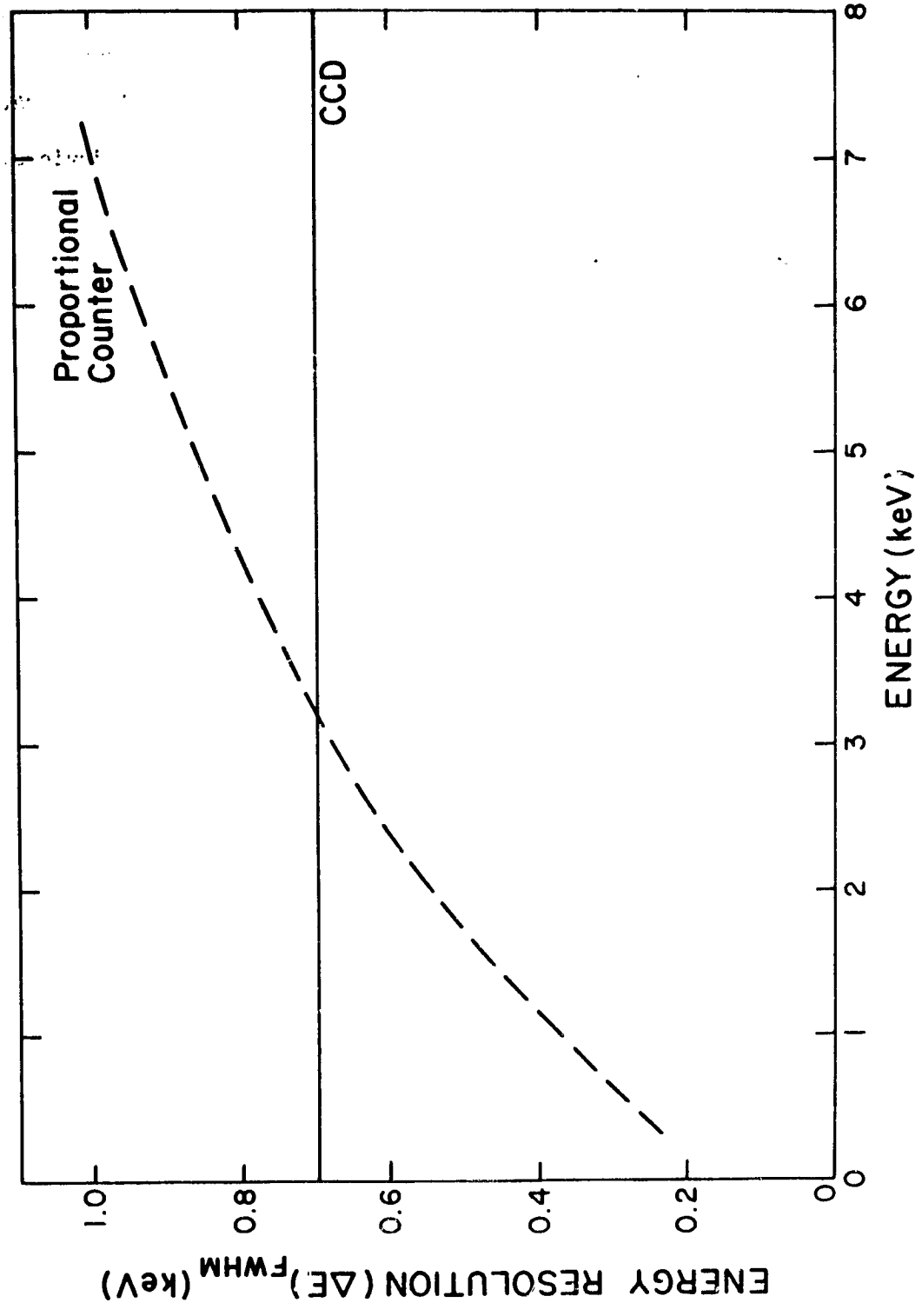


Figure 3.20 - Energy resolution as a function of energy for a proportional counter and a CCD.

to be about 20% FWHM at 1.5 keV and about 40% FWHM at 0.28 keV. This performance has been demonstrated in the laboratory.

Figure 3.21 is a conceptual drawing showing the operating principles of the device. An incident X-ray absorbed in the GaAs crystal results in a large number of electrons emitted at the back surface. These electrons are accelerated to the phosphor screen where they result in a pulse of visible light. The visible light signal is then converted to an electrical signal by means of a visible light image intensifier. Both positional and X-ray energy information can be obtained. A 7 mm diameter GaAs photocathode has been fabricated and it appears, at the present time, that there are no technical problems preventing the fabrication of a device with a 25 mm photocathode.

The quantum efficiency and energy resolution of the NEAD depend upon crystal parameters including thickness, surface yield, and diffusion length, and can be "fine-tuned" for a particular spectral region in the range 0.1 - 7 keV. Figures 3.22 and 3.23 show the predicted performance for a typical photocathode.

(3) Microchannel Plate Detector (MCP). The only fully developed high spatial resolution X-ray detector is the Einstein HRI detector. This device has two microchannel plates in cascade followed by a crossed grid of wires for position sensing. The 15 μm resolution over a 25 mm field corresponds to 0.3 arcsecond resolution over an 8 arcminute diameter field for the AXAF.

The most significant shortcomings of this detector are: the low quantum efficiency, the lack of energy resolution, and the small size. Typical values for the quantum efficiency are 35% at 0.27 keV, 12% at 1 keV, and 2% at 6 keV. Another potential problem area for MCP detectors is count lifetime, although no degradation has been observed in one year of operation of Einstein. Should this become a real problem, it can probably be alleviated by operating the plates at

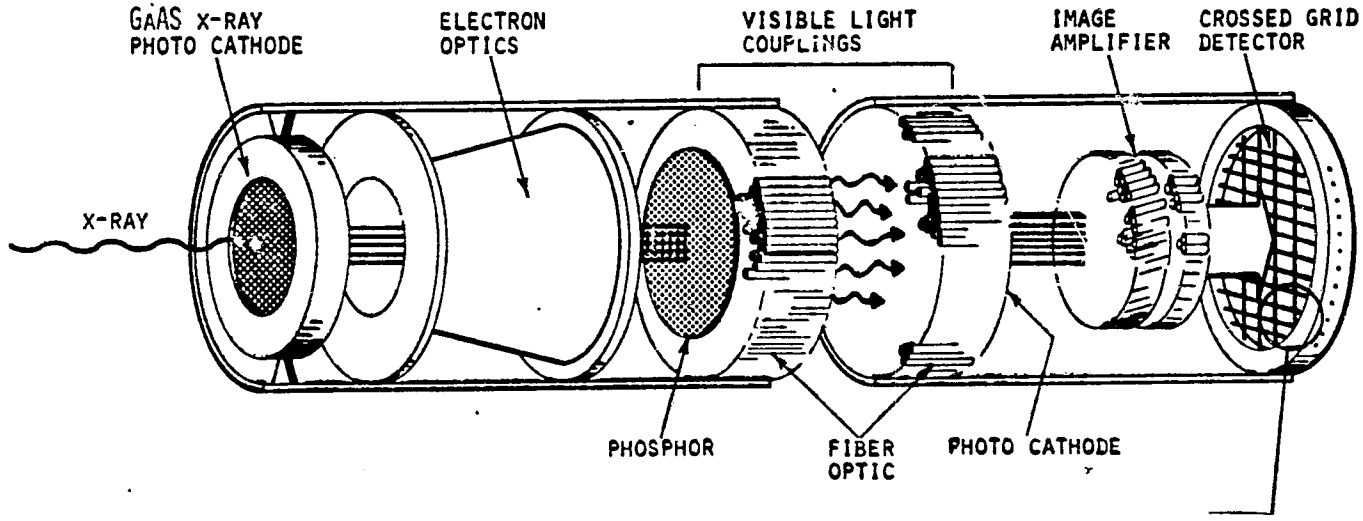


Figure 3.21 - Negative electron affinity photocathode geometry. Each X-ray photon yields many photoelectrons. The photoelectrons are accelerated and focused onto a phosphor and the resulting visible light image is detected with an image intensifier. The volume between the photocathode and the phosphor is permanently sealed and the gate valve permits the crystal to be isolated from atmospheric pressure.

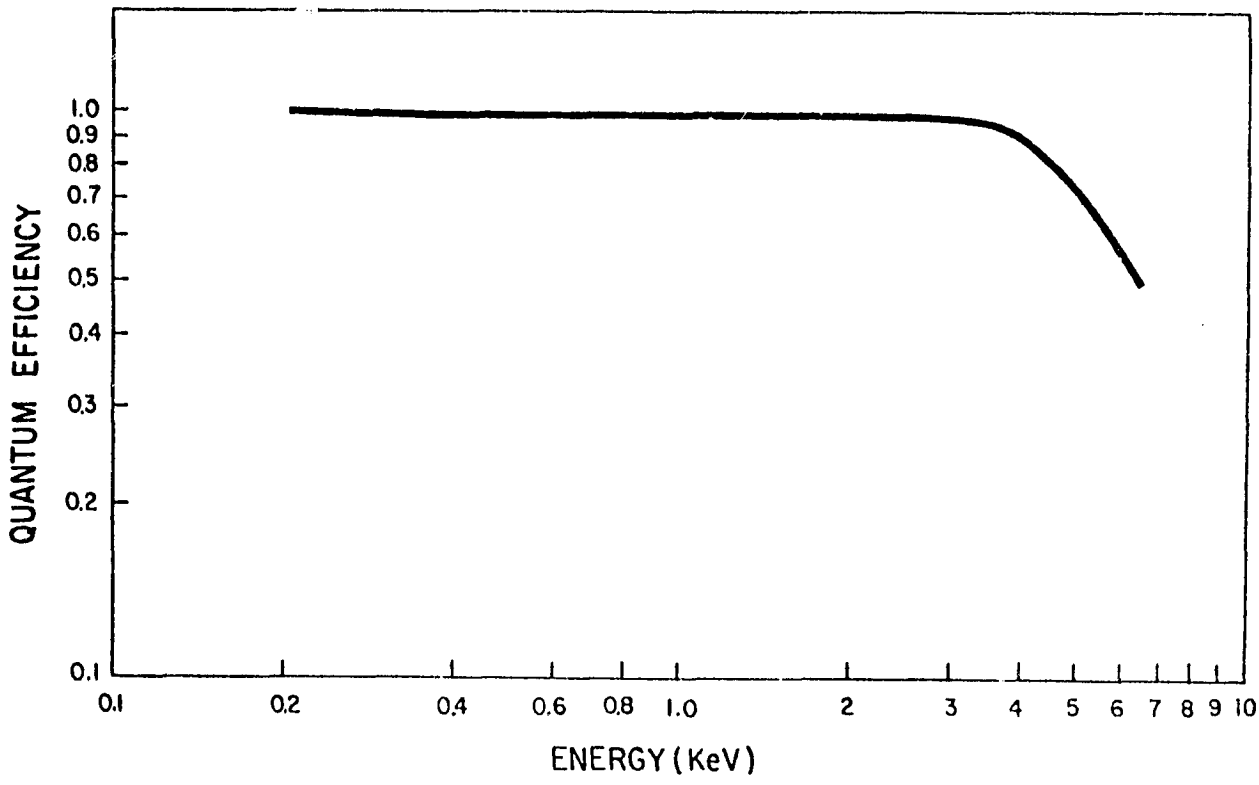


Figure 3.22 - Quantum efficiency of activated GaAs X-ray photocathode.

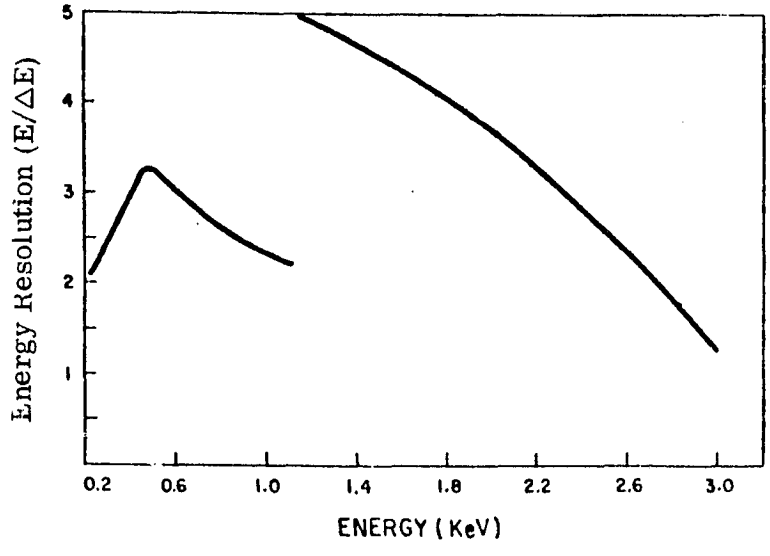


Figure 3.23 - Predicted energy resolution of the NEAD.

a lower gain.

8.5 cm diameter MCP's are now available and these would provide an $\sim$ 30 arcminute diameter field. A readout system for a detector of this size requires an extension of current readout systems. The quantum efficiency can possibly be improved through the use of coatings on the front surface of the MCP.

(4) Imaging Proportional Counter (IPC). The most widely used detector in X-ray astronomy to date has been the gas-filled proportional counter. They were used in most of the early rocket experiments, as well as in the Uhuru, OSO-7, Ariel V, SAS-3, and HEAO-1 satellites. An imaging version of this detector has been developed and is used with the Einstein X-ray telescope. Proportional counters have the virtues of providing high efficiency over the energy range 0.1 to 8 keV and above, good time resolution, background rejection, and moderate energy resolution. They have an excellent record of reliability and can be made arbitrarily large in size.

The Einstein Imaging Proportional Counter covers a region 70 x 70 mm in size and has a spatial resolution of 1 mm. Its energy resolution $E/\Delta E$ is $\sim 1.5 \sqrt{E(keV)}$ . It will not be difficult to construct a detector that is a factor of three larger in scale. This will cover the whole field of the AXAF. Recent developments have shown that IPC's can be built with a spatial resolution of a few tenths of a millimeter. If we assume that the spatial resolution is 0.5 mm, an IPC in the focal plane of the AXAF will have an angular resolution of 10 arcseconds. An energy resolution $E/\Delta E \gtrsim 2 \sqrt{E(keV)}$ is also achievable.

An IPC can also be used effectively as the detector for an objective grating spectrometer. For a 3000 line/mm grating, an IPC could cover both sides of the dispersed spectrum down to 0.2 keV and at 0.5 keV the energy resolution $E/\Delta E$ would be $\sim$ 100.

(5) Imaging Gas Scintillation Proportional Counter (IGSPC). An imaging gas scintillation proportional counter is a possible focal plane instrument on the AXAF. Such an instrument would have twice the energy resolution of conventional proportional counters, a position resolution of 1 arcminute or better at 2 keV, and background rejection capabilities similar to conventional proportional counters. The improved energy resolution and the large field of view (1° x 1°) of the IGSPC are well suited to mapping spectral features such as iron emission lines in galactic supernova remnants, interstellar hot gas, and clusters of galaxies out to Z = 0.5. The high quantum efficiency ( > 50% over most of the bandwidth from 0.1 to 8 keV) and good background rejection characteristics of the IGSPC will permit one to obtain detailed spectrophotometry of active galaxies and quasars out to Z = 3. Figure 3.24 demonstrates the dramatic improvement in spectral information obtainable with a IGSPC measurement of Cas A as compared with that obtainable by a conventional proportional counter. Iron L, silicon K, sulfur K, and iron K lines as well as the interstellar oxygen absorption edge are clearly distinguishable in the IGSPC simulation of a 1000 second AXAF observation.

Large area (250 $cm^2$), high sensitivity non-imaging GSPC's have now been built and successfully tested for flight on sounding rockets. Smaller GSPC modules with micron thin polypropylene windows have been shown to work successfully down to 0.1 keV, yielding better energy resolution at 0.28 keV ($E/\Delta E = 2.8$) than any other broad-band instrument available today (Figure 3.25). Efforts are currently underway to test the imaging capabilities of such an instrument. Several alternative approaches have been suggested to provide position information without compromising the good energy resolution. The most straightforward approach follows: an Anger camera design. A multiple phototube array is used behind a 20 x 20 cm parallel grid GSPC to view the ultraviolet photons

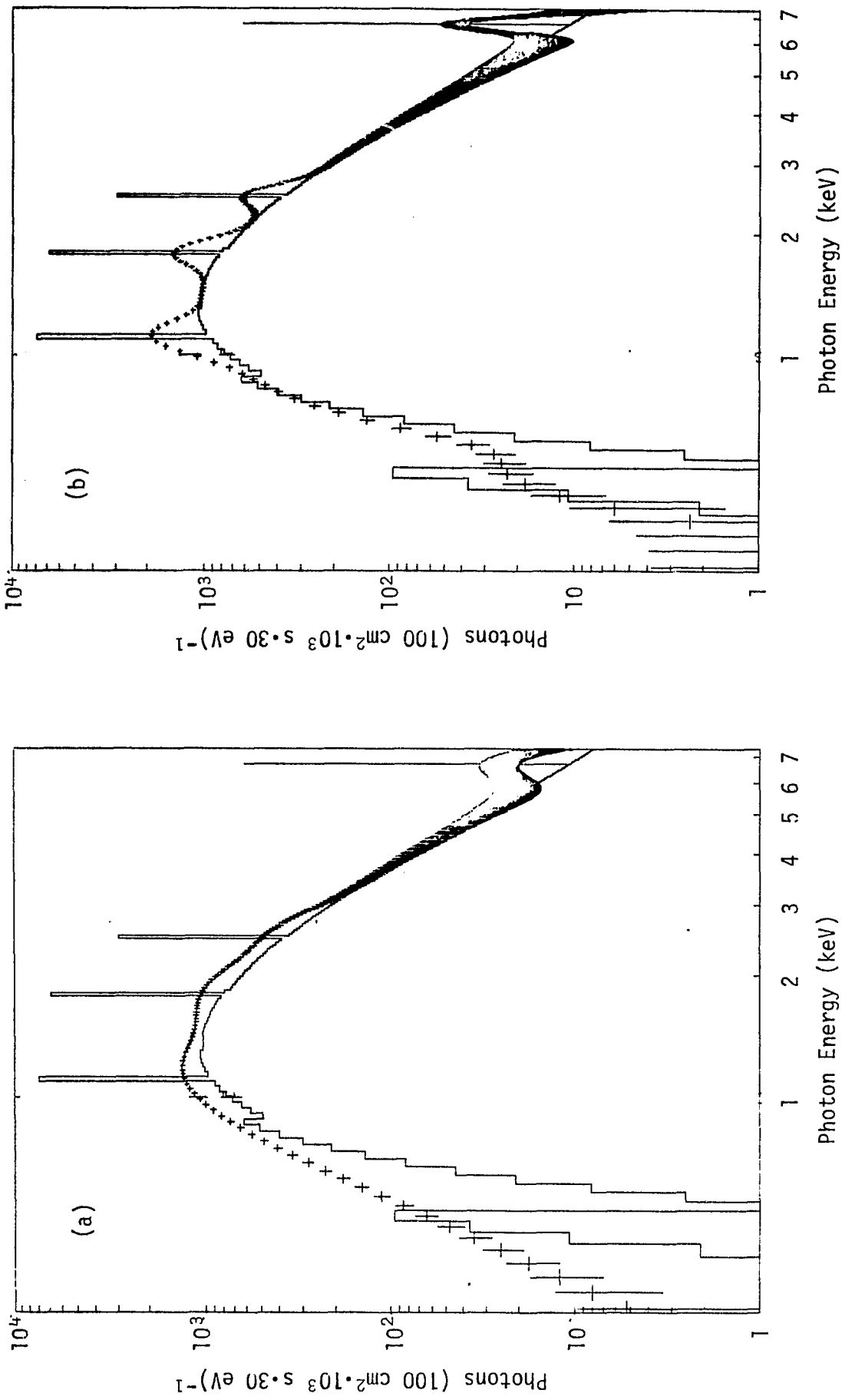


Figure 3.24 - Response of (a) a conventional proportional counter and (b) an imaging gas scintillation proportional counter to a hypothetical Cas A spectrum (histogram). A 1000 second observation with a minimum of 100 $cm^2$ over the 0.2 - 7 keV band width is assumed.

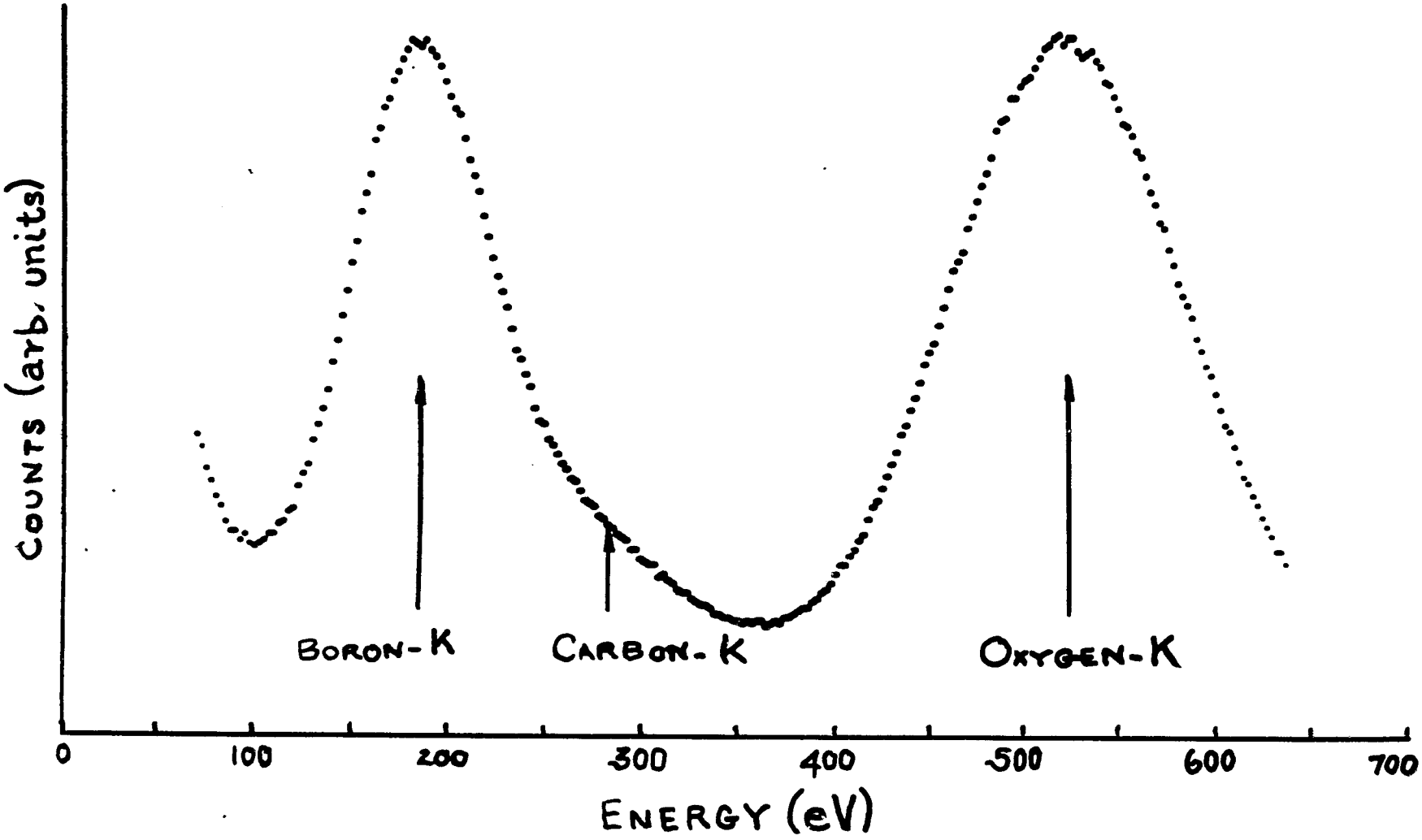


Figure 3.25 Response of a laboratory GSPC module to fluorescence boron-K (185 eV) and oxygen-K (523 eV) lines produced by a Po-α source. Carbon K (283 eV) is also present on the high energy side of the 185 eV boron line. The boron line has a FWHM resolution of 45%. The oxygen line at 523 eV is clean and has a measured FWHM resolution of 27%.

produced in a high voltage light multiplication region in the xenon gas cell. Information regarding the position of the initial ionization may be obtained by recording the light produced for each event in several phototubes and calculating the center of gravity. Monte Carlo simulations of an array of 16 phototubes of 50 mm diameter reveal that such a technique can permit position resolutions of 3 mm at 2 keV to be achieved quite easily. Recently a position resolution of 2.7 mm at 30 keV has been demonstrated with just such a technique. Energy resolution of the summed phototube signal is uncompromised. Given such position sensing capabilities and the ability to discriminate background events on the basis of the pulse rise time, the imaging GSPC should have equal, if not better, background rejection characteristics than conventional proportional counters.

The important instrument parameters are summarized:

| | |
|---|---|
| Field of view | 1° x 1° |
| Energy resolution (E/ΔE) | 2.8 at 0.28 keV<br>6.5 at 1.5 keV<br>13 at 6 keV |
| Position resolution* | 2 arcmin at 0.5 keV<br>1 arcmin at 2 keV<br>30 arcsec at 8 keV |
| Time resolution | 10 μs |
| Quantum efficiency | 80% at 0.25 keV and 0.6 keV<br>100% at 1 keV |
| Background anticipated in orbit | 0.01 counts $[(1 \text{ arcmin})^2 \text{ keV}]^{-1}$ |

* Approaches other than the Anger camera design promise to reduce the position uncertainty to a fraction of a millimeter.

Table 3.3 summarizes the properties of the five imaging detectors discussed in this section and provides a brief comment on their status.

TABLE 3.3 - CANDIDATE AXAF IMAGING DETECTORS

| Detector | Size | Spatial Resolution | Quantum Efficiency | E/ΔE 1 keV | E/ΔE 6 keV | Status |
|---|---|---|---|---|---|---|
| 1. CCD | ⩾ 25 mm x 25 mm ( ⩾ 8 x 8 arc min) | 15 - 25 μm (0.3-0.5 arc sec) | high | 1 | 9 | needs substantial development |
| 2. NEAD | ⩾ 25 mm diameter (⩾ 8 arc min diam) | 15 μm (0.3 arc sec) | high | 5 | 1 | needs substantial development |
| 3. MCP | 85 mm diam ( ∿ 30 arc min diam) | 15 μm (0.3 arc sec) | low | 0 | | needs development* |
| 4. IPC | 180 mm x 180 mm (1° x 1°) | < 0.5 mm ( < 10 arc sec) | high | 2 | 5 | needs development* |
| 5. IGSPC | 180 mm x 180 mm (1° x 1°) | < 0.5 mm ( < 10 arc sec) | high | 5 | 12 | needs substantial development |

* Smaller versions of these detectors are on the Einstein Observatory.

### 3.5.2 Spectroscopy

Many cosmic X-ray sources are known to emit characteristic lines or show absorption features. Theoretical models of supernova remnants, of binary sources, and of cluster sources, all of which appear to be essentially thermal in nature, have predicted the existence of atomic emission lines in the spectra of these sources. Edge structure due to self absorption within the source or in circumstellar material is expected in the spectra of binary sources. The spectra of all X-ray sources must also have absorption features due to interstellar material. Such features should contain unique information on the structure and composition of the interstellar medium and on the distance of the source.

Predictions of spectroscopic structure have now been confirmed by the Ariel V, OSO-8, and HEAO-1 observations of emission features near 6 keV, presumably due to transitions in ions of iron. These features have appeared in the spectra of supernova remnants, binary X-ray sources, active galaxies, and clusters of galaxies. Detailed study of the elemental abundances and physical conditions for these sources, however, have been hampered by the inherently low resolution of the proportional counters employed to make the observations. High resolution Bragg reflection crystal spectrometers on ANS, Ariel V, and OSO-8, because of lack of sensitivity, failed to detect lines. However, evidence for Ly $\alpha$ radiation from hydrogenic oxygen (O VIII) was found in a Bragg reflection spectrum of the Pupis A supernova remnant obtained in a rocket flight.

The Einstein Observatory has provided the first opportunity for moderate ($E/\Delta E \gtrsim 10$) and high energy resolution ($E/\Delta E \sim 100$-$1000$) studies at a reasonable sensitivity level (Figures 3.26 and 3.27). However, the high resolution spectrometer has an effective area less than 1 $cm^2$ and none of the instruments respond above 4 keV (the telescope cut-off is 4 keV), so that they are incapable of observing the important iron line complex between 6 and 7 keV. Nevertheless,

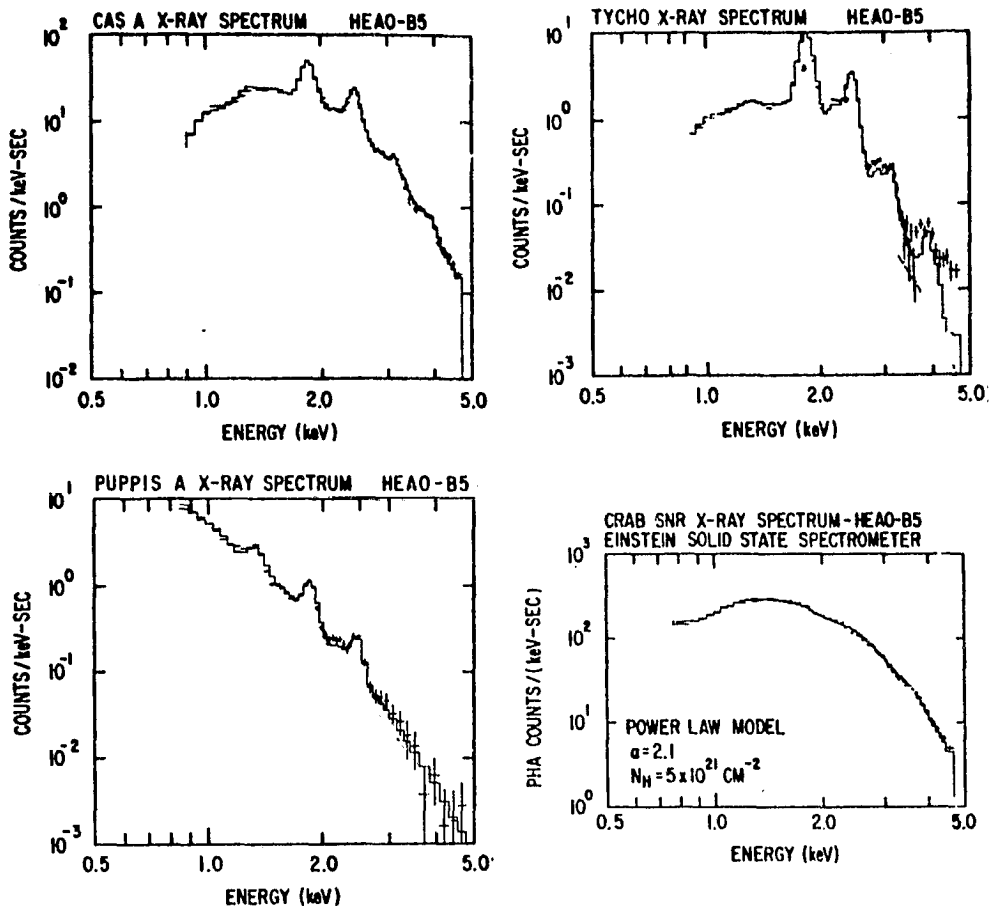


Figure 3.26 - Einstein Solid State Spectrometer (SSS) experimental spectra of four supernova remnants.

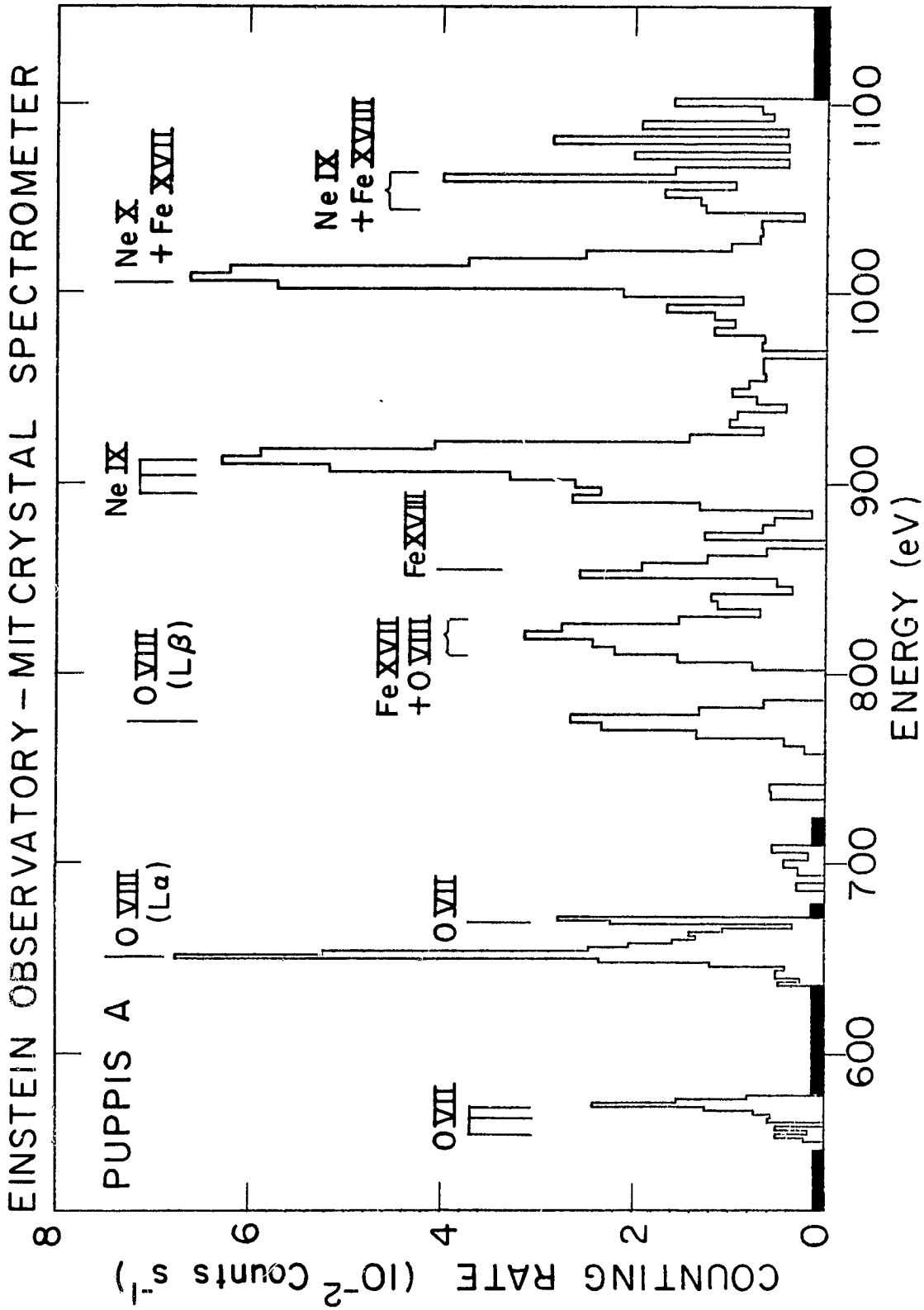


Figure 3.27 - The spectrum of Puppis A obtained with the Einstein Observatory Focal Plane Crystal Spectrometer (FPCS).

the Focal Plane Crystal Spectrometer (FPCS) data on Puppis A show a plethora of emission lines from various ionic species of oxygen, iron, and other common elements, and among these are lines whose relative strengths can be used in determining the temperatures and equilibrium states of the emitting plasma.

The spectroscopic instruments on the AXAF will provide the higher sensitivity, improved spectral resolution, and wider energy coverage that will make possible detailed and spatially resolved spectrometry of many supernova remnants in various stages of development, objects for which such data may well prove as critical to our understanding as optical spectroscopy has proved to be since its introduction into astronomy nearly 100 years ago.

Spectroscopic studies with the AXAF will encompass a wide range of objectives. For example, with an objective transmission grating and a high resolution imaging detector in the focal plane, spectra of compact faint sources can be obtained with a resolution $E/\Delta E \sim 100$. Effective areas a factor of 100 or more than the Einstein Objective Grating Spectrometer are possible. Observations of diffuse extended objects and compact sources with a focal plane crystal or grating spectrometer will provide high resolution ($E/\Delta E > 500$) spectra at sensitivities a factor of 10 to 20 better than the Einstein FPCS. A solid state spectrometer will have a collecting area > 200 $cm^2$ and a resolution $E/\Delta E \gtrsim 25$. It will be capable of detecting iron lines from distant clusters of galaxies and measuring their redshifts to $Z \geq 2$.

(1) Spectrometers. The AXAF has the capability of providing for the first time an integrated facility for the complete spectroscopic study of cosmic X-ray sources. By virtue of the spacecraft pointing capability, long observation times, large collecting area and extended energy response of the mirror assembly, detailed high resolution studies of line emission from previously unaccessible

X-ray sources will be possible.

Table 3.4 is a representative list of candidate instruments with their characteristics. These instruments, in total, provide sufficient flexibility to meet the spectroscopic objectives of the AXAF. However, it should not be considered exhaustive, since new ideas for spectroscopic instruments are being studied at many laboratories.

(2) Areas of Development.

(a) Bragg Crystals. The effectiveness of a Bragg spectrometer depends on the peak reflectivity and rocking curve width of its crystal diffractors. These properties vary greatly from one crystalline substance to another, and can be greatly affected, for better or worse, by treatment of the crystal surfaces. Various crystals with comparable 2d spacing may well differ by factors of 3 or more in resolution and reflectivity. These differences translate into differences in throughput and, consequently, into amounts of observing time required to achieve scientific goals. Thus, the search for better crystals (or pseudocrystals), and systematic studies of the effects of various surface treatments on the critical performance characteristics of crystals should be pursued.

There are problems to be solved in the bending of certain crystals that have desirable reflection characteristics, and in the mounting of bent crystals so as to preserve their qualities in a satellite application. In the case of Einstein, the choice of crystals were restricted to those which had already been successfully bent. Several of the mounted crystals developed hairline cracks because of imperfect technique in bonding the crystal facets to their mounts. It appears that the techniques for preparing bent crystal facets could be significantly improved with a resulting improvement in resolution and throughput of AXAF focal plane spectrometers.

(b) Cooling for CCD's and Solid State Detectors. The scheme used for cooling

TABLE 3.4

| Spectrometer | Energy Range (keV) | Resolution* | Configuration | Location |
|---|---|---|---|---|
| Filter | 0.1 - 8 | 3 | 10-position wheel | in optical path |
| Objective Grating | 0.1 - 4 | 100 - 200 | see Figure 3.28 | behind mirror assembly |
| Solid State Detector | 0.4 - 8 | 15 - 50 | cooled detector | in focal plane |
| Objective Crystal | 0.5 - 8 | 500 - 10,000 | see Figure 3.29 | in front of mirror assembly |
| Focal Plane Crystal | 0.5 - 8 | 500 - 3,000 | see Figure 3.30 | in focal plane |
| Focal Plane Grating | 0.1 - 1 | 500 | see Figure 3.31 | in focal plane |
| Gas Scintillation | 0.1 - 8 | 10 - 15 | | in focal plane |

* $E/\Delta E = \lambda/\Delta\lambda$, and is energy dependent.

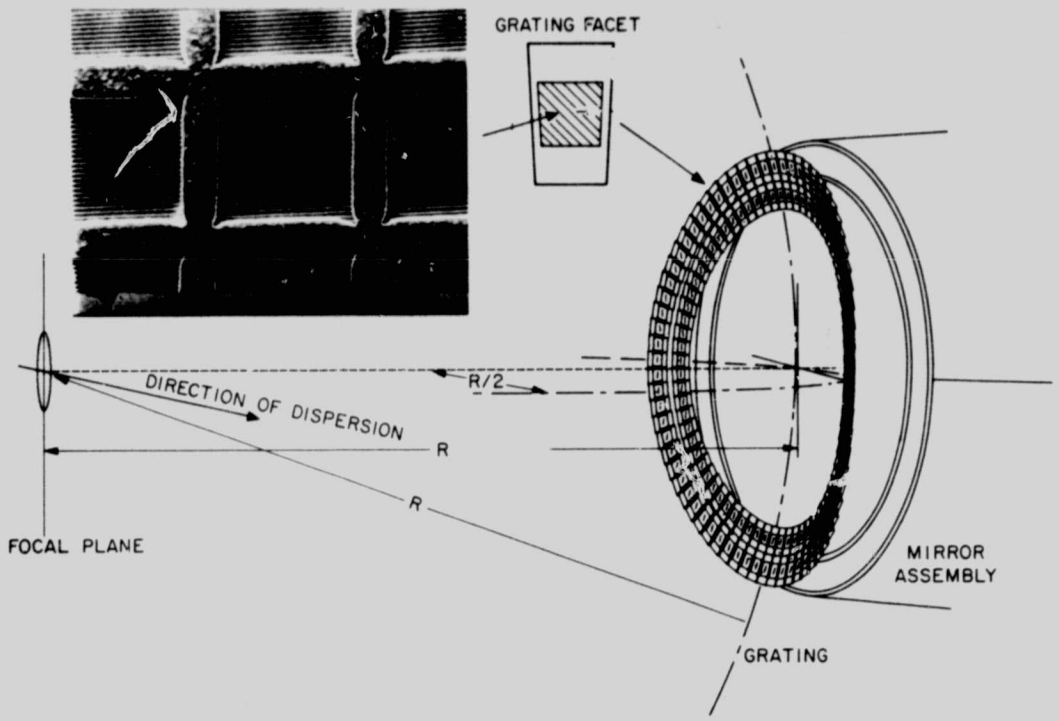


Figure 3.28 - A Coma-corrected objective grating spectrometer. Constant period grating facets are mounted on a toroidally curved frame to remove primary abberations due to the converging beam of the mirror assembly. This spectrometer will simultaneously image and disperse the spectra of all sources in the field.

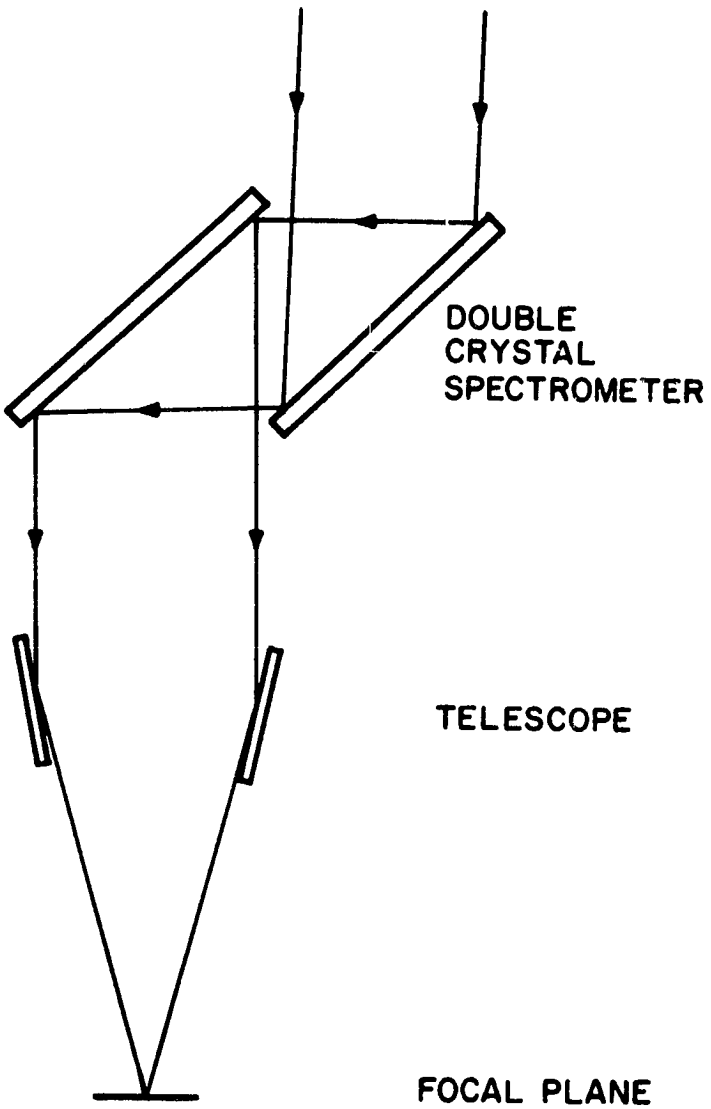


Figure 3.29 - Principle of an Objective Crystal Spectrometer. Incident X-rays are doubly Bragg reflected before entering the telescope. This double crystal configuration has distinct advantages for the study of an extended source, e.g., supernova remnant or a cluster of galaxies. If we wish to study the distribution of an emission line in a source with an angular extent of 30 arcmin (e.g., Puppis A) with a resolution of 20 arcsec, we can image a strip 20 arcsec by 30 arcmin (90 image elements) with a given setting of the spectrometer. With the focal plane crystal spectrometer, although efficiency is higher, we would require a 90 line point scan to achieve the same source exposure.

Thus, the objective crystal spectrometer can achieve a gain of from 10 - 50 in throughput compared to a focal plane instrument in the study of extended sources. Note that the problem of source confusion which exists for the objective grating is not present for the objective crystal configuration.

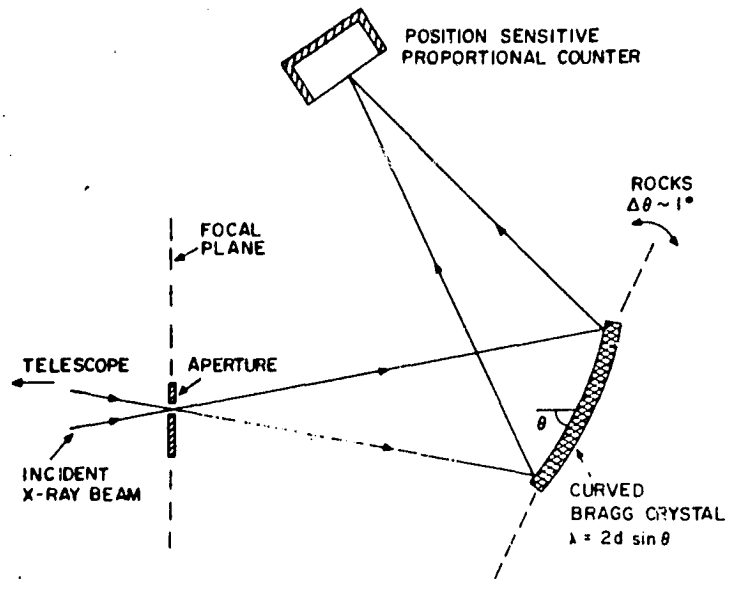


A schematic diagram of the Focal Plane Crystal Spectrometer on the Einstein Observatory.

**Figure 3.30 - Schematic of the Einstein FPCS. In order to compensate for aberrations inherent in the above configuration, the detector is moved forward of the Rowland circle. The relative positions of the focal point, crystal, and detector must be adjusted in scanning a spectrum with this mounting.**

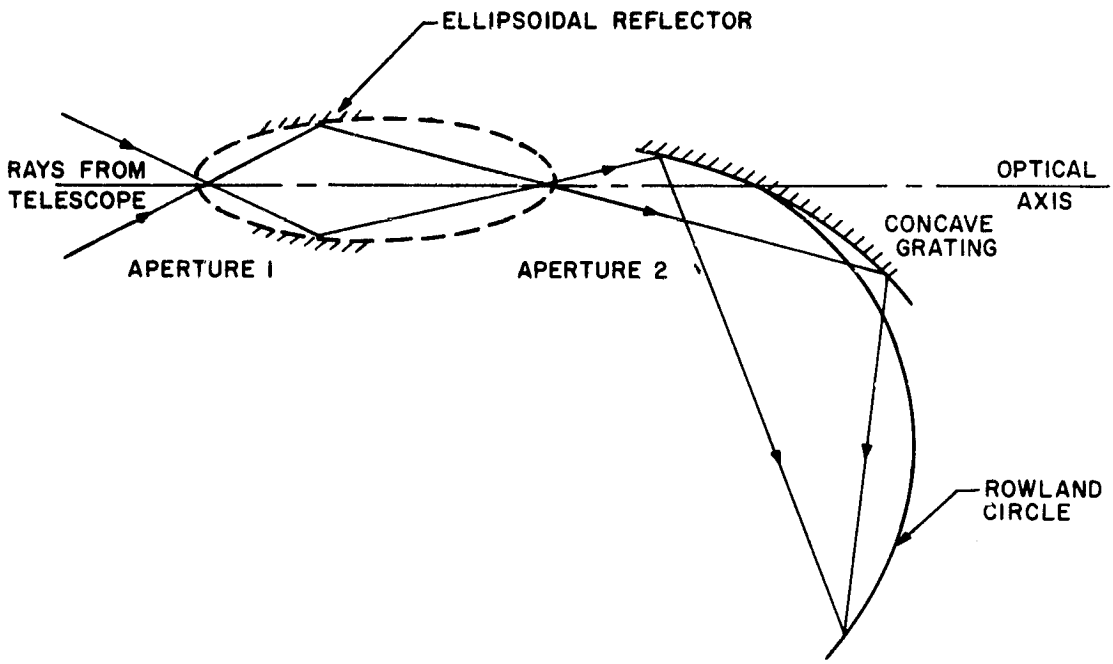


Figure 3.31 - As is well known, the problem of using a glancing incidence grazing spectrometer with a Wolter telescope is the matching of f-numbers. Since the f-number of the cone of rays entering the telescope focal plane for Wolter type I optical systems is about 4 - 5, there is an especially severe problem. This problem can be solved for $\lambda \gtrsim 15$ Å by adding a small ellipsoidal element behind the focal plane would change the beam divergence to an acceptable value. The beam would then be directed onto the entrance slit of a conventional glancing incidence spectrometer.

the solid state detector onboard Einstein (i.e., a solid cryogen sublimation system) has one virtue: its relative reliability in the short term. It has however, several severe drawbacks: expense (in both initial cost and special handling during integration), mass ( $\sim$ 100 pounds per year of lifetime), and constrained lifetime via the finite mass allowed.

There are two alternatives worth investigating for a mission with a long life. One is the use of a completely passive cooling system, i.e., a radiator which dumps heat to cold space. Such radiators have been used successfully in spaceborne experiments in other disciplines, but the spacecraft aspect is severely constrained by such a system. The radiator must always avoid sun- or earth-shine, and a near-earth orbit with a pointed mission probably cannot accommodate this requirement.

The other alternative is the use of a mechanical refrigerator. There are disadvantages relative to a subliming system, including large power drains during operation of the refrigerator (it cannot be operated while the detector is in a data taking mode). To minimize the temperature drift during data acquisition intervals, the detector must be sunk to a thermal reservoir, so that power requirements rise even more. The problem of ice buildup is accommodated by the natural defrosting of such a system.

(c) Transmission Gratings. The gratings currently employed on Einstein are produced by a holographic technique. Individual grating elements (either 500 or 1000 lines per mm) are gold plated on a glass substrate which has been coated with photo-resist and exposed to an interface pattern created with an Ar-Kr laser system. Standing wave patterns in the photo-resist limit the thickness of the exposed material to about 1/2 wavelength. Thus, it is most difficult to produce gratings with wires that are thicker than $\sim$ 2000 Å. This leads to a weak system of wires which may not be a difficulty in laboratory applications, but which

without additional support structure is not suitable for space applications. Thick irregular patterns of primary and secondary support wires, as well as a plastic substrate, are necessary to meet space requirements. This leads to several undesirable results:

1. The supporting wires obscure a considerable area, thereby reducing the system throughput.

2. A diffraction halo caused by the irregular support structure surrounds each diffraction order.

3. The thin grating wires become semi-transparent at energies corresponding to regions of anomalous dispersion in gold.

4. The absorption in the plastic substrate causes substantial loss of efficiency at low energies.

Current state of the art microlithographic technology provides several alternatives which will help overcome the difficulties described above. The most important one is the development of X-ray microlithography. This technique involves the use of a master pattern in close contact with a photo-resist coated substrate. The photo-resist is exposed with soft X-rays which cause a much deeper region of exposure in the photo-resist and, therefore, a thicker grating wire. Once this most difficult structural problem is solved, the emphasis can shift towards choosing the optimum grating material and geometry for the spectrometer. Line densities of 3000 lines per mm appear feasible with this technique.

The mechanical ruling of a master grating and the subsequent fabrication of replica gratings is another approach to the production of thick gratings. Width to thickness ratios of 1:1 are feasible. So far the feasibility of this technique has been demonstrated up to line densities of 2000 lines per mm.

### 3.5.3 Polarimetry

X-ray polarimetry promises to provide critical tests on the emission

mechanisms which are important in both galactic and extragalactic X-ray sources. For example, until the discovery of X-ray polarization in the Crab Nebula served to confirm the synchrotron nature of this source, thermal models of emission could not be ruled out.

The AXAF provides a unique opportunity for greatly extending such studies. This mission is presently baselined to operate for ten years. If 5 to 10% of this time is devoted to X-ray polarimetric observations, then 200 to 300 days of polarization measurements could be carried out while leaving most of the time for other classes of observations. With a mosaic graphite Bragg crystal polarimeter, we find that we could study $\sim$ 50 Uhuru sources to the 5% level ($3\sigma$ confidence) in 200 days. We could study 20 sources to the 1% level in only 80 days.

The sources that could be studied include extragalactic objects as well as galactic sources such as compact X-ray systems, globular clusters, etc. For example, although at radio wavelengths emission from Cen A is via synchrotron radiation, both inverse Compton and synchrotron mechanisms have been proposed to explain X-ray emission. A straightforward way to resolve this controversy is via polarimetry. On AXAF, a sensitivity of 5% could be obtained in an observation time of 5 or 6 days. As such extragalactic sources are known to be synchrotron emitters in other spectral regions, they may well exhibit 10% to 20% X-ray polarization, comparable to the polarization at radio wavelengths. If, however, the X-rays are produced by the inverse Compton process, the polarization would almost certainly be very much less. Thus, a study of extragalactic sources with an AXAF polarimeter could provide critical evidence with regard to the emission mechanisms in such sources.

Many of the extragalactic sources exhibit radio and optical polarization so that one has a basis for comparing the predictions of various models. A comparison of the degree and position angles of the polarized radiation in these different

spectral regions will provide a great deal of information on the physical conditions which exist in these sources.

In the case of compact sources, one expects polarization from accretion disks. In the case of Cygnus X-2, OSO-8 observations indicate $\sim$ 5% polarization at $\sim 3.5\sigma$ confidence level. X-ray polarimetry of accretion disk sources can provide a direct indication of the inclination angle of the disk. More importantly, if the inclination angle is known, polarization measurements allow one to choose between two-temperature models and accretion disk models.

The radiation mechanism in X-ray pulsars is not well understood, but if the field at the surface is of the order of $10^{11}$ gauss, the Larmor frequency, given by:

$$h\nu = 1.2\ (B/10^{11})\ \text{keV}$$

is likely to be in the X-ray band. This suggests that the X-ray emission in pulsed sources, like Cen X-3 and Her X-1, may be due to electrons radiating at the cyclotron frequency or low harmonics thereof. In fact, evidence has been obtained for a cyclotron line in the spectrum of the binary pulsar Her X-1 with an energy of 55 keV. The polarization may be as high as 75% perpendicular to the field lines. Moreover, the polarization would be expected to vary as a function of pulse phase, with the maximum polarization occuring in the wings of the pulse. Alternatively, the observed X-rays may be associated with thermal processes, but in this case, the opacity of matter in the accretion column will be strongly affected by the magnetic field. For example, a beam emerging along the field lines should be strongly circularly polarized. In general, the expected polarization would be elliptical.

A particularly exciting possibility is that X-ray polarimetry may provide a direct test for the existence of rapidly rotating black holes. Recent

publications show that an accretion disk surrounding a rapidly rotating black hole will exhibit an energy dependent position angle, whereas in the Newtonian approximation, the position angle is independent of energy. In the particular case of Cyg X-1, it is predicted that the position angle may change by as much as 40% between 1 and 10 keV. The OSO-8 polarimeter has indicated a polarization in the high state of Cyg X-1 of about 3% at the 2.5$\sigma$ confidence level. An observation of Cyg X-1 with AXAF for a period of 4 or 5 days would significantly improve this measurement since it would be sensitive to polarized emission of $\leq$ 1%. X-ray polarization measurements by the AXAF would provide one of the few direct tests for the existence of a rapidly rotating black hole in the Cyg X-1 system.

X-ray astronomy has made very great strides with photometric observations and certainly such observations will continue. The spectroscopic and spatial mapping capabilities of the Einstein mission will certainly vastly extend our knowledge of the X-ray sky. It is imperative that we begin to obtain a deeper insight into the emission mechanisms in the presently known sources. This goal will be furthered if polarimetric observations are included on the AXAF.

(1) Thomson Scattering Polarimeter. As a direct consequence of Brewster's Law, scattering of X-rays at 45° incidence angle yields a 100% polarized beam; conversely scattering can be used as an analyzer. Figure 3.32 shows the principle of a Thomson scattering polarimeter.

The efficiency of such an instrument is determined by the competition between scattering and photoelectric absorption in the scattering material. Because of the relatively low energy response of grazing incidence mirrors, a scattering polarimeter operating in conjunction with the AXAF mirror assembly would have an unacceptably low efficiency.

(2) Bragg Crystal Polarimeters. Bragg reflection at 45° incidence angle offers

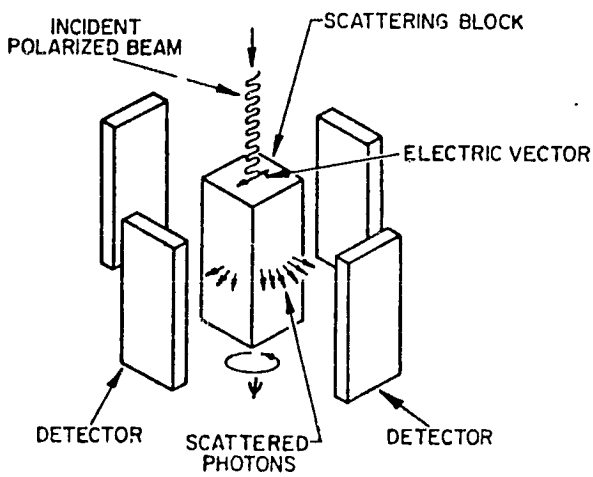


**Figure 3.32** Principles of a Thomson scattering polarimeter. The polarized beam is scattered with a distribution proportional to $\cos^2\psi$ (projected in the plane of the scattering surface). If the detectors are rotated about the direction of the X-rays with a frequency $\omega$, net polarization of the incident radiation will cause a signal with frequency $2\omega$.

an alternative to Thomson scattering in order to measure polarization at the low energies for which grazing incidence mirrors are sensitive.

The crystal polarimeters make use of the fact that when X-rays are Bragg reflected through 90°, only the polarization component of the incident flux that is normal to the incident and reflected rays contributes to the reflected power. The component parallel to the reflected ray is absorbed. During an observation, the instrument would be rotated about the line of sight to the source so that polarization, if present, would result in a modulation of the detected signal at twice the frequency of rotation. By expoliting the properties of mosaic crystal with high integrated efficiencies, an efficient Bragg crystal polarimeter can be made.

Figure 3.33 shows the principle of a Bragg crystal polarimeter operating with a grazing incidence mirror; Figure 3.34 shows the expected sensitivity of a mosaic graphite Bragg crystal polarimeter operating at the focal plane of the AXAF.

3.5.4 Auxiliary Instruments

(1) Monitor Counter (0.5 - 100 keV). The Monitor Counter will provide both spectral and temporal data. This non-focal plane instrument continuously monitors the flux of sources being observed simultaneously by one of the focal plane instruments. Such monitoring is important because it provides broad energy range data to complement the narrow band observations of these instruments. In addition, its potential, high temporal resolution capability will permit the study of high frequency flux variations. The Monitor Counter would have a collimator whose axis is aligned with the optical axis of the X-ray telescope.

(2) All-Sky Monitor. An All Sky Monitor would be used to continuously view the X-radiation from all bright sources not contained within the $< 10^{-4}$ of the sky which represents the instantaneous field of view of the telescope and monitor

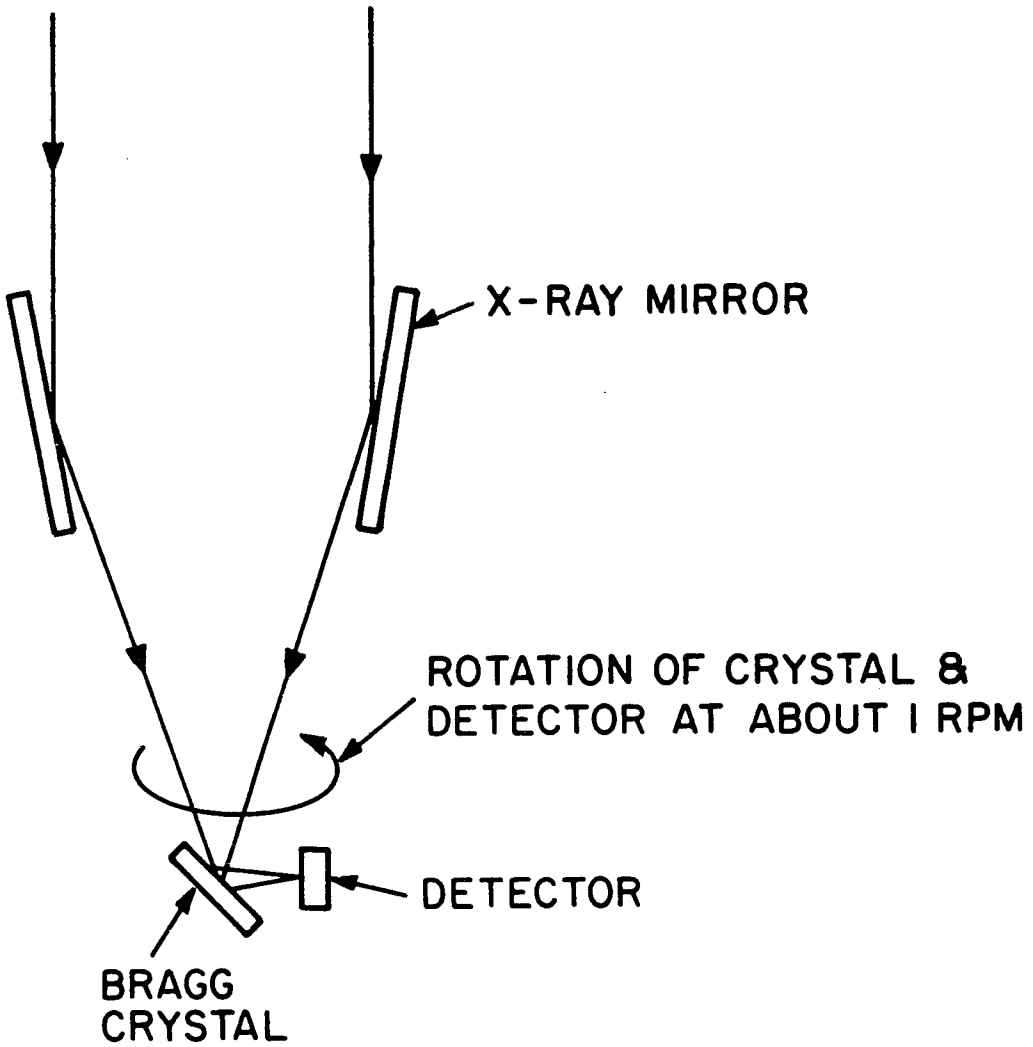


Figure 3.33 - Principle of operation of a Bragg crystal polarimeter.

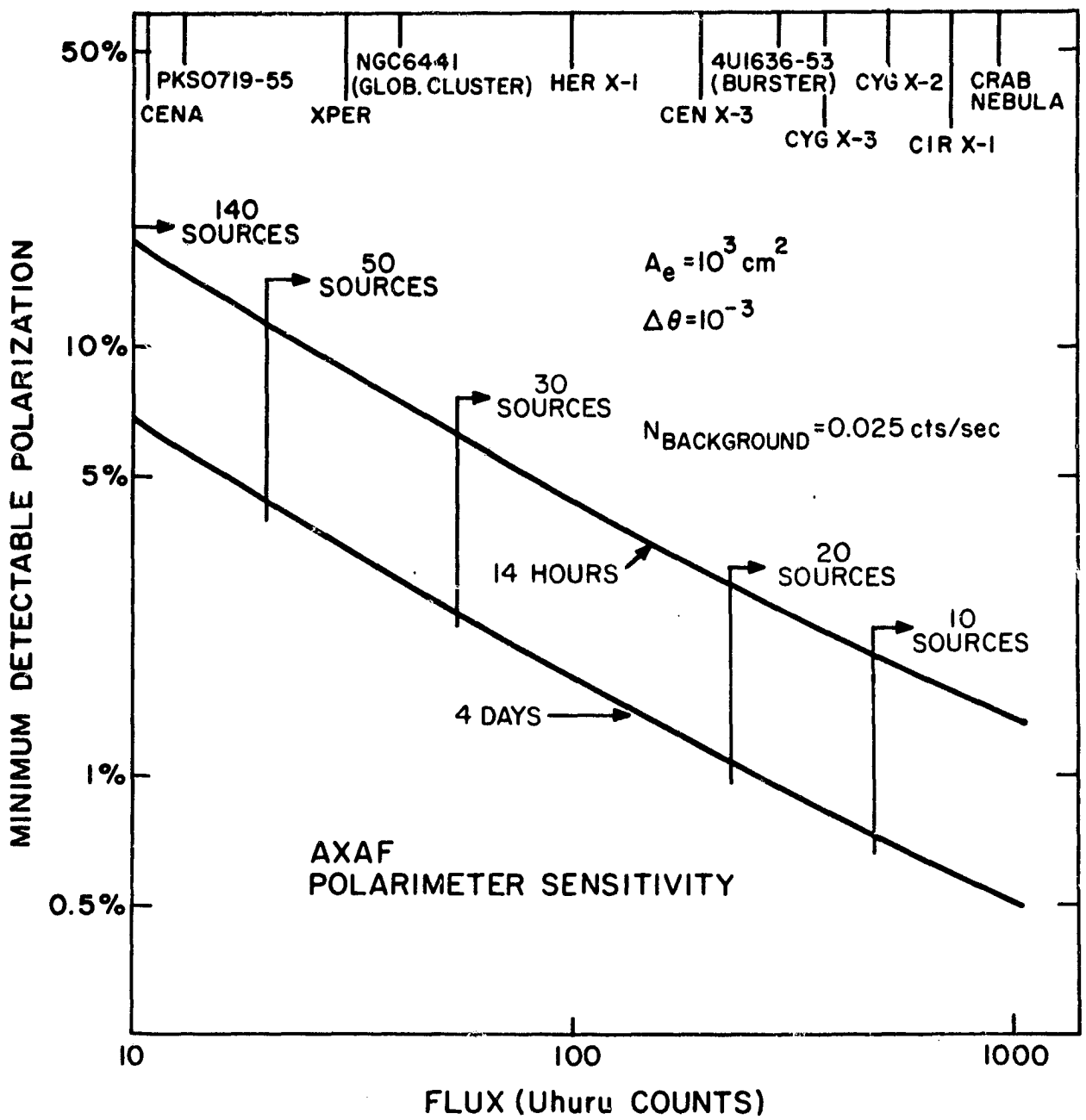


Figure 3.34 - The expected sensitivity of a mosaic graphite Bragg crystal polarimeter operating at the focal plane of the AXAF.

proportional counter. Its primary purpose is the monitoring of the entire sky for new sources and for anomalous variations in the intensity of already known sources, so that the telescope may be promptly trained in the direction of transient phenomena which would otherwise be missed. As an adjunct to this function, the constant monitoring of bright sources in the sky will undoubtedly yield a wealth of data on the long-term behavior of these objects which would otherwise be unmeasurable (e.g., periodicities on time scales from minutes to months, temporal spectra of fluctuations), even if the telescope cannot always respond to the transient phenomena detected by the instrument.

### 3.5.5 Summary

The following represents a selection of classes of instruments that would exploit the scientific capabilities of the AXAF. Some are state of the art, others are modest extensions, and a few would represent substantial development. This list can be understood as a strawman payload for spacecraft engineering tradeoff studies.

(1) Imaging.

High resolution detector: high quantum efficiency, 0.5 arcsecond spatial resolution, some energy resolution. (MCP, NEAD, CCD)

Moderate resolution detector: high quantum efficiency, 5-10 arcsecond spatial resolution, moderate energy resolution, large format. (IPC, IGSPC)

(2) Spectroscopy.

Objective grating ($E/\Delta E \gtrsim 100$)

Band-pass filters

Solid state spectrometer

Focal plane crystal spectrometer

(3) Polarimetry.

Focal plane Bragg reflection polarimeter

(4) Auxiliary (not pre-focal or focal).

Monitor proportional counter

All-sky monitor

Table 3.5 shows the expected performances of this instrument complement. The Einstein instrument characteristics are shown for comparison.

## AXAF and EINSTEIN OBSERVATORY INSTRUMENT PARAMETERS COMPARED

(Einstein parameters are in parentheses)

| | Outer Diameter | # of Elements | Focal Length | Focal Plane Scale | Field of View (diameter) | Spatial Resolution | Effective Area ($cm^2$) @ 0.25 | 2 | 4[a] | 7 keV | Energy Range (keV) | Energy Resolution (E/ΔE) @ 0.25 | 2 | 4 | 7 keV |
|---|---|---|---|---|---|---|---|---|---|---|---|---|---|---|---|
| Mirror Assembly | 1.2 m (0.6 m) | 6 (4) | 10 m (3.4 m) | 50 μm/arcsec (17 μm/arcsec) | 60 arcmin (80 arcmin) | 0.5 arcsec (4 arcsec) | 1600 (400) | 1100 (250) | 500 (50) | 200 (0) | 0.1–8 keV (0.1–4 keV) | | | | |
| Instruments[b] | | | | | | | | | | | | | | | |
| High Resolution Imager (HRI) | | | | | 25 arcmin (25 arcmin) | 0.5 arcsec (4 arcsec) | 250 (15) | 250 (5) | 150 (0.5) | 75 (0) | 0.15–8 keV (0.15–3 keV) | | 4 (no energy resolution) | 8 | 10 |
| Imaging Proportional Counter (IPC) | | | | | 1° x 1° (1° x 1°) | 10 arcsec (1 arcmin) | 400 (100) | 500 (100) | 200 (20) | 200 (0) | 0.15–8 keV (0.15–4 keV) | 1 (0.5) | 4 (3) | 5 (4) | 7 |
| Solid State Spectrometer (SSS) | | | | | 2 arcmin (6 arcmin) | 2 arcmin (6 arcmin) | 4 (1) | 950 (200) | 200 (20) | 200 (0) | 0.4 – 8 keV (0.4 – 4 keV) | 3 (2) | 20 (15) | 40 (25) | 70 |
| Focal Plane Crystal Spectrometer (FPCS) | | | | | 2 arcmin (6 arcmin) | 2 arcmin (6 arcmin) | 2 (0.1 – 1) | 10 | 7 | 0.5 (0) | 0.2 – 8 keV (0.2–3.5 keV) | 400 (50 – 100) | 2000 | 1000 (100 – 1000) | 1000 |
| Objective Grating Spectrometer[c] (OGS) | | | | | 25 arcmin (25 arcmin) | 1 arcsec (4 arcsec) | 170 (1) | 120 (0.2) | 60 (.03) | (0) | 0.15–8 keV (0.2 – 3 keV) | 500 (10 – 50) | 200 | 100 | 50 |
| Polarimeter (Einstein has no polarimeter) | | | | | | | | | | | 1 – 8 keV | | | | |

a High energy cut-off of Einstein in 4 keV.
b The instruments for AXAF are considered to be representative only (see Section 3.2).
c With HRI.

## 4.0 TEST FACILITIES

A significant step in establishing the AXAF involves ground testing of both the X-ray mirrors and instrumentation. Such ground testing is mandatory in establishing the actual X-ray performance in order to assure that the program's engineering specifications and scientific goals are met and to calibrate the telescope and instruments. The importance of this cannot be overemphasized.

Early testing must be done on development mirrors to evaluate the X-ray reflection efficiency and resolution. The need for any possible design modifications can thereby be determined and corrective actions taken as required.

Calibration and final alignment testing will be done on the completed system. This will involve the alignment of the multiple X-ray mirror system, X-ray instruments, and aspect sensors.

Furthermore, it is the general experience with such complex systems, such as the AXAF, that, regardless of how well designed and constructed, functional testing is a mandatory step toward the achievement of the final performance specification.

The instruments involved in this program together with others operating at the extreme ultraviolet region of the electromagnetic spectrum share a common requirement for testing in a facility with a long evacuated path length to provide a nearly parallel beam of radiation that can be used for testing, calibration, and alignment. The requirement for the long path length is necessary because X-ray light cannot be reflected at large angles. This means that collimating mirrors (as used with visible light) cannot be used to achieve a parallel beam. The practical means for testing is to provide a nearly parallel beam of radiation by having a long distance between the radiation source and instruments. Since the radiation at X-ray wavelengths is heavily attenuated in air, the path of the radiation must be evacuated.

## 5.0 SPACECRAFT AND SUPPORT SUBSYSTEMS

The work performed by MSFC concerning spacecraft and support subsystems is documented in considerable detail in "Advanced X-ray Astrophysics Facility Conceptual Design", NASA/MSFC, May 1978. The majority of the summary information and recommendations presented in this section is extracted from that report.

Any spacecraft limitations, such as pointing performance, power provisions, and communications and data handling, will set restrictions on the quality and quantity of scientific data that can be taken and returned to the principal investigators. Conversely, the scientific complement and its support requirements dictate the spacecraft functions and capabilities to achieve the mission objectives.

Three typical spacecraft are illustrated in Figure 5.1 - the Space Telescope Support Systems Modules (SSM), the Multi-mission Modular Spacecraft (MMS), and the HEAO Spacecraft Equipment Module (SEM) - and are candidates for the AXAF mission. These spacecraft have been or are being developed to use standard components when possible, and can be adapted to a wide range of missions. Considerable development cost can be saved by using an existing spacecraft for the AXAF. Although the AXAF support system requirements are not completely established and both the MMS and SSM are surrently under development, the candidate spacecraft represent current state of the art technology and their characteristics and performance estimations are representative of Shuttle-era spacecraft which could be modified to meet the AXAF support requirements.

### 5.1 Support Subsystems

Although the support subsystem requirements are not well defined, no unusual or extremely demanding requirements are anticipated. Available spacecraft modules can be adapted to AXAF. If spacecraft modifications or add-ons are needed, the components should be available. No development or technology tasks were identified.

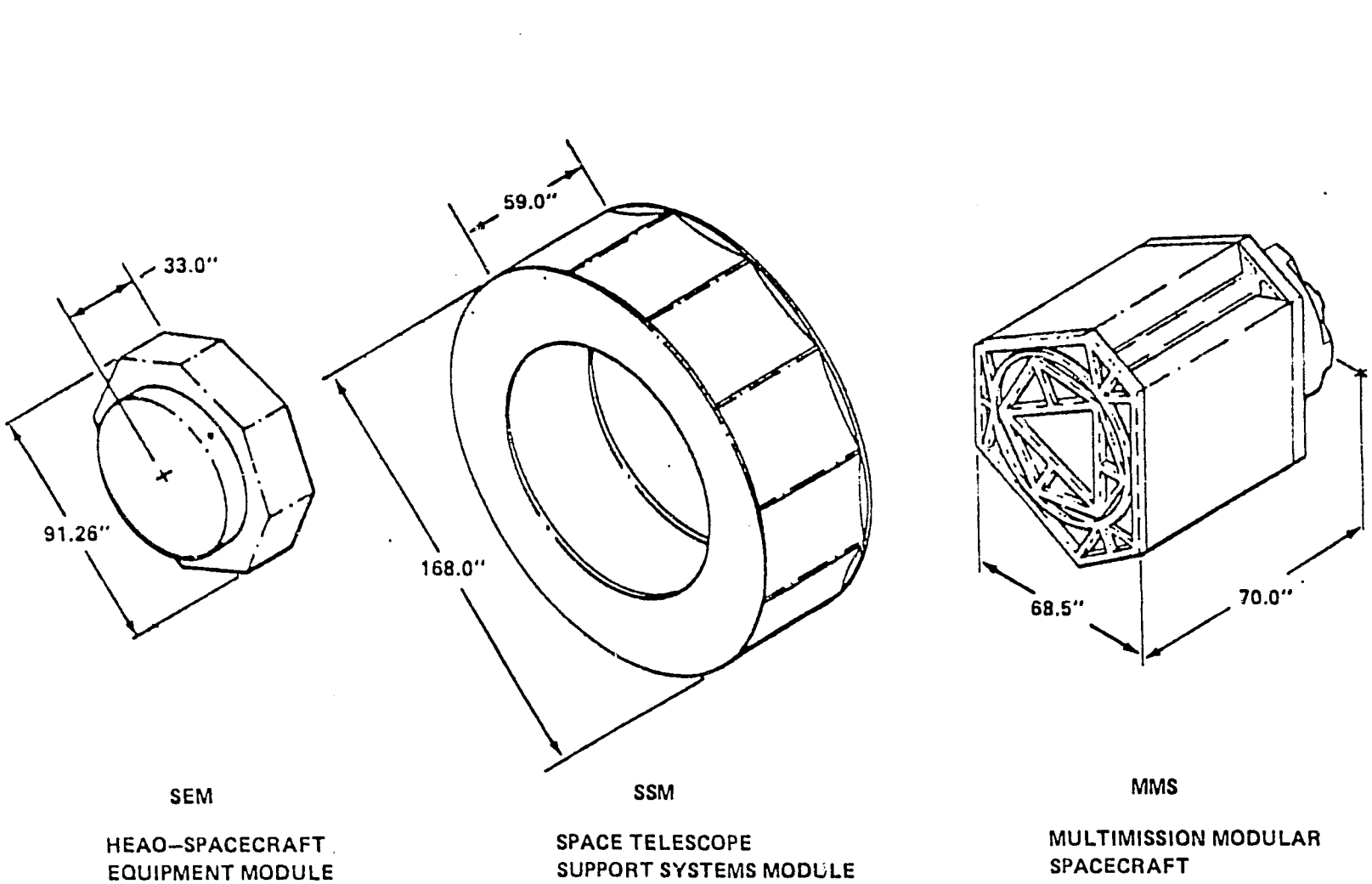


Figure 5.1 - Possible spacecraft candidates for the AXAF mission.

5.1.1 Attitude Control. The 30 arcsecond pointing requirements can be satisfied using existing components. Depending on the configuration moments of inertia, four reaction wheels sized at 100 to 400 ft-lb-sec each, and magnetic torquer bars sized at 3000 to 6000 A-m per control axis should be adequate for AXAF. The navigation base, star cameras, and rate gyros should be located on the mirror assembly for greater stability.

5.1.2 Propulsion. No hard requirement for a Reaction Control System (RCS) was identified since the magnetic system provides momentum management.

5.1.3 Electrical Power. The estimated power requirement of 600 W for science and 600 W for support subsystems can be provided by either the MMS (1200 W) or the SSM (2100 W), or by modifying the SEM (600 W). Articulated solar arrays permit all sky viewing anytime and are rolled or folded up for protection during ground and launch operations.

5.1.4 Communications and Data Management. The estimated science data rate ranges from 6 to 1000 kbps. Considering the planned in-orbit refurbishment of focal plane instruments, we recommend adopting the higher data rate, to accommodate future requirements. If the science data rate is low ( < 25 kbps), then the data can be combined with the engineering data on a common data bus and single access Tracking and Data Relay Satellite System (TDRSS) service can be used. Separate science formatters and recorders are recommended for higher data rates and multiple access TDRSS service must be used. The SSM can provide either type data management (up to 1000 kbps) and provides both single and multiple TDRSS service. No cost advantages were defined to discriminate between single or multiple access TDRSS service, and either can be implemented using standard components.

## 5.2 Candidate Spacecraft

Three candidate spacecraft modules were assessed for application to AXAF. The capabilities of each module were compared with the AXAF support subsystems requirements, and modifications and add-ons were defined as needed. Components from each major subsystems of each spacecraft are listed in Table 5.1. A check mark indicates that the component can be used to satisfy an AXAF requirement without modification. Only the SSM can satisfy the AXAF subsystem requirements without any modifications; however, two additional magnetic torquer bars are recommended.

Both the MMS and SEM attitude control actuators must be replaced with much larger units. The size of these new actuators require new structural modules on MMS and major modifications inside SEM to provide installation volume. Since the SEM communications systems is designed for STDN, major modifications are required to convert it to TDRSS. Also, the electrical power system of SEM must be doubled in capacity to provide the anticipated AXAF power needs. Assuming that the AXAF science data rate will be high enough to preclude combining it with engineering data on the spacecraft data bus, separate science data formatters and recorders are added to both MMS and SEM. The modifications and add-ons, however, can be accomplished using state of the art components (e.g., recorders will be NASA standard). Structural modifications are required on both MMS and SEM to attain the spacecraft module mounting near the system center of mass, as recommended for AXAF. The support subsystems can be implemented using components from either existing spacecraft or from presently existing flight hardware items. By mounting the support subsystem components in boxes, the spacecraft then becomes several boxes that are attached to the outer shell near the system center of mass to mimimize the principal moments of inertia.

TABLE 5.1 - Candidate Spacecraft for AXAF

| Subsystem | SSM | MMS | SEM |
|---|---|---|---|
| Reaction Wheels | ✓ | Replace | Replace |
| Magnetic Torquers | Add 2 Bars | Replace | Add System |
| Communications | ✓ | ✓ | Modify for TDRSS |
| Recorders | ✓ | Add as Required | Replace as Required |
| Computer | ✓ | ✓ | Add 16K Memory |
| Data Management | ✓ | ✓ | Modify for High Rates |
| High Science Rates | ✓ | Add Science Formatter | Add Science Formatter |
| Batteries | ✓ | ✓ | Add as Required |
| Solar Arrays | ✓ | Add as Required | Replace |
| Structure | ✓ | New Module for RWA | Modify for RWA; Batt |
| Toroid Mounting | ✓ | Replace Structure | Major Modifications |

( ✓ = use as is)

## 5.3 Facility Integration

5.3.1 Reference Configuration. The design reference selected for a large portion of this study is a 33 ft focal length telescope integrated with the spacecraft module. The 43 ft long, 22000 lb configuration shown in Figure 5.2 fulfilled the initial design requirements very well and provided an excellent basis for detailed trade study. A pictorial illustration of the AXAF elements is given in Figure 5.3.

The facility design incorporates an insulated aluminum outer shell which provides thermal isolation for the telescope assembly and mounting provisions for the solar array system, the low and high gain antennae, the magnetic torquer system, and all sky monitor instruments. Structural interface with the Orbiter is also provided by the outer shell and spacecraft module. A conical ring adapter, located near the facility center of mass, connects the telescope assembly to the outer shell and spacecraft module. This support concept essentially decouples thermal distortions of the outer structure from the telescope. The outer shell is made of several segments with varying thickness that carry very small loads. However, the center section must be thick enough to carry the optical bench loads directly to the Orbiter attachments, and to provide the interface with the spacecraft module (or boxes) and the conical ring adapter.

The telescope assembly includes the mirror assembly, optical bench, and focal plane assembly (carousel with instruments). The optical bench must be made of materials with a low coefficient of expansion and be dimensionally stable over the facility lifetime. Graphite epoxy is recommended, however, other materials such as aluminum can marginally satisfy the requirements. Coatings and insulation are used on the outer shell to produce a stable temperature of about 69°F for the telescope assembly. Variation of optical bench temperature from side to side or from end to end is less than 1°F.

ORBITER BAY CONFIGURATION,
DEPLOYABLE SUNSHADE -33 ft FOCAL LENGTH

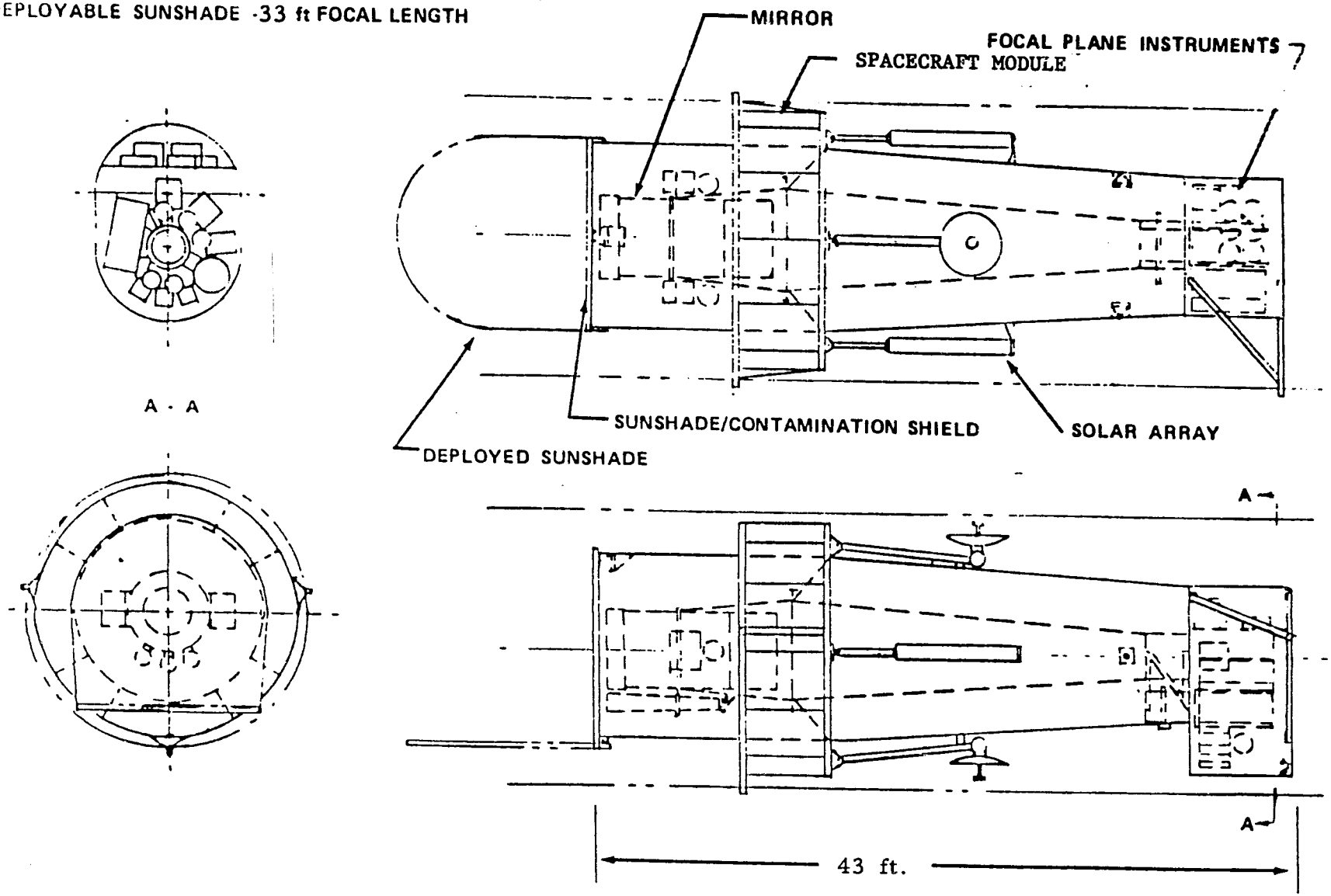


Figure 5.2 - AXAF configuration.

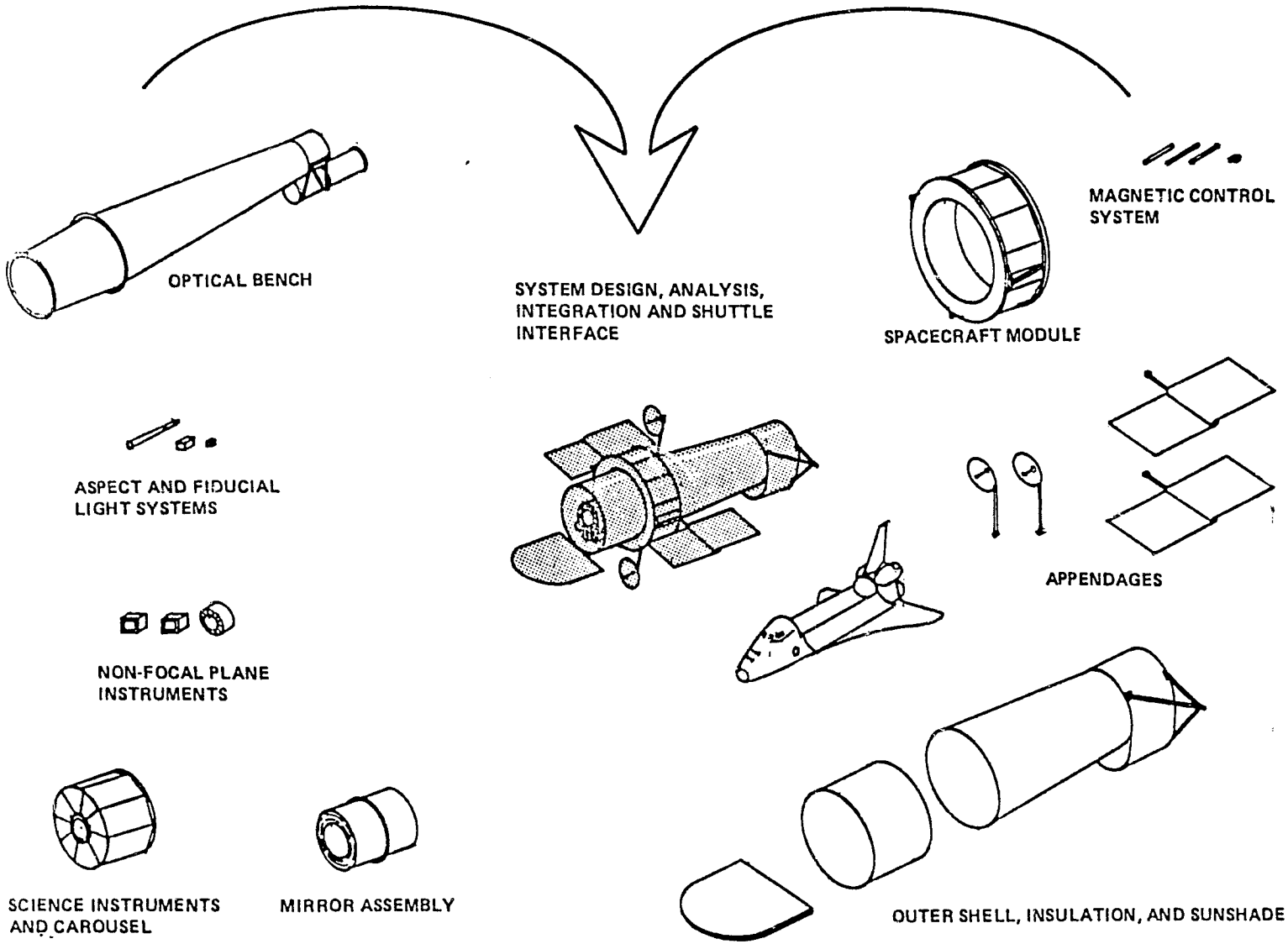


Figure 5.3 - Facility integration.

Structural and thermal analyses performed on this configuration reveal no particular problems and all parameters chosen for and derived from the analyses are reasonable and reflect current state of the art capability. The analyses show considerable design margins in most cases which could allow alternate design approaches and alternate material selections.

Although other telescope configurations and spacecraft options were considered, they all employ the isolated optical bench approach. Configurations with a toroidal-type spacecraft and a deployable sunshade allow a focal length of ~ 33 ft within the Orbiter payload bay.

5.3.2 Facility Integration with Orbiter. Figure 5.4 depicts the Orbiter launch and return capabilities for the aft facing, 33 ft focal length configuration. As shown, the composite payload center of gravity of this configuration is within the Orbiter capability when one OMS kit is used.

The figure also shows that the 43 ft AXAF with a 33 ft focal length, and servicing/tilt table structure (3 ft), OMS kit (10 ft), and required EVA space (4 ft) fill the payload bay thus, without changing the servicing approach and possibly the orbit selection, a 33 ft focal length is the maximum length that can be accommodated.

Other configurations with shorter focal lengths do not have significant Orbiter constraints, and none of the configurations are constrained by the Orbiter load carrying capability.

5.3.3 Mission Operations and Performance. The design reference 28.5 deg/460 km orbit was selected on the basis of scientific objectives, STS performance capabilities, and operational considerations. No upper stage of sufficient capability to permit a significantly lower inclination orbit is currently planned to be available for a 1986-7 AXAF launch date. The orbital altitude of 460 km results in a 2 to 4% loss of observing time due to the South Atlantic Anomaly,

PAYLOAD CENTER-OF-GRAVITY WITH OMS KIT —
33 ft FOCAL LENGTH

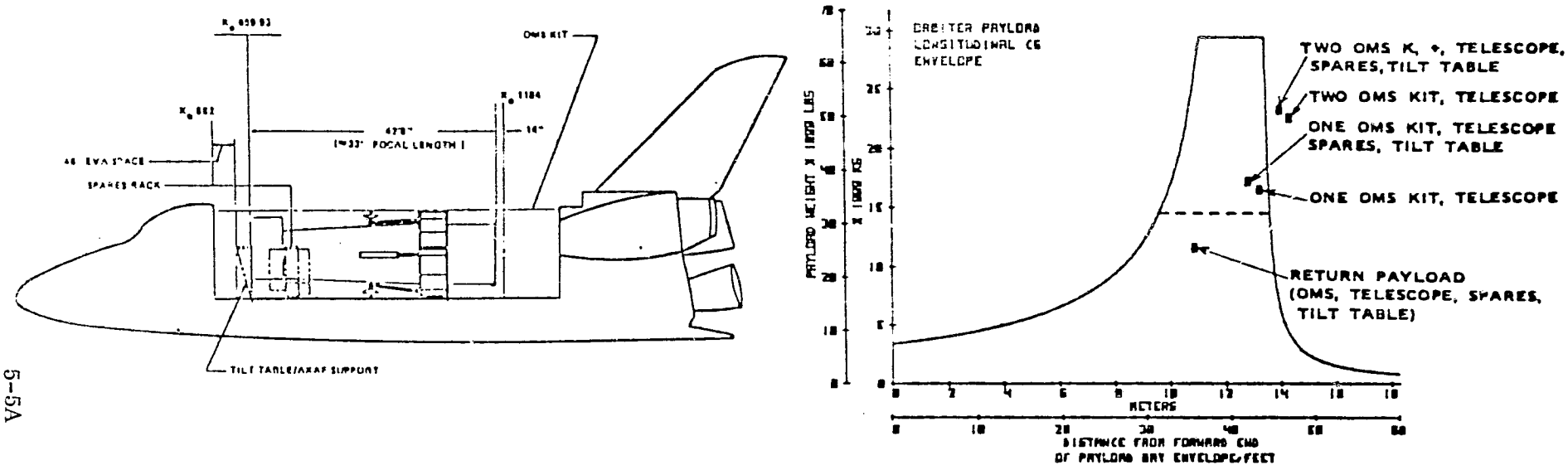


NOTE: A 10 percent WEIGHT CONTINGENCY IS INCLUDED IN THE C. G. CALCULATIONS.

Figure 5.4 - Payload center of gravity with OMS kit.

yet provides an orbital lifetime which gives reasonable assurance that revisit will not be required because of orbit decay.

To obtain this orbit, either an OMS kit or a "mini" upper stage is necessary; $\sim$ 10 ft of the cargo bay is required for this purpose. The capabilities of the Shuttle, with and without an OMS kit, and with use of such an upper stage to perform delivery, retrieval, and maintenance missions, have been assessed.

Maintenance concepts, from fully automated servicing mechanisms through unaided EVA, have been considered. An EVA maintenance concept as shown in Figure 5.5 has been selected. From the standpoints of scientific objectives and economics, orbital maintenance is preferred; contingency retrieval must be allowed for in-operations planning. Replacement and/or maintenance of scientific instruments is recommended by the AXAF scientific working group.

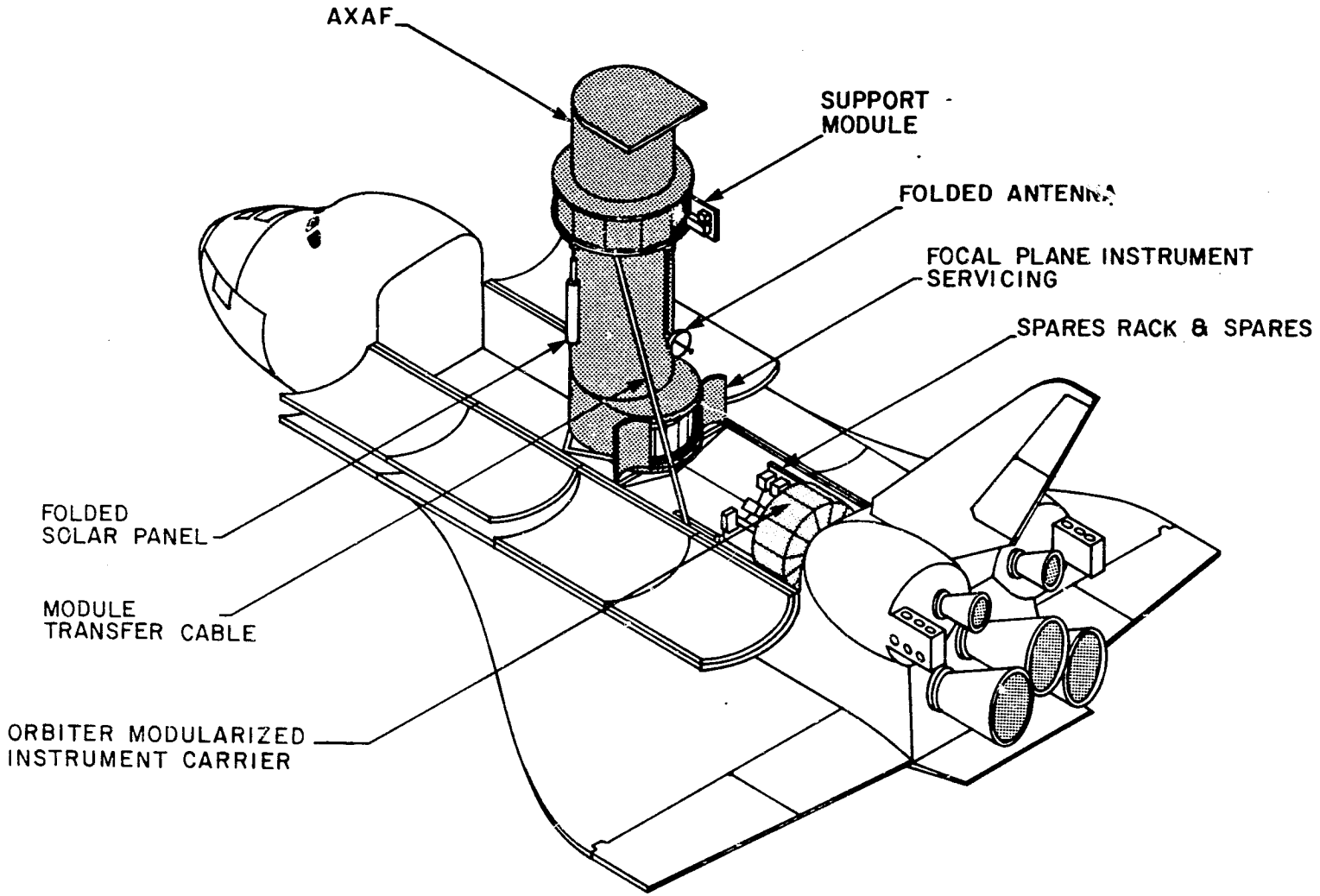


**AXAF ON-ORBIT SERVICING**
(CAROUSEL FPA CONCEPT)

Figure 5.5 - EVA maintenance concept.

# APPROVAL

## ADVANCED X-RAY ASTROPHYSICS FACILITY (AXAF) SCIENCE WORKING GROUP REPORT

By the Program Development Directorate

The information in this report has been reviewed for technical content. Review of any information concerning Department of Defense or nuclear energy activities or programs has been made by the MSFC Security Classification Officer. This report, in its entirety, has been determined to be unclassified.

James A. Downey III

W. R. MARSHALL
Director, Program Development

☆ U.S. GOVERNMENT PRINTING OFFICE: 1980—640-247/3 REGION NO.4